

ALEXANDROS KOSTOPOULOS

Diploma Thesis

Evaluation of the performance and power requirements of a high-pressure hydraulic system using a control-volume strategy versus classical servovalve actuation.

Section: Mechanical Design & Automatic Control

Supervisor: Vasilios Spitas, Associate Professor NTUA

Athens, March 2022



SCHOOL OF MECHANICAL ENGINEERING

First of all, I would like to thank my family for all their support throughout the years. Also, I want to thank my supervisor professor, Mr. Visilios Spitas, for his valuable guidance and for the time he spend on resolving all my questions. Finally, I would like to thank Mr. Efstratios Tsolakis, doctoral student of the lab, for the excellent cooperation at resolving some technical issues during the completion of the Diploma Thesis.

ABSTRACT

The main objective of this Diploma Thesis is to investigate the difference in power consumption of two control strategies in a hydraulic configuration that uses a hydraulic cylinder. Initially, a theoretical analysis of hydraulic systems is done followed by an analysis of the two control strategies that are under investigation. Then the values of the system parameters are being defined and the components of both systems are selected. Finally, the simulation results for the power consumption, mean chamber pressure and position error are presented for each system. In addition, the effect of inertia and friction losses are also investigated in a separate model.

Contents

List of Figures	9
List of Tables	11
1. Hydraulic Systems Theory.....	13
1.1. Introduction.....	13
1.2. Hydraulic Power Supply	13
1.3. Control Elements.....	14
1.3.1. Lands and ports	14
1.3.2. Center type	15
1.3.3. Servo valve.....	16
1.4. Actuators	17
2. System analysis	19
2.1. Problem description	19
2.2. Hydro-mechanical servo system	19
2.2.1. Hydro-mechanical system	19
2.2.2. Servo valve modeling.....	23
2.3. Active system	26
3. System parameters and Sizing.....	30
3.1. System sizing	30
3.2. Value selection	33
3.3. Final simulation parameters	37
4. Results.....	40
4.1. Model Description.....	40
4.2. Effect of hydraulic losses on the system	42
4.3. Hydraulic – Active system comparison	56
4.3.1. Main results	56
4.3.2. Piston Position Results.....	63
4.4. Conclusion	63
Bibliography	65
Appendix	67
A. Mean simulation values	67
B. Position plots	69
C. Matlab codes.....	80

a) Main code	80
b) PID Gains.....	89
c) Sizing.....	91
D. KDamper	93

List of Figures

Figure 1-1: Typical configuration of valve spools [2]	15
Figure 1-2: Types of valve lapping at neutral position [2]	15
Figure 1-3: Typical valve flow gain [2]	16
Figure 1-4: Servo valve, no signal [3]	16
Figure 1-5: Signal applied to electric motor and spool about to move [3].....	17
Figure 1-6: Equilibrium condition with signal applied [3].....	17
Figure 1-7: 3D model of a hydraulic cylinder	18
Figure 1-8: An axial piston hydraulic motor.....	18
Figure 2-1: Functional schematic of hydro-mechanical servo system	19
Figure 2-2: Servo valve port area	24
Figure 2-3: Step response of the MOOG D936 servo valve	24
Figure 2-4: Digitalized step response of the MOOG D936 servo valve	25
Figure 2-5: Spool stroke - Valve settling time diagram.....	25
Figure 2-6: Functional schematic of active hydraulic system	26
Figure 2-7: Simplified electric motor circuit	27
Figure 3-1: Time – Theoretical force diagram.....	31
Figure 3-2: Time – Power diagram.....	32
Figure 3-3: Fourier transformation of the system power.....	33
Figure 3-4: Bosch Rexroth Series CDH3 hydraulic cylinder.....	34
Figure 3-5: ME1302 (DLC-28) Brushless 15 kW - 38 kW Liquid-Cooled PMAC Motor.	35
Figure 3-6: Bosch Rexroth Axial Piston Fixed Pump A2FO series 6	36
Figure 3-7: D936 Servo-Proportional Valve	37
Figure 4-1: Simple system Simulink model	40
Figure 4-2: Full system Simulink model	41
Figure 4-3: Hydro-mechanical servo system model	41
Figure 4-4: Active system model.....	42
Figure 4-5: Time – Piston position diagram	43
Figure 4-6: Time – Piston position diagram (detail)	43
Figure 4-7: Time – Hydraulic power diagram	44
Figure 4-8: Time – Piston chamber pressure diagram.....	45
Figure 4-9: Time – Ring chamber pressure diagram.....	45
Figure 4-10: Time – Inertia losses in piston chamber diagram.....	46
Figure 4-11: Time – Inertia losses in ring chamber diagram	47
Figure 4-12: Time – Friction losses in piston chamber diagram	47
Figure 4-13: Time –Friction losses in ring chamber diagram.....	48
Figure 4-14: Time – Piston position diagram	49
Figure 4-15: Time –Hydraulic power diagram	49
Figure 4-16: Time – Piston chamber pressure diagram.....	50
Figure 4-17: Time – Ring chamber pressure diagram.....	50
Figure 4-18: Time – Inertia losses in piston chamber diagram.....	51
Figure 4-19: Time – Inertia losses in ring chamber diagram	51
Figure 4-20: Time – Friction losses in piston chamber diagram	52

Figure 4-21: Time – Friction losses in ring chamber diagram.....	52
Figure 4-22: Time – Inertia losses in piston chamber diagram.....	53
Figure 4-23: Time – Inertia losses in ring chamber diagram	54
Figure 4-24: Time – Friction losses in piston chamber diagram.....	54
Figure 4-25: Time – Friction losses in ring chamber diagram.....	55
Figure 4-26: Frequency – Power diagram.....	57
Figure 4-27: Frequency – Power diagram (detail)	57
Figure 4-28: Frequency – Percent Power Loss diagram	58
Figure 4-29: Frequency – Piston Chamber Pressure diagram	59
Figure 4-30: Frequency – Ring Chamber Pressure diagram	59
Figure 4-31: Frequency – Piston Absolute Position Error diagram	60
Figure 4-32: Frequency – Piston Percent Position Error diagram	61
Figure 4-33: Frequency – Piston Position at 10Hz diagram.....	62
Figure 4-34: Frequency – Piston Position at 10Hz diagram (detail)	62
Figure B-1: Frequency – Piston Position at 0.1Hz diagram ($V_g = 5\text{cm}^3/\text{rev}$)	69
Figure B-2: Frequency – Piston Position at 0.2Hz diagram ($V_g = 5\text{cm}^3/\text{rev}$)	69
Figure B-3: Frequency – Piston Position at 0.4Hz diagram ($V_g = 5\text{cm}^3/\text{rev}$)	70
Figure B-4: Frequency – Piston Position at 0.6Hz diagram ($V_g = 5\text{cm}^3/\text{rev}$)	70
Figure B-5: Frequency – Piston Position at 0.8Hz diagram ($V_g = 5\text{cm}^3/\text{rev}$)	71
Figure B-6: Frequency – Piston Position at 1Hz diagram ($V_g = 5\text{cm}^3/\text{rev}$)	71
Figure B-7: Frequency – Piston Position at 2Hz diagram ($V_g = 5\text{cm}^3/\text{rev}$)	72
Figure B-8: Frequency – Piston Position at 4Hz diagram ($V_g = 5\text{cm}^3/\text{rev}$)	72
Figure B-9: Frequency – Piston Position at 6Hz diagram ($V_g = 5\text{cm}^3/\text{rev}$)	73
Figure B-10: Frequency – Piston Position at 8Hz diagram ($V_g = 5\text{cm}^3/\text{rev}$)	73
Figure B-11: Frequency – Piston Position at 10Hz diagram ($V_g = 5\text{cm}^3/\text{rev}$)	74
Figure B-12: Frequency – Piston Position at 0.1Hz diagram ($V_g = 10\text{cm}^3/\text{rev}$)	74
Figure B-13: Frequency – Piston Position at 0.2Hz diagram ($V_g = 10\text{cm}^3/\text{rev}$)	75
Figure B-14: Frequency – Piston Position at 0.4Hz diagram ($V_g = 10\text{cm}^3/\text{rev}$)	75
Figure B-15: Frequency – Piston Position at 0.6Hz diagram ($V_g = 10\text{cm}^3/\text{rev}$)	76
Figure B-16: Frequency – Piston Position at 0.8Hz diagram ($V_g = 10\text{cm}^3/\text{rev}$)	76
Figure B-17: Frequency – Piston Position at 1Hz diagram ($V_g = 10\text{cm}^3/\text{rev}$)	77
Figure B-18: Frequency – Piston Position at 2Hz diagram ($V_g = 10\text{cm}^3/\text{rev}$)	77
Figure B-19: Frequency – Piston Position at 4Hz diagram ($V_g = 10\text{cm}^3/\text{rev}$)	78
Figure B-20: Frequency – Piston Position at 6Hz diagram ($V_g = 10\text{cm}^3/\text{rev}$)	78
Figure B-21: Frequency – Piston Position at 8Hz diagram ($V_g = 10\text{cm}^3/\text{rev}$)	79
Figure B-22: Frequency – Piston Position at 10Hz diagram ($V_g = 10\text{cm}^3/\text{rev}$)	79
Figure D-1: Schematic presentation of KDamper	93
Figure D-2: KDamper: (a) Static equilibrium under gravity force, (b) perturbed position after dynamic excitation	94
Figure D-3: Conceptual configuration of the negative stiffness spring in KDamper ...	94
Figure D-4: Simplified model of the hydraulic actuator	95

List of Tables

Table 3-1: System parameter values	37
Table 3-2: Hydraulic cylinder parameter values	37
Table 3-3: Load parameter values	38
Table 3-4: Electric motor parameter value	38
Table 3-5: Hydraulic pump parameter value	38
Table 3-6: Servo valve parameter value	38
Table 3-7: Control volume parameter value	38
Table 3-8: Hydraulic oil parameter value	39
Table 4-1: Mean absolute values of the Pressure Losses	55
Table A-1: Mean System Power	67
Table A-2: Mean Piston Chamber Pressure	67
Table A-3: Mean Ring Chamber Pressure	68
Table-A-4: Mean Absolute Error	68
Table A-5: Mean Percent Error	68

1. Hydraulic Systems Theory

1.1. Introduction

The function of hydraulic systems is based on Pascal's law, which states that applying a pressure to a fluid inside a closed circuit, will result in the transmission of this pressure equally in all directions. So, a hydraulic system functions by using a fluid which is under pressure to produce work.

A hydraulic system comprises of interconnected components that transfer fluid in order to perform a desired function. These components usually are [1]:

- hydraulic power supply
- control elements
- actuators
- other elements (pipelines, measuring devices, etc.)

The hydraulic power supply usually consists of a pump connected to a prime mover (electric or diesel motor). The pump then converts the available mechanical power of the prime mover to hydraulic power at the actuator, which can either be a hydraulic cylinder for translational motion or a hydraulic motor for rotational motion. In addition, control elements, such as valves, control the flow direction, pressure and power at the actuator.

1.2. Hydraulic Power Supply

Hydraulic pumps are machines that convert the available mechanical power from an electric or diesel motor into hydraulic power of the fluid flowing through them. The rotating speed of the pump determines the flow rate of the fluid whereas the pressure developed is determined by the load at the pump outlet. The main types of hydraulic pumps are:

- **External gear pumps** use two gears rotating against each other to provide fluid flow. As the gears rotate away from each other, fluid trapped in the slots between the teeth is carried around and discharged at the outlet port.
- **Internal gear pumps** have two gears, an inner gear which is inside an outer gear. The shaft of the motor drives the inner gear which in turn moves the outer gear. Fluid is trapped between the teeth of the two gears and is transferred from the inlet to the outlet port.
- **Rotary vane pumps** consist of variable length vanes mounted to an off-centered shaft. As the shaft rotates, the vanes slide in and out in order to maintain contact with the pump housing and so chambers of varying sizes are created inside the pump. The fluid enters the pump at the largest chamber which becomes smaller in size as the fluid exits through the discharge port.
- **Swash-plate piston pumps** have a rotating shaft connected to a cylinder block which contains pistons. These pistons are pressed against a swash plate which sits at an angle to the cylinder. As the shaft rotates, the pistons move against

the swash-plate which causes them to reciprocate within the piston block. The pistons create a vacuum which forces fluid inside them during the intake stroke and expel it during the discharge stroke.

- **Radial piston pumps** have pistons that are arranged around the cylinder block with an eccentric cam mounted on the drive shaft. As the shaft rotates, the cam moves towards the pistons forcing them down into the cylinder block and discharging the fluid.
- **Screw pumps** consist of two screws that intermesh with each other. As the screws rotate, a vacuum is created at the inlet causing fluid to fill the space between the treads and the housing.

1.3. Control Elements

The most important control element in a hydraulic circuit are the hydraulic valves. There are four basic types of valves in hydraulic systems [1].

- **Pressure valves** are used to maintain and/or select the desired pressure level in the hydraulic system.
- **Check valves** are a special type of directional valves which only allow fluid flow in one direction while preventing the flow in the reverse direction.
- **Flow control valves** are used to regulate the flow rate of the fluid from one part of the hydraulic circuit to another.
- **Directional control valves (DCVs)** are used to control the direction of fluid flow into various paths. They are characterized by the number of connected lines (ways), the number of control positions and the number of lands. The most common type of DCVs consist of a spool inside a cylinder (sleeve) and the position of the spool determines the direction of flow. A special type of DCV is the servo controlled valve.

1.3.1. Lands and ports

The spool of a DCV can have different number of connected lines (ways) and lands, depending on the application. Since a supply, a return and at least a line to the actuator is needed, the spool needs to have three or more ports. Some examples of valve spools are shown in the figure below [2].

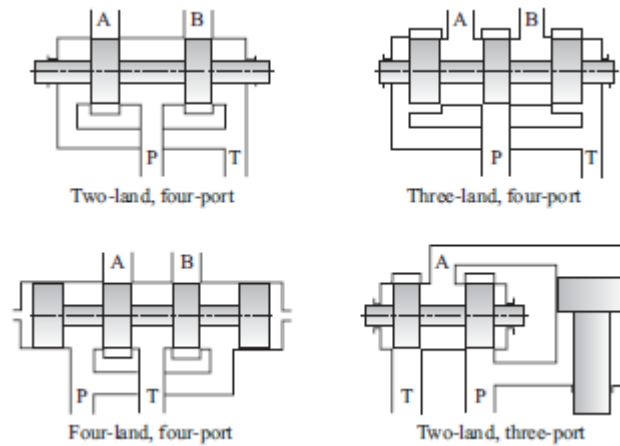


Figure 1-1: Typical configuration of valve spools [2]

1.3.2. Center type

The center type of a valve is defined by the “lap”, which is the width of the spool land relative to the width of the port in the valve sleeve. Based on this, there are three main categories of center types [1] [2].

- **Open center or under-lapped** where the width of the land is smaller than the width of the port. In this case, there is a moment where all ports are connected to each other. This results in smooth, continuous flow during the valve operation.
- **Closed center or over-lapped** where the width of the land is larger than the width of the port. In this type of valves, there is a length around the neutral position of the spool where all the ports are not connected, which in turn causes a dead-band in flow.
- **Critical center or zero-lapped** where the width of the land is equal to the width of the port. They are the most common type of valves and is because of their geometry, they can achieve a linear flow gain around the neutral position.

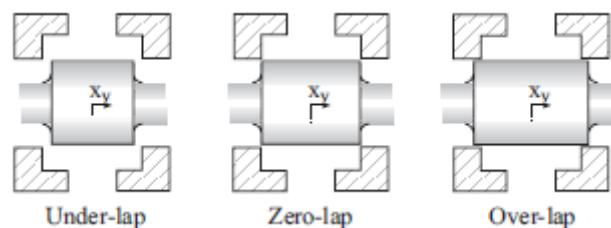


Figure 1-2: Types of valve lapping at neutral position [2]

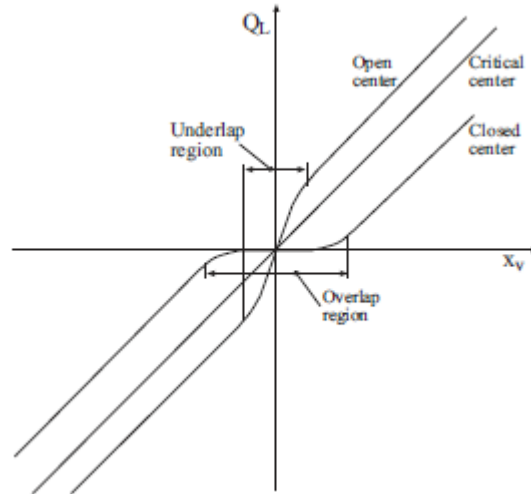


Figure 1-3: Typical valve flow gain [2]

1.3.3. Servo valve

Servo valves are fast responding DCVs that incorporate a control law in order to accurately control motion, force and other parameters. “In its simplest form, a servo or a servomechanism is a control system, which measures its own output and forces the output to quickly and accurately follow a command signal” [2]. A typical type of a hydraulic servo valve is the two stage flapper-nozzle valve (figure 1-4). An electrical current in the torque motor causes the armature to rotate which displaces the flapper between the two nozzles. This displacement makes the area of the nozzle that comes closer to the flapper, smaller, lowering the flow rate and increasing the pressure on that side. Then, the pressure increase moves the spool to the opposite direction and continues to move it until the feedback signal matches the desired signal.

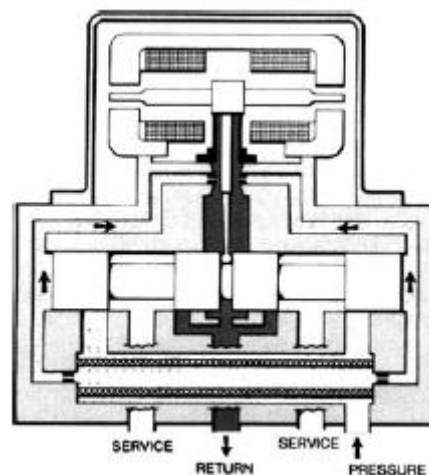


Figure 1-4: Servo valve, no signal [3]

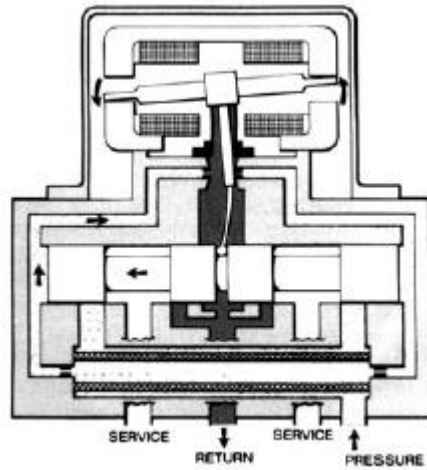


Figure 1-5: Signal applied to electric motor and spool about to move [3]

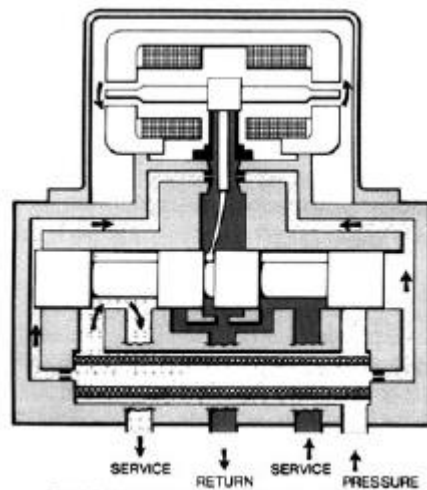


Figure 1-6: Equilibrium condition with signal applied [3]

Although servo valves have many advantages, they are not energy efficient due to the heavy throttling losses they introduce to the system. For example, “the nominal flow capacity of a servo valve is specified at a total valve pressure drop of 70 bar. Assuming a supply pressure of 210 bar gives that only the valve losses represents 33% of the input power at nominal flow conditions and only 67% remains for load actuations” [2].

1.4. Actuators

Hydraulic actuators are components that convert hydraulic power, delivered by the pump, to mechanical power in the desired form. There are two main types of actuators, the hydraulic cylinder and the hydraulic motor.

Hydraulic cylinders convert the hydraulic power of the fluid into mechanical power, performing a translational motion. The pressure of the fluid is converted into force acting on the piston whereas the flow rate determines the piston velocity.

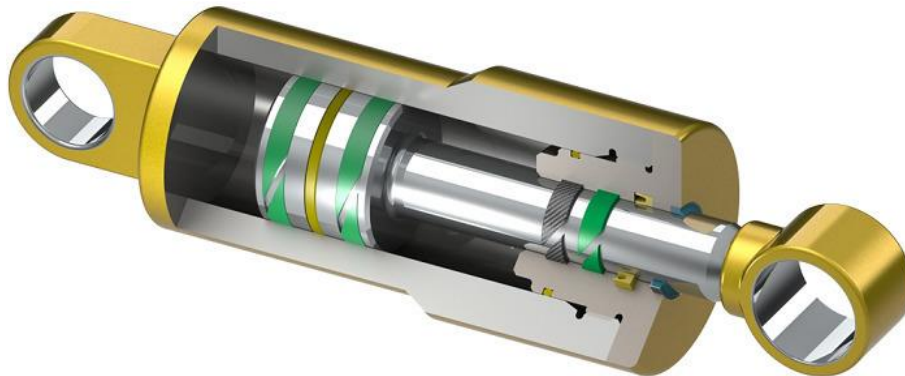


Figure 1-7: 3D model of a hydraulic cylinder

Hydraulic motors have similar function to the pump, in the reverse way. Instead of pushing fluid into the system, they are pushed by the fluid and thus convert the fluid pressure and flow rate into torque and rotary velocity at the shaft.



Figure 1-8: An axial piston hydraulic motor

2. System analysis

2.1. Problem description

As stated in chapter 1.3.3, although the servo valve offers quick and accurate system control, it forces the liquid to pass through narrow ports and orifices which leads in heavy energy losses. This is further increased by the frequency of the system, making the servo valve a non-optimal control choice for systems operating at high frequencies.

In this thesis an alternative control configuration is being investigated. This configuration consists of a cylindrical mass connected to one of the chambers of a hydraulic cylinder and can freely move in and out of the chamber with the help of an electric motor. The position of the control volume affects the pressure and the size of the cylinder chamber that is connected, which in turn causes the cylinder piston to move at the desired direction.

2.2. Hydro-mechanical servo system

2.2.1. Hydro-mechanical system

Consider a hydro-mechanical system consisting of a servo valve controlled hydraulic piston connected to a mass. The analysis for the aforementioned configuration has already been done in previous works [2] [3], but it is critical to repeat the analysis for completeness reasons.

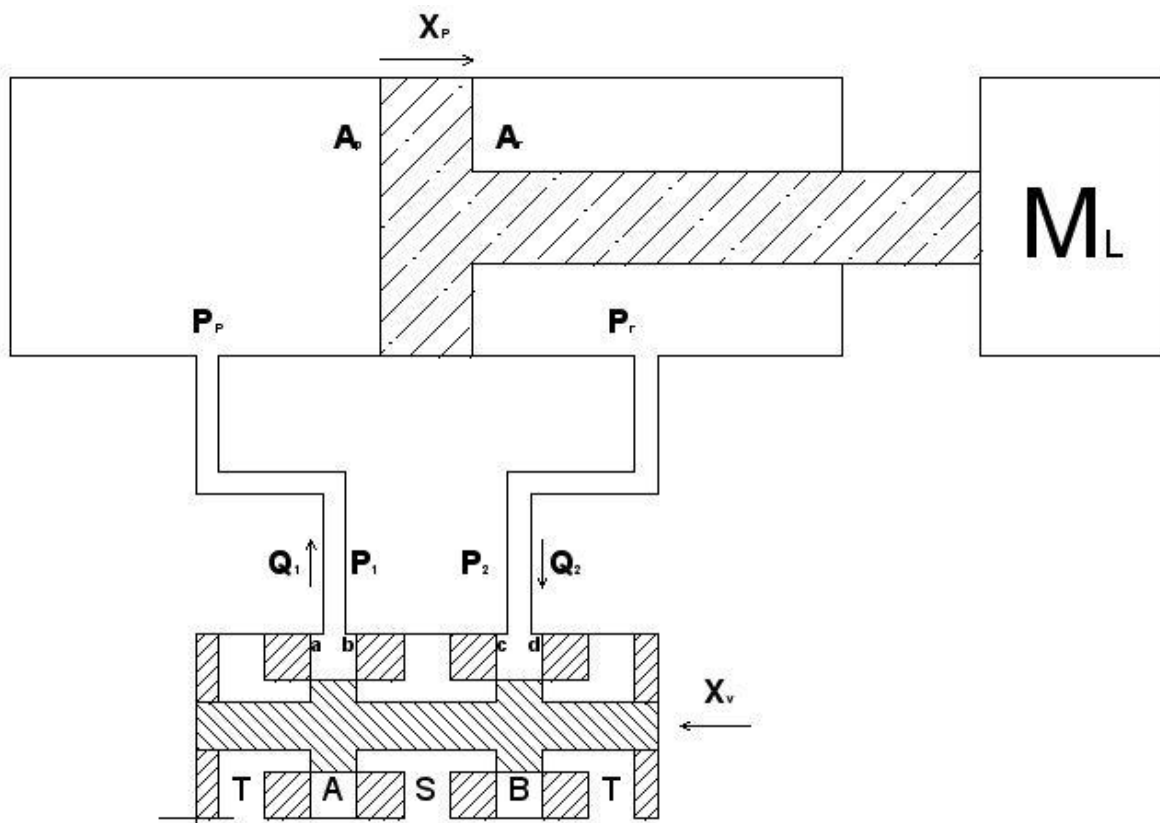


Figure 2-1: Functional schematic of hydro-mechanical servo system

It is assumed that the servo valve is critical center and symmetrical, the supply pressure is constant and the tank pressure is zero. Also, it is assumed that the leakages inside the servo valve are zero, as well as the effect of inertia, compressibility and friction of the oil inside the hydraulic lines connecting the supply and tank to the corresponding piston chamber.

The flow rate equations through the restriction areas of the servo valve can be written as:

$$Q_1 = C_d A_{b(x_v)} \sqrt{\frac{2}{\rho} (P_s - P_1)} - C_d A_{a(x_v)} \sqrt{\frac{2}{\rho} (P_1 - P_t)} \quad (2-1)$$

$$Q_2 = C_d A_{c(x_v)} \sqrt{\frac{2}{\rho} (P_s - P_2)} - C_d A_{d(x_v)} \sqrt{\frac{2}{\rho} (P_2 - P_t)} \quad (2-2)$$

where:

- Q_i : Servo valve flow rate
- C_d : Discharge coefficient
- $A_{i(x_v)}$: Restriction areas
- ρ : Oil density
- P_s : Supply pressure
- P_t : Tank pressure
- P_1 : Servo valve pressure in land 1
- P_2 : Servo valve pressure in land 2

It is assumed that the valve is matched ($A_{a(x_v)} = A_{c(x_v)}$ and $A_{b(x_v)} = A_{d(x_v)}$) and symmetrical ($A_{a(-x_v)} = A_{b(x_v)}$ and $A_{c(-x_v)} = A_{d(x_v)}$) type. Also, the radial clearance of the spool is considered to be zero. So, the restriction areas (assuming they are rectangular) are calculated as follows:

$$\left. \begin{array}{l} A_a = A_c = 0 \\ A_b = A_d = A = wx_v \end{array} \right\} \text{For } x_v > 0 \quad (2-3)$$

$$\left. \begin{array}{l} A_a = A_c = A = wx_v \\ A_b = A_d = 0 \end{array} \right\} \text{For } x_v < 0 \quad (2-4)$$

where:

- x_v : Spool displacement/stroke
- w : Port width
- A : Servo valve port area

The hydraulic oil flow is actually a spatial distributed physical system and the mathematical model that describes it is too complicated when taking into consideration all the parameters that affect it. For this reason, a lumped element model is used in order to simplify the behavior of the system. Except from the driving forces, the motion of hydraulic oil is also affected by oil inertia and compressibility, during transient conditions, and, as well as, friction. The effect of inertia, resistance and capacitance in each piston chamber are considered to be separate from each other.

The walls of the hydraulic cylinder can be considered rigid compared to the hydraulic oil due to the effect of oil compressibility and therefore, the deformation of the hydraulic cylinder walls is zero. Applying the continuity equations to the piston chambers results in the following equations:

$$Q_1 - A_p \frac{dX_p}{dt} - Q_{leak} - Q_{ep,leak} = \frac{V_p}{\beta_e} \frac{dP_p}{dt} \quad (2-5)$$

$$Q_2 + A_r \frac{dX_p}{dt} + Q_{leak} - Q_{er,leak} = \frac{V_r}{\beta_e} \frac{dP_r}{dt} \quad (2-6)$$

where:

- A_p : Piston area without rod (Piston Chamber)
- A_r : Piston area with rod (Ring Chamber)
- X_p : Piston displacement
- V_p : Volume of Piston Chamber
- V_r : Volume of Ring Chamber
- P_p : Pressure inside Piston Chamber
- P_r : Pressure inside Ring Chamber
- β_e : Bulk modulus
- Q_{leak} : Internal leakage flow
- $Q_{ei,leak}$: External leakage flow

The internal and external leakage flows of the hydraulic cylinder are considered to be linear to the pressure difference and are calculated as:

$$Q_{leak} = K_{leak}(P_p - P_r) \quad (2-7)$$

$$Q_{ei,leak} = K_{ei,leak}P_i \quad (2-8)$$

where:

- K_{leak} : Internal leakage coefficient
- $K_{ei,leak}$: External leakage coefficient

Considering equations (2-5) and (2-6) and the direction of individual flow rates at the corresponding piston chambers, the total flow rate inside each chamber is:

$$Q_A = Q_1 - Q_{\text{leak}} - Q_{\text{ep,leak}} - \frac{V_p}{\beta_e} \frac{dP_p}{dt} \quad (2-9)$$

$$Q_B = Q_2 + Q_{\text{leak}} - Q_{\text{er,leak}} - \frac{V_r}{\beta_e} \frac{dP_r}{dt} \quad (2-10)$$

The pressure inside the servo valve is different from the pressure inside the cylinder chambers due to liquid inertia and friction affecting the formation of pressure inside the cylinder chambers. Considering the oil inertia and friction inside the hydraulic cylinder chambers, the following equations can be deduced:

$$P_1 - P_p = I_p \frac{dQ_A}{dt} + R_p Q_A \quad (2-11)$$

$$P_2 - P_r = I_r \frac{dQ_B}{dt} + R_r Q_B \quad (2-12)$$

where:

- I_i : Oil inertia in chamber i
- R_i : Oil resistance in chamber i

The oil inertia and resistance in the cylinder chambers, assuming a linear flow, are calculated as:

$$I_i = \frac{4\rho L_i}{\pi D_i^2} = \frac{\rho L_i}{A_i} \quad (2-13)$$

$$R_i = \frac{128\mu L_i}{\pi D_i^4} = \frac{8\mu\pi L_i}{D_i^2} \quad (2-14)$$

where:

- μ : Oil viscosity
- L_i : Chamber length

Combining equations (2-1) and (2-2) with equations (2-11) and (2-12), the flow rate equations can be written as:

$$Q_1 = C_d A_{b(x_v)} \sqrt{\frac{2}{\rho} \left(P_s - P_p - I_p \frac{dQ_A}{dt} - R_p Q_A \right)} - C_d A_{a(x_v)} \sqrt{\frac{2}{\rho} \left(P_p + I_p \frac{dQ_A}{dt} + R_p Q_A - P_t \right)} \quad (2-15)$$

$$Q_2 = C_d A_{c(x_v)} \sqrt{\frac{2}{\rho} \left(P_s - P_r - I_r \frac{dQ_B}{dt} - R_r Q_B \right)} - C_d A_{d(x_v)} \sqrt{\frac{2}{\rho} \left(P_r + I_r \frac{dQ_B}{dt} + R_r Q_B - P_t \right)} \quad (2-16)$$

The final equation derives from the force equilibrium on the piston:

$$A_p P_p - A_r P_r = M_L \frac{d^2 X_P}{dt^2} + B_L \frac{dX_P}{dt} + K_L X_P + \Delta F_L \quad (2-17)$$

where:

- M_L : Load mass
- B_L : Friction coefficient
- K_L : Load stiffness
- ΔF_L : External loading force

2.2.2. Servo valve modeling

In the hydro-mechanical system analysis, it was assumed that the servo valve port has a rectangular shape. This is not the case for the selected servo valve which has a circular port. Thus, the restriction area of the servo valve must be calculated.

For a circular shaped area, the central angle is:

$$\theta = 2 \cos^{-1} \left(1 - \frac{|x_v|}{R} \right) \quad (2-18)$$

The circular segment area (green area) can be calculated as:

$$A = \frac{R^2}{2} (\theta - \sin \theta) \quad (2-19)$$

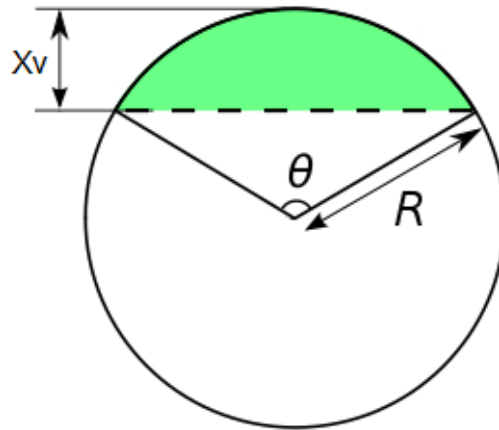


Figure 2-2: Servo valve port area

To continue the analysis, MOOG D936 Series is selected as servo valve that has a maximum nominal flow rate of $40 \frac{l}{min}$, which is considered sufficient for the specific application. From servo valve theory [2], as well as, from the step response of the servo valve, it is deduced that it can be modelled as a first order system. The transfer function of the servo valve can be written as:

$$G_{sv} = \frac{1}{\tau s + 1} \quad (2-20)$$

where τ is the settling time. The manufacturer states that the maximum settling time is 11ms, which can also be seen in the step response diagram (figure 2-3).

Step Response

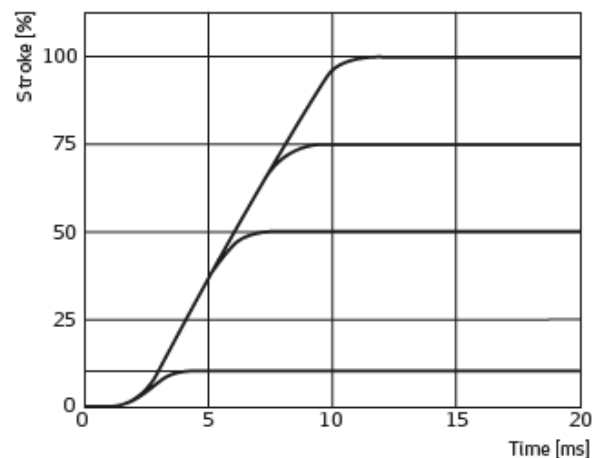


Figure 2-3: Step response of the MOOG D936 servo valve

The above value of the settling time is true in the case that the spool moves from 0 to 100% of its stroke. Because the needed stroke of the servo valve constantly varies

depending on its operation, a relationship between stroke and settling time must be established. For this reason, the step response of the servo valve was digitalized. Also, a line that connects the settling time points for the various strokes was created in order to correlate the two parameters, as shown in the figure below.

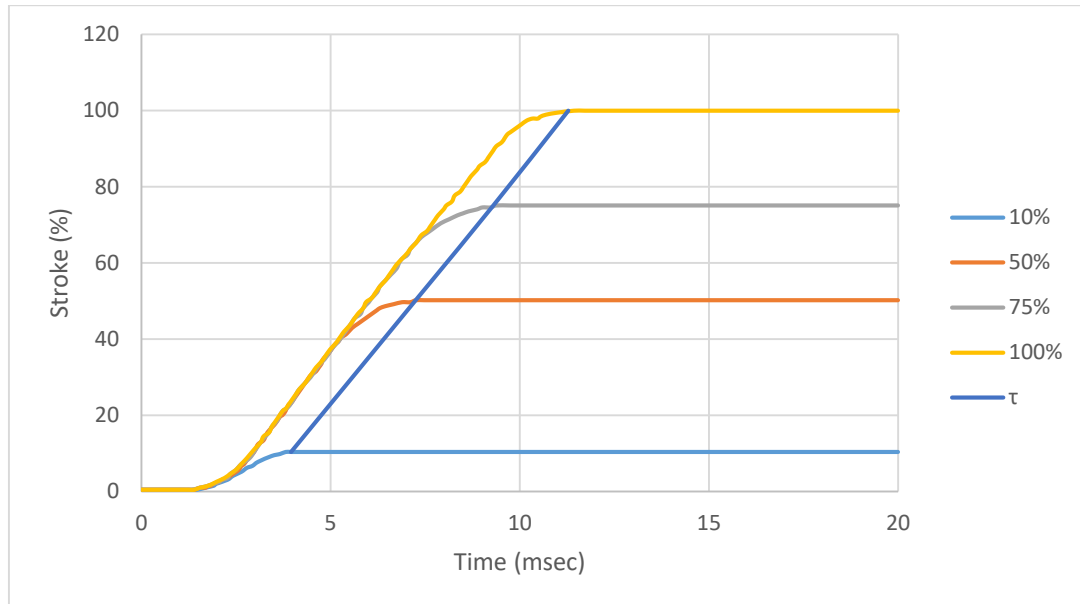


Figure 2-4: Digitalized step response of the MOOG D936 servo valve

It is observed that the line connecting the settling time points is almost straight and it can be safely linearized without important error. It is also assumed that the maximum stroke of the servo valve equals to the maximum port width, which is the maximum port diameter for a circular shaped port. By plotting the valve stroke on x-axis and settling time on y-axis, an equation for the two parameters can be obtained.

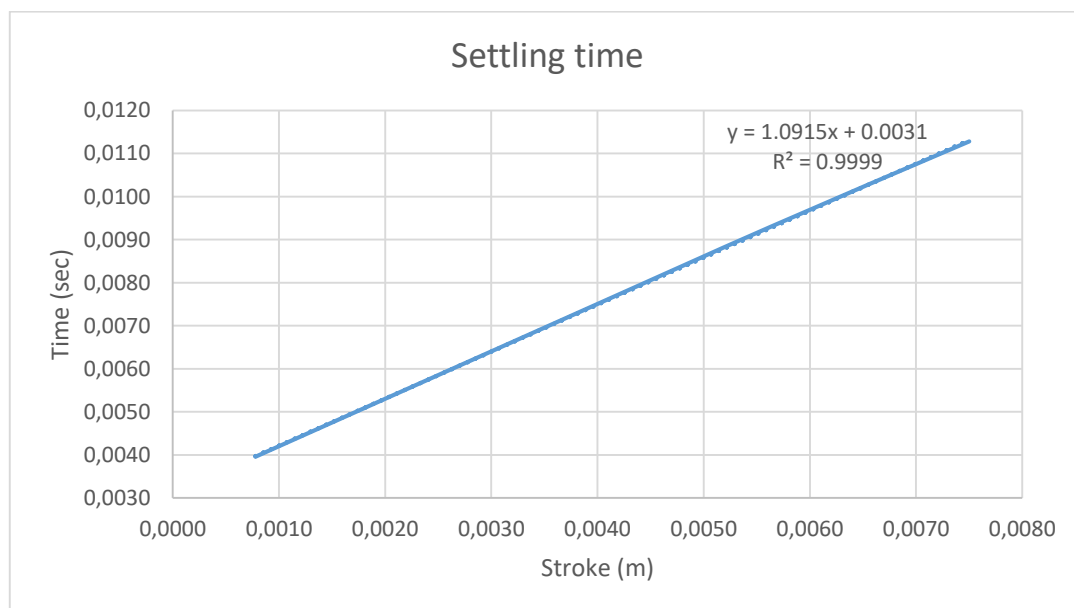


Figure 2-5: Spool stroke - Valve settling time diagram

From the above diagram, the equation that relates valve stroke with settling time is:

$$y = 1.0915|x_v - x_{v,previous}| + 0.0031 \quad (2-21)$$

2.3. Active system

The active hydraulic system consists of a hydraulic cylinder with pre-pressurized oil in both cylinder chambers and a small control volume/mass that is connected to the piston chamber. The control volume can move in and out of the chamber with the help of an electric motor and thus, respectively decreasing and increasing the volume of the chamber and ultimately increasing or decreasing the pressure of the chamber. This causes the piston to move in the desired direction.

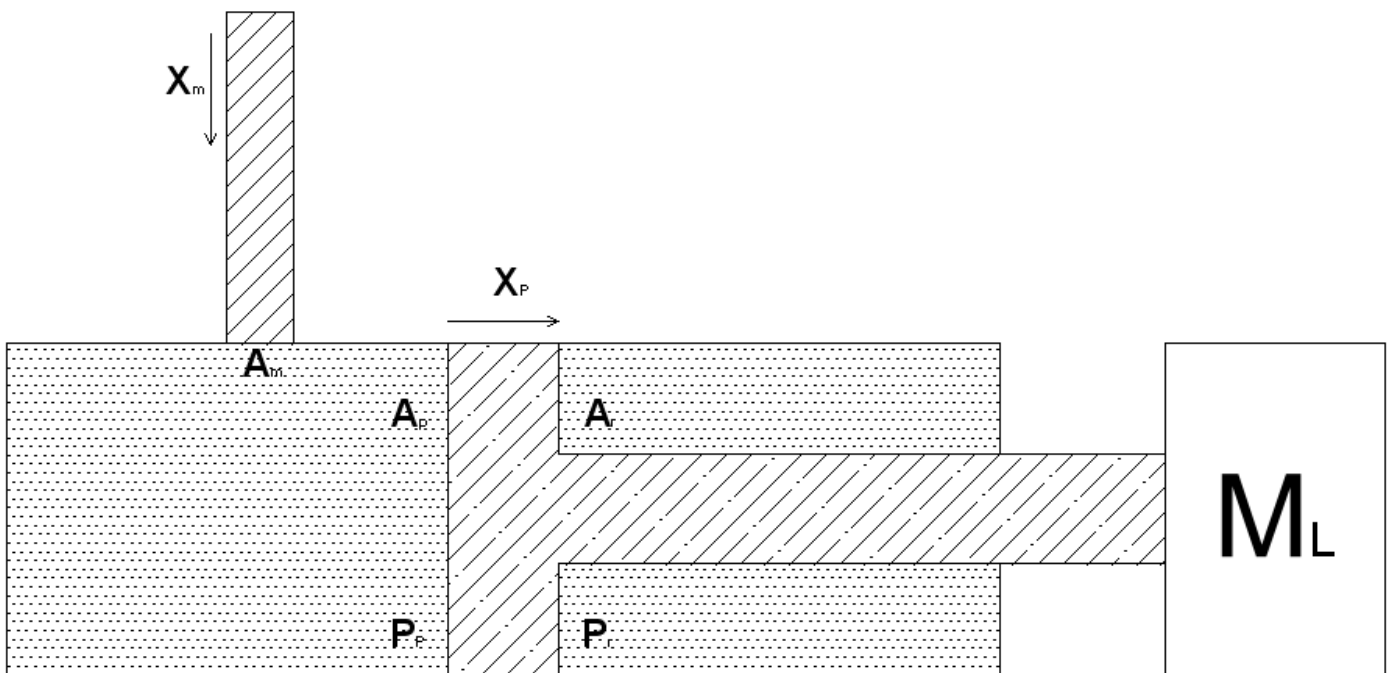


Figure 2-6: Functional schematic of active hydraulic system

The volume of each chamber can be calculated by the following equations:

$$V_p = X_p A_p - X_m A_m \quad (2-22)$$

$$V_r = (L - X_p) A_r \quad (2-23)$$

where:

- V_i : Chamber volume
- L : Total length of hydraulic cylinder
- X_m : Control volume displacement
- A_m : Control volume area

Applying the continuity equation to each hydraulic cylinder chamber results in:

$$\frac{dX_m}{dt} A_m - \frac{dX_p}{dt} A_p - Q_{\text{leak}} - Q_{\text{ep,leak}} = \frac{V_p}{\beta_e} \frac{dP_p}{dt} \quad (2-24)$$

$$A_r \frac{dX_p}{dt} + Q_{\text{leak}} - Q_{\text{er,leak}} = \frac{V_r}{\beta_e} \frac{dP_r}{dt} \quad (2-25)$$

The force equilibrium equation on the hydraulic piston is the same as in the servo valve analysis.

$$A_p P_p - A_r P_r = M_L \frac{d^2 X_p}{dt^2} + B_L \frac{dX_p}{dt} + K_L X_p + \Delta F_L \quad (2-26)$$

A DC motor is a common actuator that provides rotary motion, which can be converted into translational motion if needed. The electrical circuit of a DC motor consists of two circuits, the armature and the field circuit. It is assumed that the field is excited by a constant voltage, thus only the armature circuit is considered. The armature circuit consist of a voltage source, an electrical resistance, an inductor and the rotor. The speed of the DC motor is proportional to armature voltage.

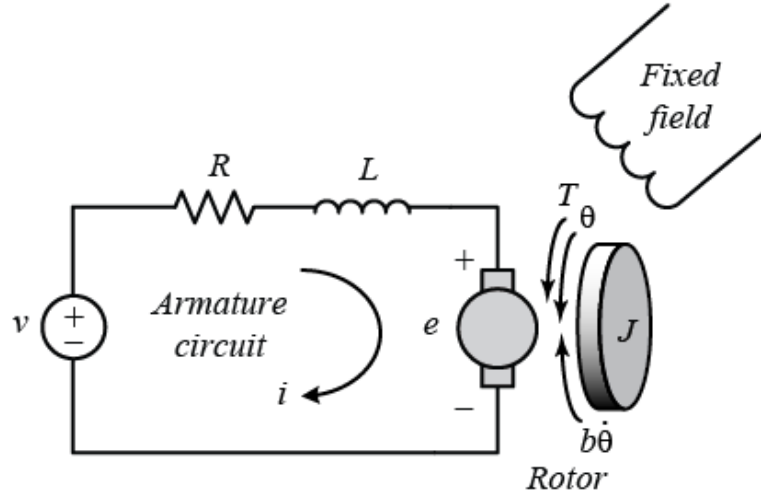


Figure 2-7: Simplified electric motor circuit

By applying Kirchhoff's law on the armature circuit, the following expression can be written:

$$v_a = i_a R_a + \frac{di_a}{dt} L_a + e_b \quad (2-27)$$

where:

- v_a : Armature voltage
- i_a : Armature current

- R_a : Armature resistance
- L_a : Armature inductance
- e_b : Back-emf

The torque of a DC motor is proportional to armature current and can be calculated as:

$$T = k_t i_a \quad (2-28)$$

where:

- T : Motor torque
- k_t : Motor torque constant

The back-emf of the DC motor is proportional to the angular velocity of the shaft:

$$e_b = k_b \frac{d\theta}{dt} = k_b \omega \quad (2-29)$$

where:

- k_b : Back-emf constant
- θ : Motor angular position
- ω : Motor angular velocity

The motor torque constant and back-emf constant are equal in SI units. Finally, by applying Newton's 2nd law the following equation is deduced:

$$T = J \frac{d^2\theta}{dt^2} + B \frac{d\theta}{dt} + T_l \quad (2-30)$$

where:

- J : Rotor moment of inertia
- B : Rotor viscous friction
- T_l : Load torque

Applying the Laplace transformation on equations (2-27) – (2-30) and then combining equations (2-28) and (2-30), results in:

$$\begin{aligned} k_t I_{a(s)} &= J s^2 \theta_{(s)} + B s \theta_{(s)} + T_{l(s)} \Rightarrow \\ I_{a(s)} &= \frac{J s^2 + B s}{k_t} \theta_{(s)} + \frac{1}{k_t} T_{l(s)} \end{aligned} \quad (2-31)$$

Again, by combining equations (2-27), (2-28) and (2-31) the final expression for the angular position is obtained:

$$\begin{aligned}
V_{a(s)} &= \left(\frac{Js^2 + Bs}{k_t} \theta_{(s)} + \frac{1}{k_t} T_{l(s)} \right) R_a \\
&\quad + \left(\frac{Js^2 + Bs}{k_t} \theta_{(s)} + \frac{1}{k_t} T_{l(s)} \right) sL_a + k_b s \theta_{(s)} \Rightarrow \\
\theta_{(s)} &= \frac{k_t}{s(JL_a s^2 + (JR_a + BL_a)s + (BR_a + k_t k_b))} \left(V_{a(s)} \right. \\
&\quad \left. - \frac{L_a s + R_a}{k_t} T_{l(s)} \right) \quad (2-32)
\end{aligned}$$

The load torque is the torque that the electric motor has to overcome in order to move the piston and it is caused by the force developed on the control volume connected to the hydraulic chamber. This force is caused by the pressure inside the hydraulic chamber and can be calculated by the equation below:

$$F_l = P_p A_m \quad (2-33)$$

where:

- F_l : Load force

Assuming that a rack and pinion mechanism is used to convert the rotational to translational movement, the load torque is given by the equation:

$$T_l = F_l R \quad (2-34)$$

where:

- R : Pinion effective/pitch radius

3. System parameters and Sizing

3.1. System sizing

For the sizing of the hydraulic circuit a few parameters need to be determined. In all cases the desired piston trajectory is a sinusoidal wave, which can be expressed by the equation below.

$$X_p = A \sin(\omega t) \quad (3-1)$$

where:

- A : Amplitude
- ω : Angular frequency
- t : Time

The angular frequency can be calculated from the desired piston frequency:

$$\omega = 2\pi f \quad (3-2)$$

The desired velocity and acceleration of the piston are found by differentiating equation (3-1):

$$u = \frac{dX_p}{dt} = A\omega \cos(\omega t) \quad (3-3)$$

$$a = \frac{du}{dt} = \frac{d^2X_p}{dt^2} = -A\omega^2 \sin(\omega t) \quad (3-4)$$

From the force analysis on the hydraulic system, the total force acting on the piston is given by the following equation:

$$F_{tot} = M_L \frac{d^2X_p}{dt^2} + B_L \frac{dX_p}{dt} + K_L X_p + \Delta F_L \quad (3-5)$$

It is assumed that no external forces are applied on the load and that the load stiffness is zero. Using equations (3-3) to (3-5), the total force can then be written as:

$$F_{tot} = -M_L A \omega^2 \sin(\omega t) + B_L A \omega \cos(\omega t) \quad (3-6)$$

The total force is a sum of two sinusoidal forces with different amplitudes and a phase shift of 90°. For this reason, the maximum force is applied at a different time than the maximum inertia and friction force, as shown in the figure below (in this example a frequency of 1Hz and an amplitude of 0.1m was used).

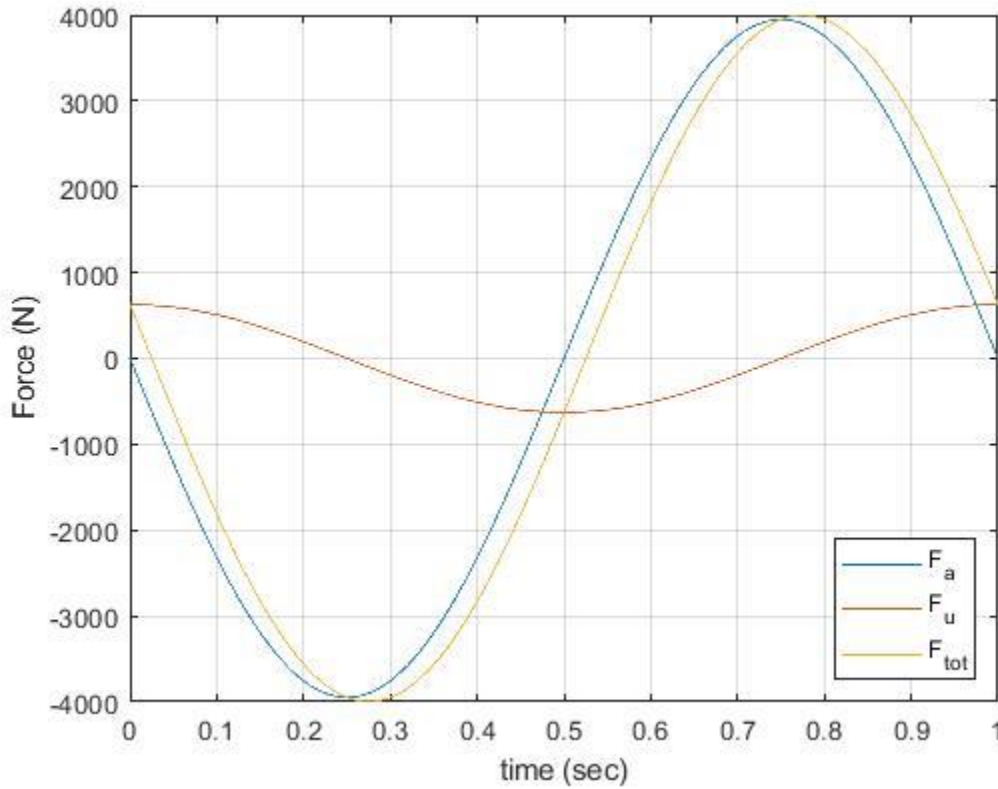


Figure 3-1: Time – Theoretical force diagram

The time, at which the maximum total force is applied, can be found by differentiating equation (3-5) and setting it to zero:

$$\begin{aligned} \frac{dF_{tot}}{dt} = 0 &\Rightarrow -M_L A \omega^3 \cos(\omega t') - B_L A \omega^2 \sin(\omega t') = 0 \Rightarrow \\ &\Rightarrow \tan(\omega t') = -\frac{M_L \omega}{B_L} \Rightarrow t' = \frac{1}{\omega} \tan^{-1} \left(-\frac{M_L \omega}{B_L} \right) \end{aligned} \quad (3-7)$$

Thus, the maximum total force can be calculated:

$$F_{tot,max} = -M_L A \omega^2 \sin(\omega t') + B_L A \omega \cos(\omega t') \quad (3-8)$$

By dividing the maximum total force with the supply pressure results into the appropriate piston area:

$$A_r = \frac{F_{tot,max}}{P_s} \quad (3-9)$$

For the typical double-acting hydraulic cylinder, the active areas of the piston head are not the same since one side of the head has the rod (ring side), thus decreasing the available area on that side. Since the desired trajectory is the same for the cylinder

extension and retraction, the area calculated above must correspond to the ring area, which is the area on the side that has the cylinder rod. The piston area can then be selected by hydraulic cylinder catalogs, since the ring area has already been determined. Also, the piston diameter can be seen in the catalog or can be calculated:

$$D_p = \sqrt{\frac{4A_p}{\pi}} \quad (3-10)$$

The power needed for the system to act can be calculated from the equation:

$$\mathcal{P} = F_{tot}u \quad (3-11)$$

From the diagram below it can be seen that the power of the system has double the frequency of the total force. This can also be confirmed by using Fourier transformation on the signal above.

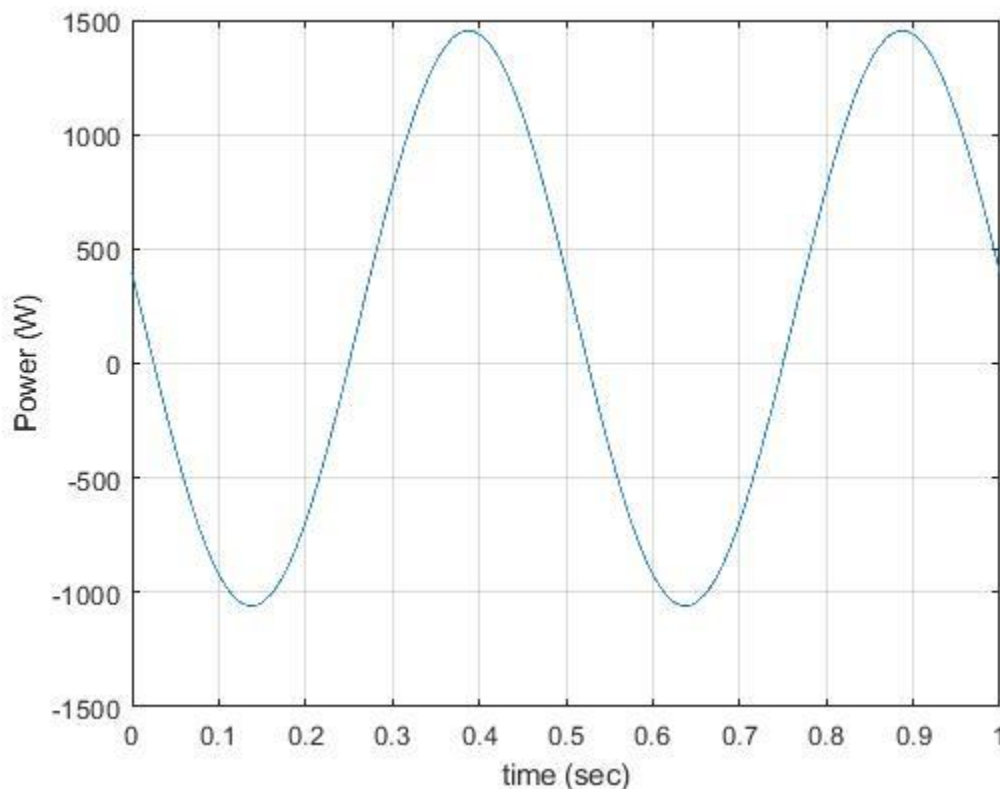


Figure 3-2: Time – Power diagram

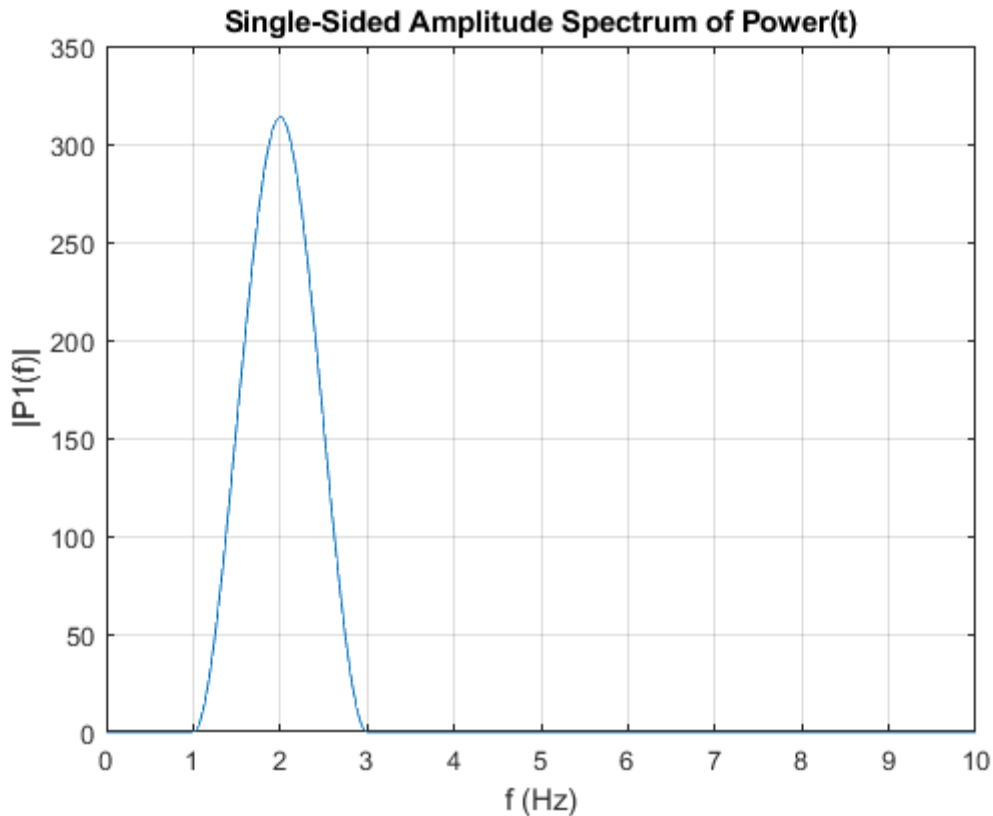


Figure 3-3: Fourier transformation of the system power

3.2. Value selection

In order to compare the two models, some parameters must first be set either by estimation, assumption or trial and error. First of all, for the active system, it is assumed that the pressure of the oil inside the hydraulic cylinder ring chamber is 280bar. Although, a high oil pressure means more required power for the electric motor, it is necessary in order to prevent vacuum inside the chambers. The vacuum may appear because moving the control volume quickly out of the chamber creates suction which is further amplified by the movement of the piston.

For the load, a mass of 1000kg is chosen with a friction coefficient of 1000Nsec/m. Also, the amplitude of the desired trajectory was set at 2.5mm and the maximum piston stroke at 0.4m.

Next, the range of frequencies that are going to be examined must be determined. For a load mass of 1000kg executing a trajectory that constantly requires it to accelerate and decelerate, a maximum frequency of 10Hz is considered as satisfactory, while the minimum frequency was set at 0.1Hz.

Since all the parameters of the load and desired trajectory are set, the maximum force can be calculated from equation (3-6) and also the ring area of the piston from equation (3-9). By searching in hydraulic cylinder catalogs, an approximate area ratio of 2 is selected and hence, the value of the appropriate piston diameter is calculated:

$$D_p = \sqrt{\frac{4A_p}{\pi}} = \sqrt{\frac{8A_r}{\pi}} = 0.0268m \quad (3-12)$$

Considering a safety factor of about 1.5, the hydraulic cylinder selected is Bosch Rexroth Series CDH3 with piston diameter of 0.04m and ring diameter (rod side) of 0.028m.



Figure 3-4: Bosch Rexroth Series CDH3 hydraulic cylinder

In order for the forces acting on both sides of piston to balance, the pressure of the oil inside the piston chamber must be equal to:

$$P_p = 280 \frac{A_r}{A_p} = 142.8bar \quad (3-13)$$

The control volume is assumed to be of cylindrical shape. The area of the control volume is selected to be five times smaller than the area of the piston mass and so, the diameter of the control volume is calculated:

$$D_m = \sqrt{\frac{4A_m}{\pi}} = \sqrt{\frac{4A_p}{5\pi}} = 0.0179m \quad (3-14)$$

Also the control volume is assumed to be made of stainless steel with density of 7500kg/m³ and that it has a length equal to the piston diameter which makes its weight equal to:

$$M_m = \rho A_m D_p = 0.0754kg \quad (3-15)$$

For the electric motor, the ME1302 DLC-28 from Electric Motorsport was selected. The manufacturer doesn't give a value for the viscous friction coefficient. By going through the literature, it can be seen that the viscous friction coefficient for a DC motor has a low value of 10^{-5} or below [4] [5]. Because the values found are for a small DC motor, a value of 10^{-3} is assumed instead. In addition, after running some simulations, the pitch radius for the pinion gear is set at 6.25mm with a module of 1.25.



Figure 3-5: ME1302 (DLC-28) Brushless 15 kW - 38 kW Liquid-Cooled PMAC Motor

For the servo valve system, by calculating the maximum desired velocity of the piston, the maximum flow rate needed can also be calculated using the equation below:

$$Q_{max} = u_{max}A_p = 11.84 \frac{l}{min} \quad (3-16)$$

The pump selected is Bosch Rexroth Axial Piston Fixed Pump A2FO series 6. For the size of the pump, two values are selected, at $5 \frac{cm^3}{rev}$ and $10 \frac{cm^3}{rev}$ since both sizes meet the requirement for the maximum flow rate. However, for these values, the pump has different maximum nominal speed, which is interesting to investigate further. Also, since the manufacturer doesn't give any information about the volumetric efficiency of the pump, a value of 0.92 is selected. The speed of the pump that is needed to provide the maximum flow rate can be calculated as:

$$n = \frac{Q_{max}}{V_g \eta_v} \quad (3-17)$$



Figure 3-6: Bosch Rexroth Axial Piston Fixed Pump A2FO series 6

Since the maximum desired piston velocity and hence, the maximum flow rate are proportional to the trajectory frequency, the speed of the pump will be as well. For this reason, the nominal pump velocity is calculated for frequency of 1Hz which results in 130rpm for the bigger pump and 260rpm for the smaller pump. This means that the appropriate speed of the pump can be easily calculated as:

$$n = n_{nom} f \quad (3-18)$$

The servo valve that is selected is MOOG D936 Series with nominal flow rate $20 \frac{l}{min}$. For maximum flow rate, the manufacturer states that the port width is designed with $\varnothing 7.5mm$. Since the maximum nominal flow rate is $40 \frac{l}{min}$, the port diameter for the wanted flow rate must be calculated. The nominal flow rate is calculated for a pressure drop of 70bar. According to the above and equation (2-1), for a positive spool displacement, the following expression can be written:

$$\begin{aligned} \frac{Q_N}{Q_{N,max}} &= \frac{C_d A_N \sqrt{\frac{2}{\rho} (\Delta p)}}{C_d A_{N,max} \sqrt{\frac{2}{\rho} (\Delta p)}} \Rightarrow \frac{Q_N}{Q_{N,max}} = \frac{A_N}{A_{N,max}} = \frac{4\pi D_N^2}{4\pi D_{N,max}^2} \\ &\Rightarrow \\ D_N &= \sqrt{\frac{Q_N}{Q_{N,max}}} D_{N,max} = 5.81mm \end{aligned} \quad (3-19)$$



Figure 3-7: D936 Servo-Proportional Valve

Finally, the discharge coefficient of the servo valve is selected at 0.611 [3]. Also, since the active model is a closed system with no oil supply, the seals of the hydraulic cylinder must be of excellent quality and, therefore, the leakage coefficient was selected at $10^{-16} \text{ Pasec}/\text{m}^3$.

3.3. Final simulation parameters

All parameters and values used in the simulations are shown in the tables below.

System

Parameter name	Value [Unit]	Description
f	0.1 – 10 [Hz]	Frequency
A	0.0025 [m]	Amplitude
$P_r = P_2$	280 [bar]	Pre-charge pressure ring chamber
$P_p = P_1$	142.8 [bar]	Pre-charge pressure piston chamber
P_t	0.1 [bar]	Tank pressure

Table 3-1: System parameter values

Cylinder

Parameter name	Value [Unit]	Description
D_p	0.04 [m]	Piston diameter
D_r	0.028 [m]	Ring diameter
K_{leak}	$1e - 16$ [Pasec/ m^3]	Leakage coefficient
$X_{p,max}$	0.4 [m]	Maximum piston stroke

Table 3-2: Hydraulic cylinder parameter values

Load

Parameter name	Value [Unit]	Description
M_l	1000 [kg]	Load mass
B_l	1000 [Nsec/m]	Load damping coefficient

Table 3-3: Load parameter values

Motor

Parameter name	Value [Unit]	Description
J_a	$45e - 4$ [kgm ²]	Armature inertia
R_a	0.013 [Ohm]	Armature resistance
L_a	$0.1e - 3$ [H]	Armature inductance
k_t	0.15 [Nm/A]	Torque constant
k_b	0.15 [Vsec/rad]	Speed constant
η_m	0.90	Motor efficiency
B_m	0.001 [Nmsec/rad]	Motor damping coefficient

Table 3-4: Electric motor parameter value

Pump

Parameter name	Value [Unit]	Description
RPM_{nom}	3150,5600 [rpm]	Nominal pump speed
RPM_m	130f, 260f [rpm]	Pump speed
V_g	5,10 [cm ³ /rev]	Pump displacement
J_p	$0.6e - 4, 4e - 4$ [kgm ²]	Pump inertia
K_p	0.63,0.92 [kNm/rad]	Pump rotary stiffness

Table 3-5: Hydraulic pump parameter value

Servo valve

Parameter name	Value [Unit]	Description
C_d	0.611	Discharge coefficient
D_{servo}	0.0053 [m]	Servo valve maximum opening

Table 3-6: Servo valve parameter value

Control volume

Parameter name	Value [Unit]	Description
D_m	0.0179 [m]	Control volume diameter
L_m	0.004 [m]	Control volume length
ρ_m	7500 [kg/m ³]	Control volume density
M_m	0.0754 [kg]	Control volume mass
R_p	0.00625 [m]	Pinion pitch radius

Table 3-7: Control volume parameter value

Oil

Parameter name	Value [Unit]	Description
ρ_o	857.2 [kg/m^3]	Oil density
ν	31.81e - 6 [m^2/sec]	Oil kinematic viscosity
β_e	1.44756e9 [Pa]	Oil bulk modulus

Table 3-8: Hydraulic oil parameter value

4. Results

4.1. Model Description

In this chapter the results of two sets of simulations are being presented. All the simulations were implemented on Matlab and specifically, Simulink and Simscape.

The first set features two models of a hydraulic servo system, consisting of a servo valve and a hydraulic cylinder connected to a mass. The first model (simple) was created using Simscape by connecting the appropriate hydraulic blocks, while the second model (full) derives from the system analysis and is using the function blocks provided. A major difference between these two models is that in the Simscape model, the effect of oil inertia and friction inside the cylinder chambers isn't simulated. So, the aim of this set is to investigate the effect of oil inertia and friction on system response. The Simulink models of the two systems are presented below.

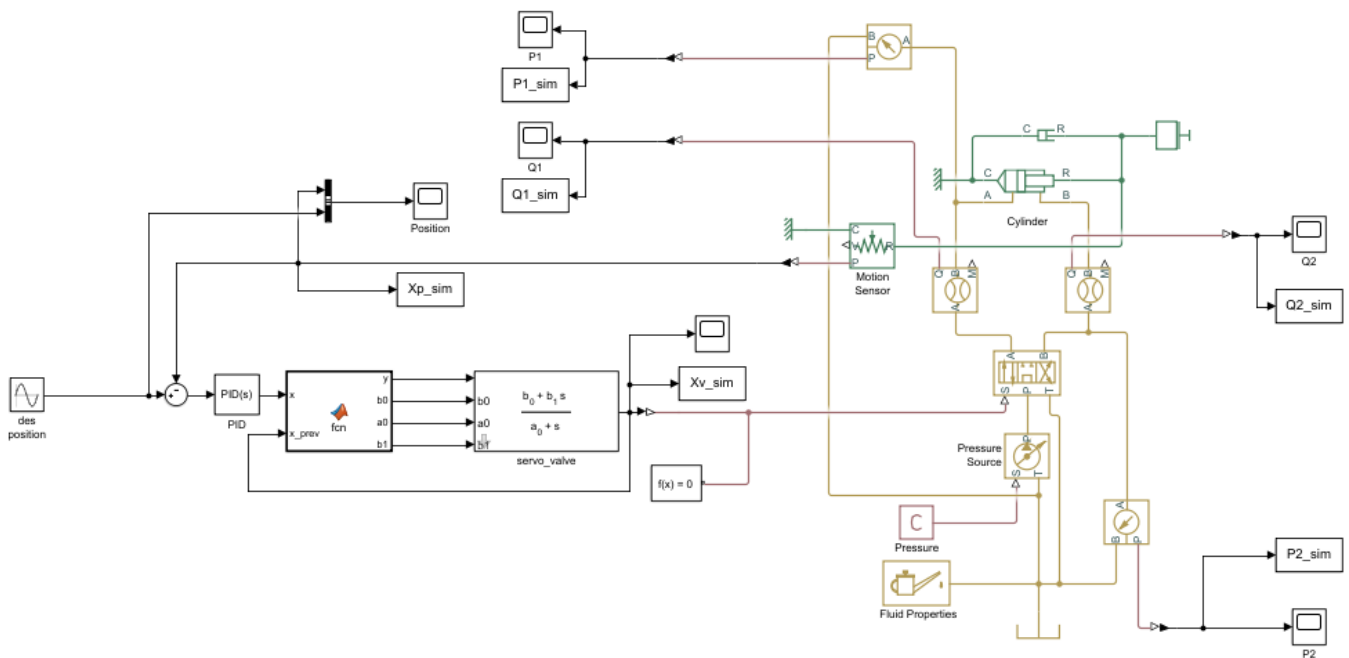


Figure 4-1: Simple system Simulink model

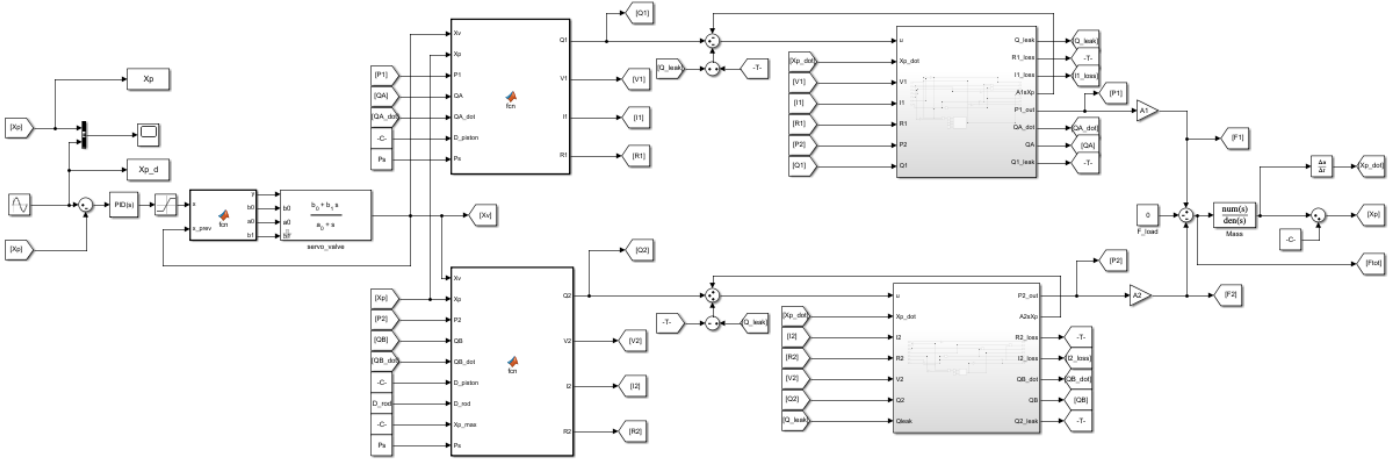


Figure 4-2: Full system Simulink model

The second set, which is the main objective of this thesis, compares a hydraulic servo system to the active system, which was presented in a previous chapter. The servo system model is implemented through Simscape hydro-mechanical blocks while for the active system model, the Matlab function blocks are used. The goal of this set is to compare the energy required for the two systems to achieve the same trajectory in a range of frequencies, as well as other parameters. The Simulink models of the two systems are presented below.

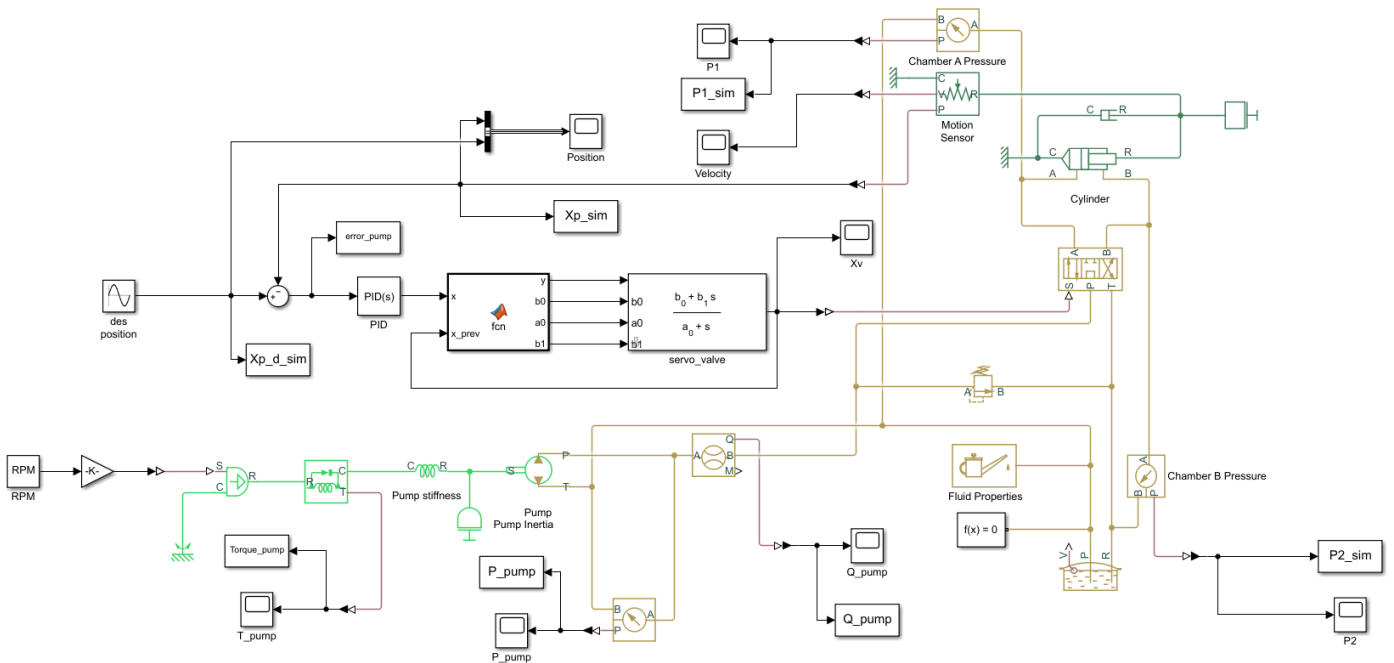


Figure 4-3: Hydro-mechanical servo system model

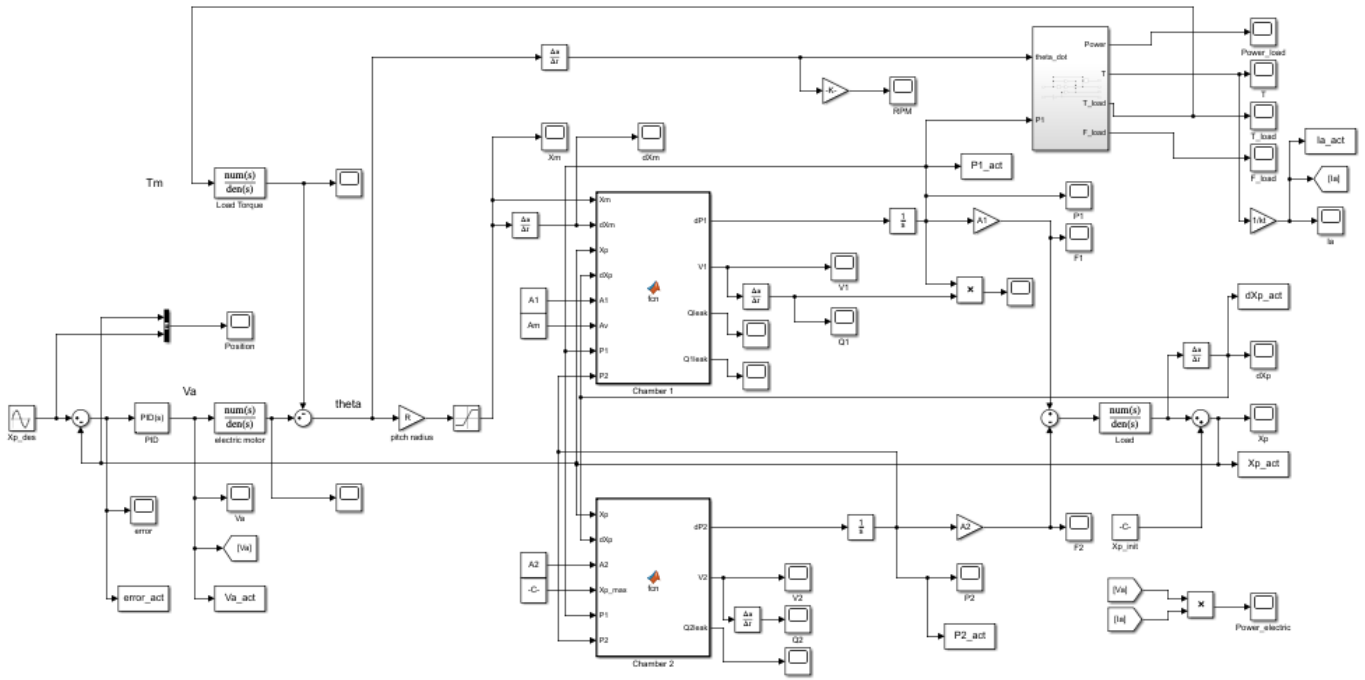


Figure 4-4: Active system model

4.2. Effect of hydraulic losses on the system

Based on the hydro-mechanical servo system analysis in chapter 2.2, a Simulink model of the complete hydraulic servo system was created in order to simulate the piston stroke. In addition, it is possible with Simulink, through Simscape, to simulate various physical models, including hydraulic systems, although some parameters such as fluid inertia and friction in a varying volume are not calculated. In order to determine the extent of which those parameters affect the system, a comparison between the two models was made.

For this comparison a sinusoidal trajectory for the piston was selected with a frequency of 1Hz and an amplitude of 0.05m. For both models a constant pressure supply of 280bar was considered while the remaining values are the same as stated in chapter 3.3. The results from the simulations are presented below.

For both models the piston position is almost the same although the trajectory of the model that has inertia and friction implemented (full model) seems less smooth especially when the piston reaches its extreme positions.

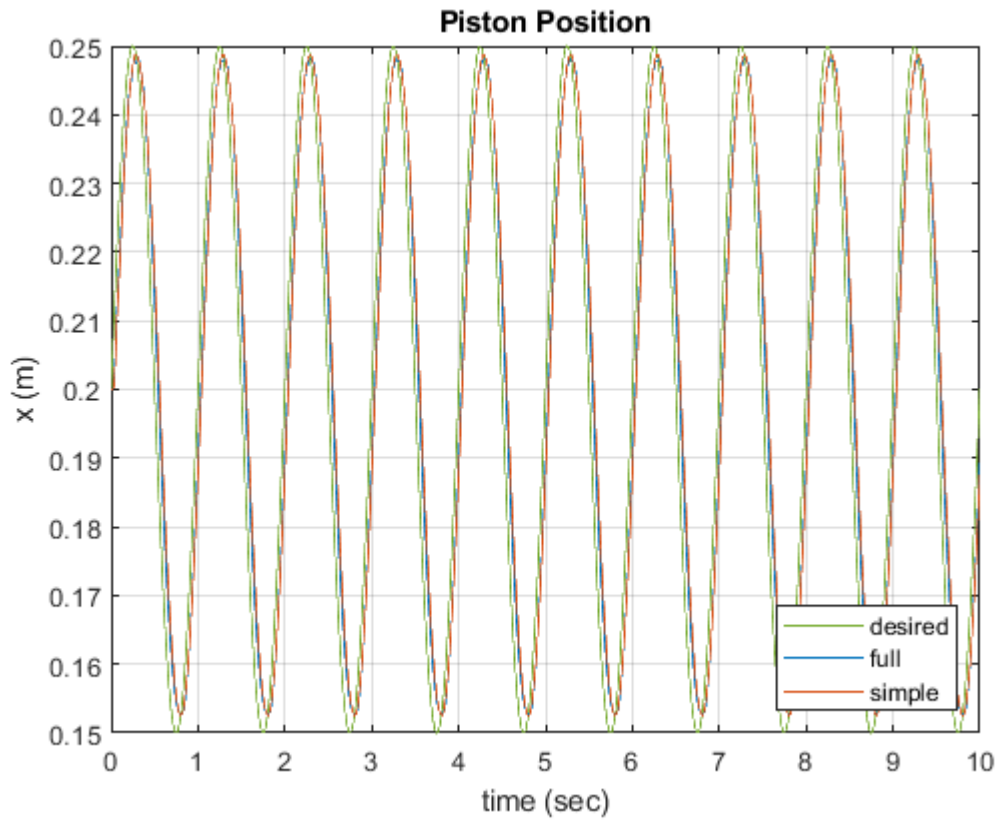


Figure 4-5: Time – Piston position diagram

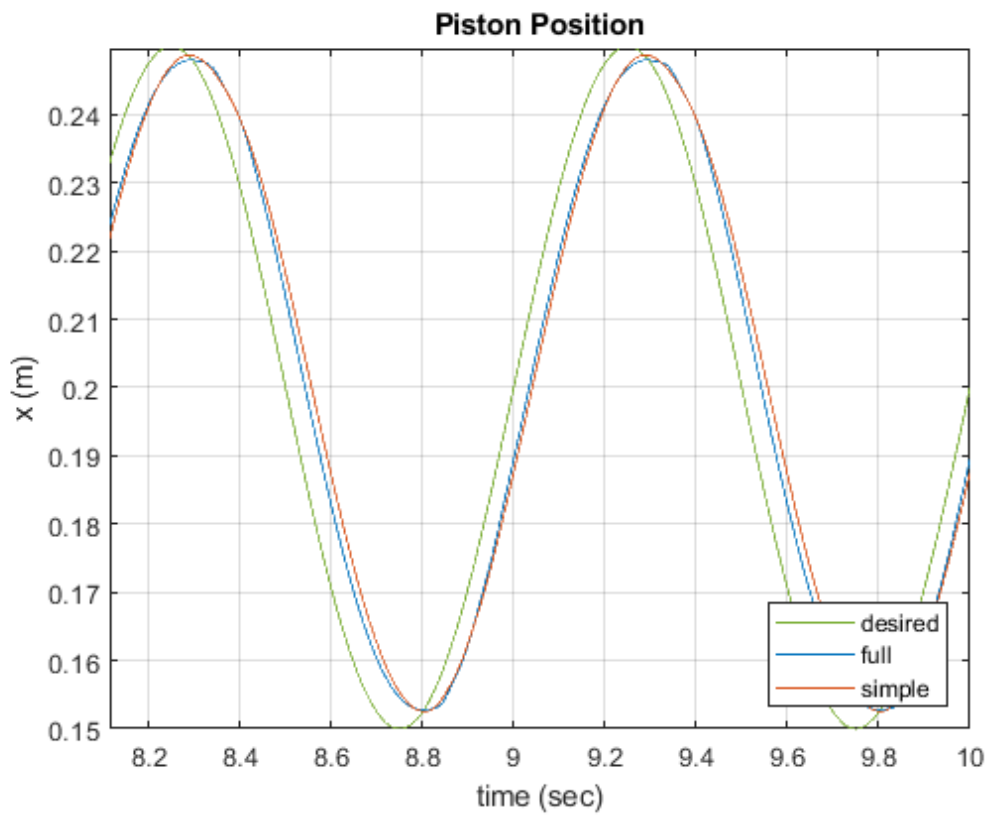


Figure 4-6: Time – Piston position diagram (detail)

In the figure below, it can be seen that the power of the hydraulic fluid in both models is again identical, with the full model having a little higher power.

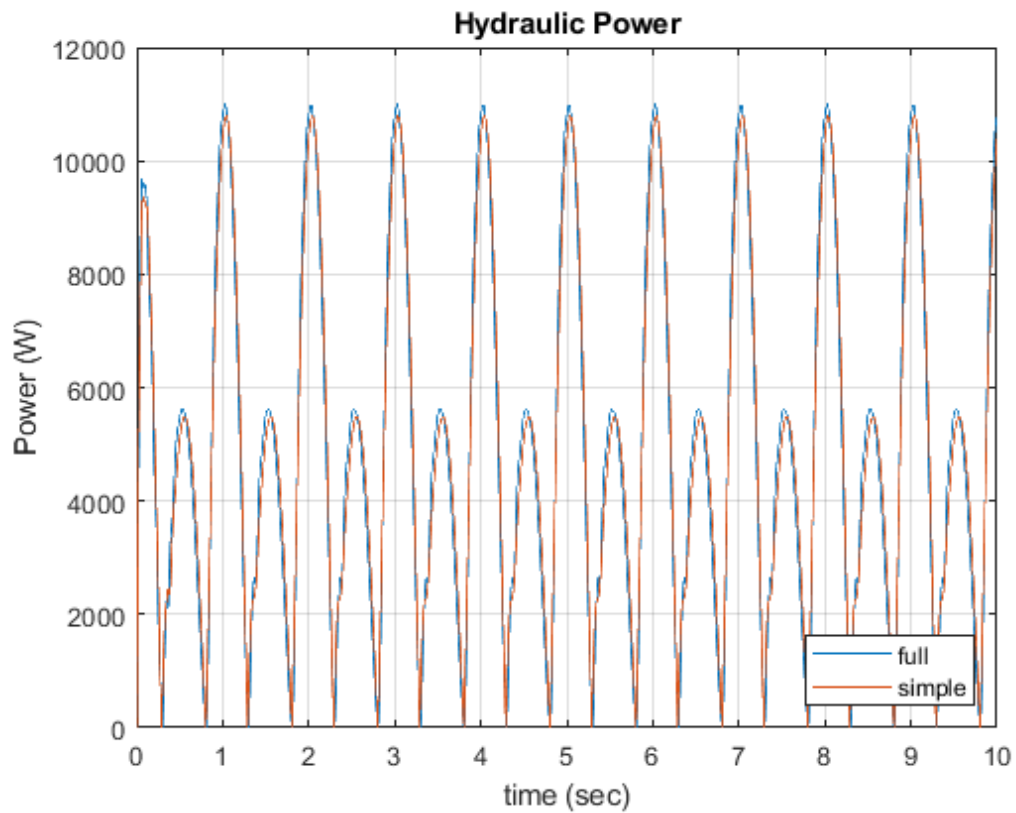


Figure 4-7: Time – Hydraulic power diagram

The pressure inside each cylinder chamber is shown below. In both cases the pressure of the two models are very close, but in the full model some oscillations appear during the piston extension, as well as, some spikes in pressure during the piston retraction probably due to the fluid inertia.

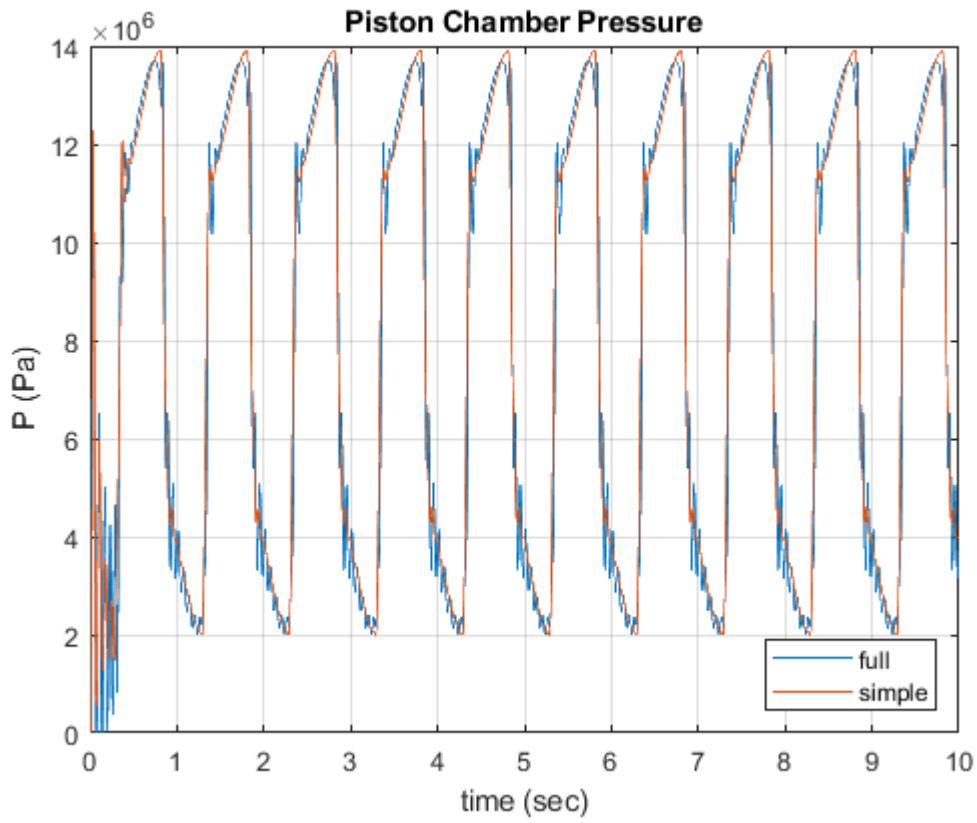


Figure 4-8: Time – Piston chamber pressure diagram

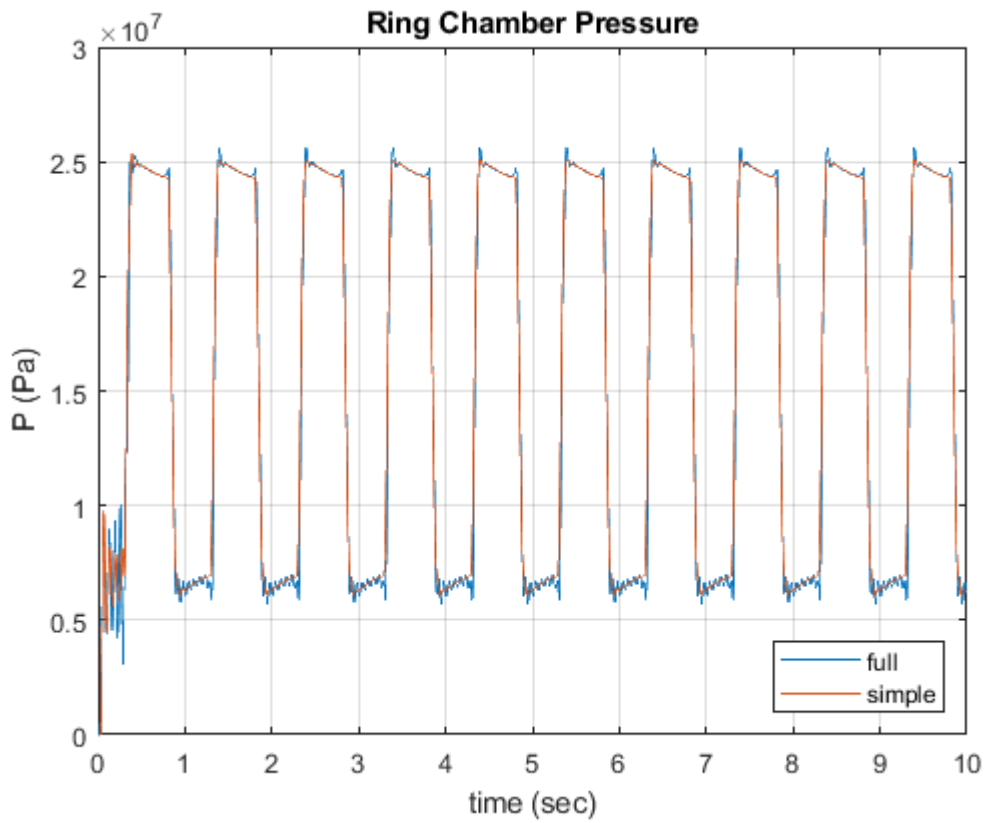


Figure 4-9: Time – Ring chamber pressure diagram

In the four diagrams below, the inertia and friction losses are shown. First of all, the inertia losses diagrams have oscillations which is expected since the desired piston stroke has a constantly varying acceleration and fluid inertia is affected by acceleration. Also, the inertia losses are about ten times higher than the friction losses but are still very small compared to the minimum pressure that is developed inside the piston chamber. All and all, the losses due to inertia and friction are very small and can be neglected without affecting the final results.

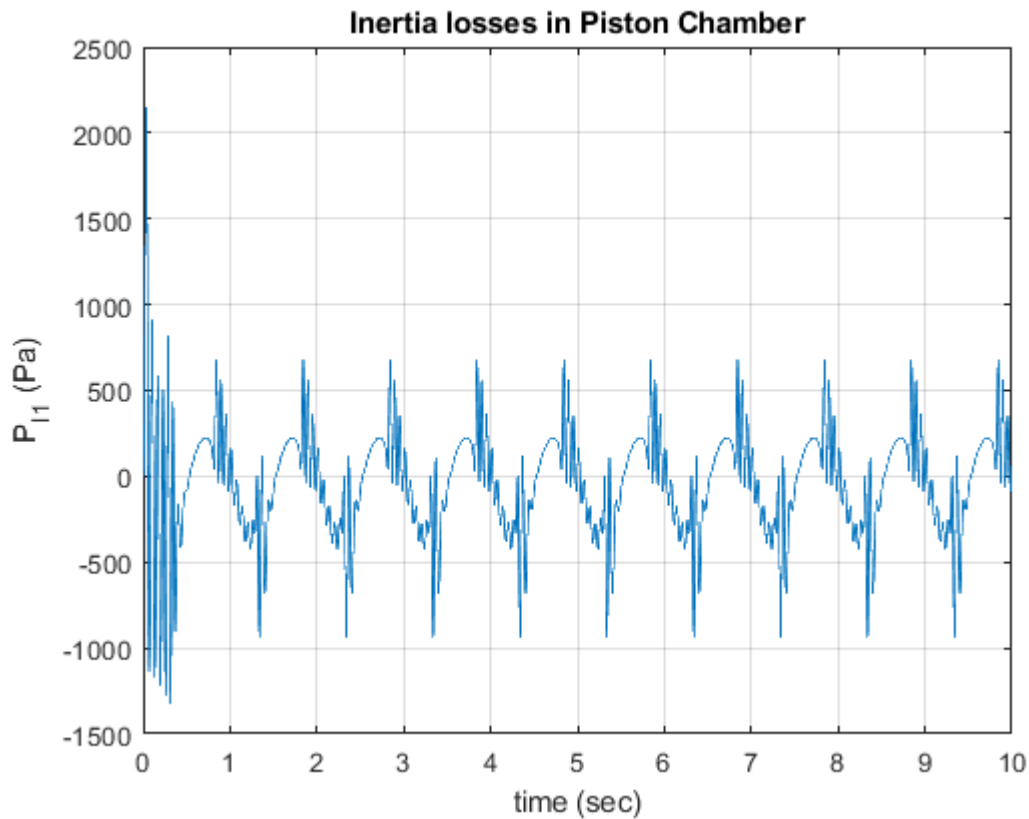


Figure 4-10: Time – Inertia losses in piston chamber diagram

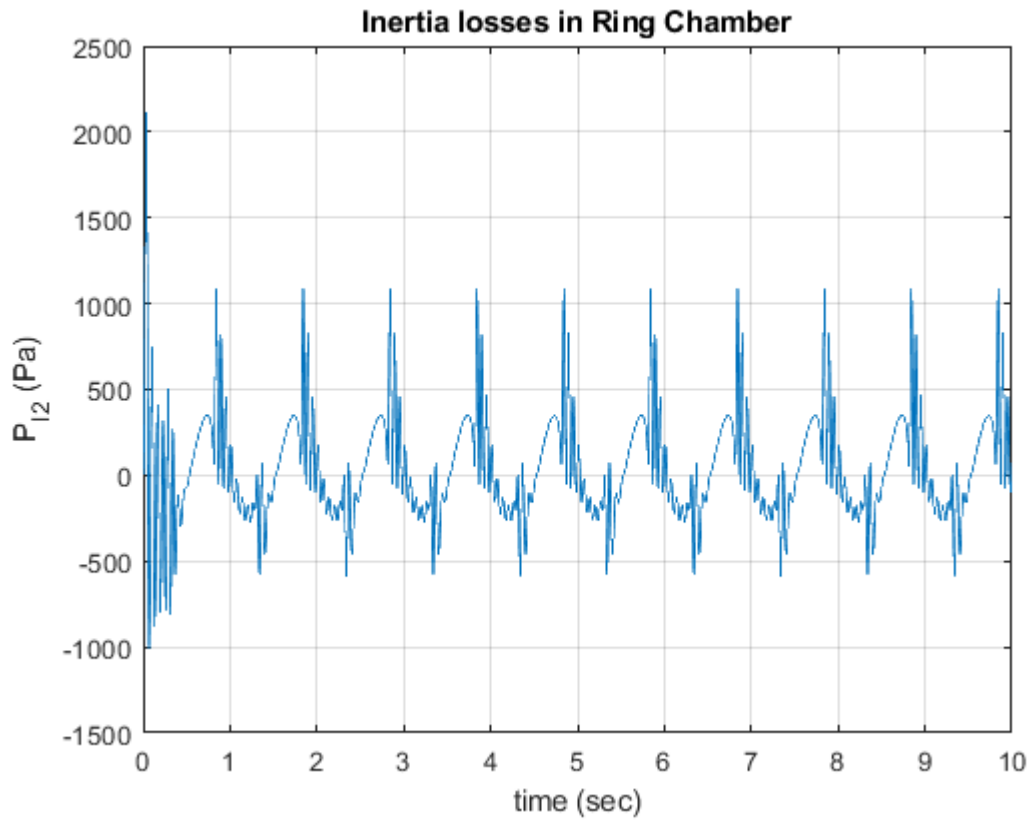


Figure 4-11: Time – Inertia losses in ring chamber diagram

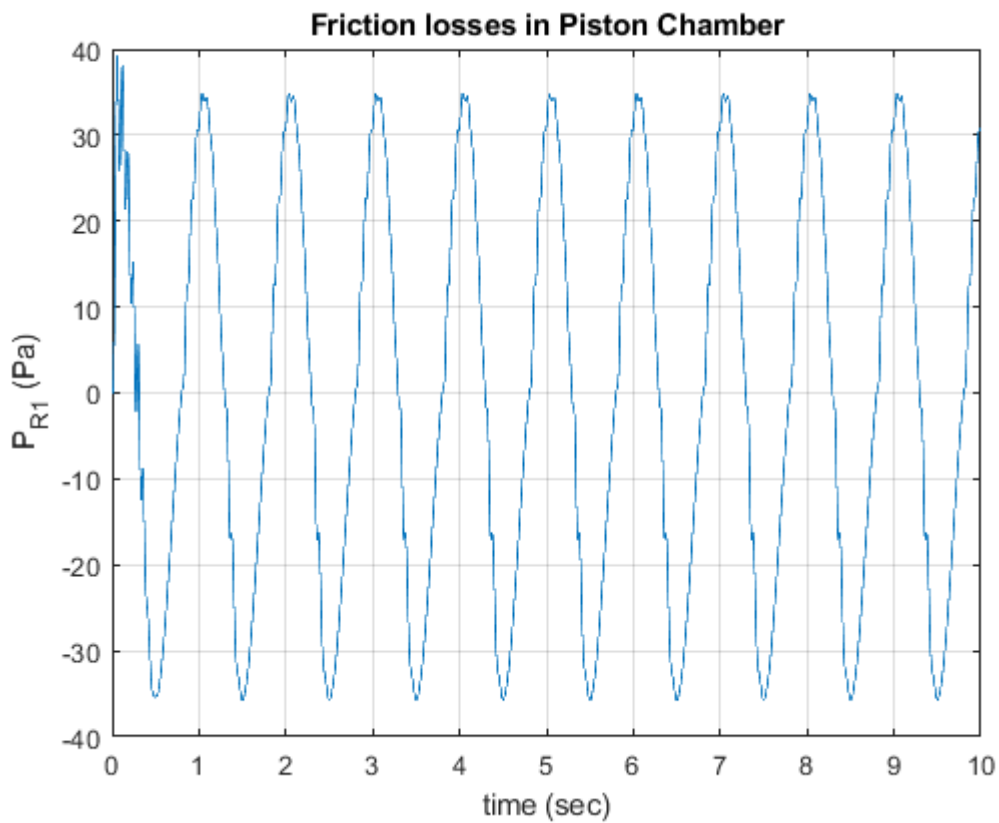


Figure 4-12: Time – Friction losses in piston chamber diagram

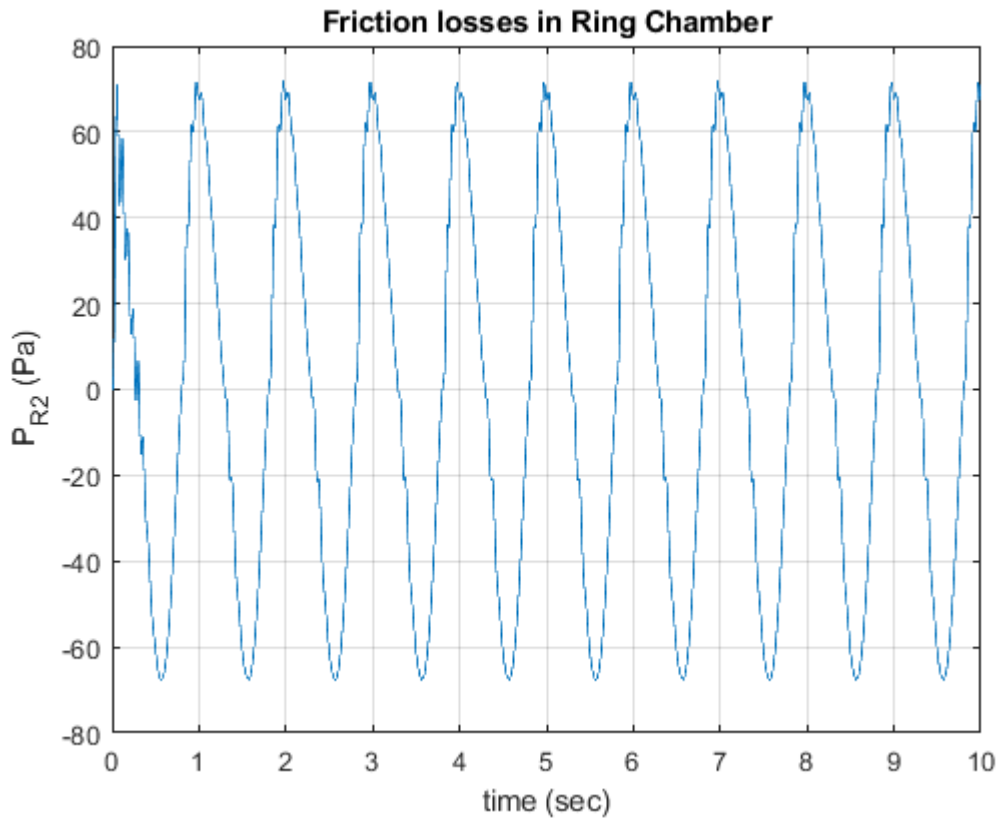


Figure 4-13: Time –Friction losses in ring chamber diagram

In addition to the above, another comparison of the two aforementioned models was done, this time with 0.0025m amplitude, which is the same as in the final simulation of the active system, so that to examine the effect of amplitude in hydraulic losses. It was observed that both models where unstable and could not be controlled simply with a proportional gain and so, a PID controller was used.

Again, it is observed that the results are very close for the two models. An important thing to notice is that both inertia and friction losses decrease as the amplitude decreased, which is expected since both the acceleration and velocity of the piston are lower. More specifically, it can be seen that decreasing the amplitude by twenty times causes the same decrease in both inertia and friction losses.

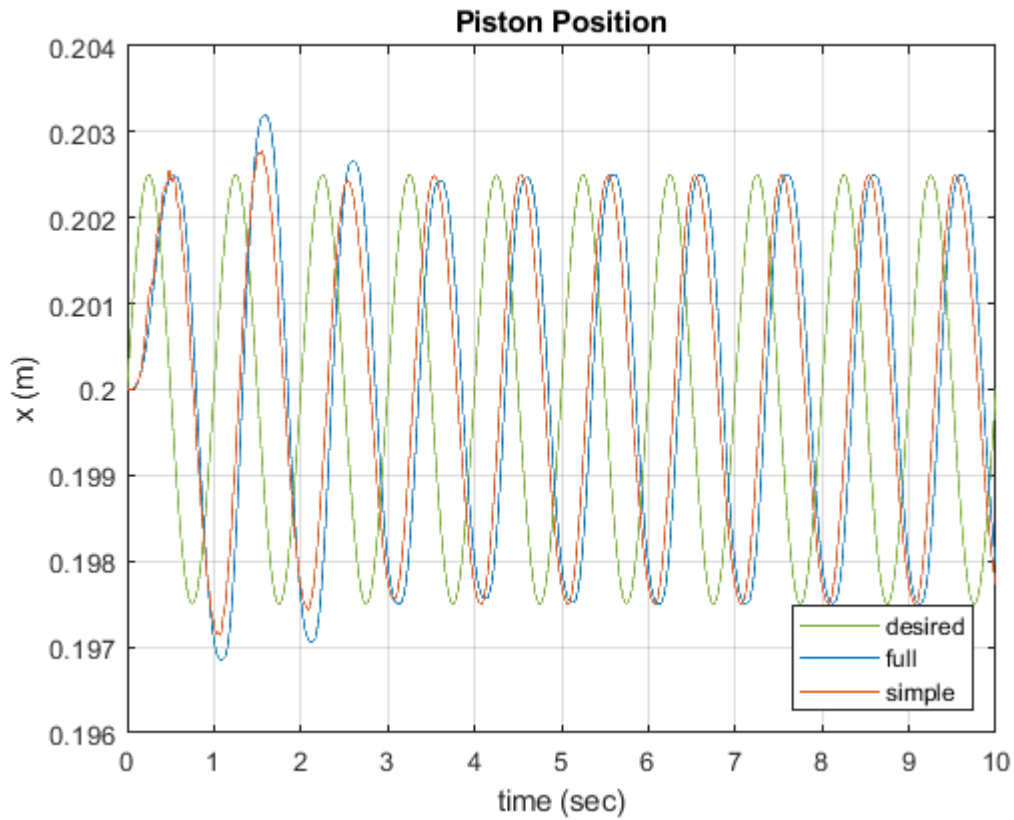


Figure 4-14: Time – Piston position diagram

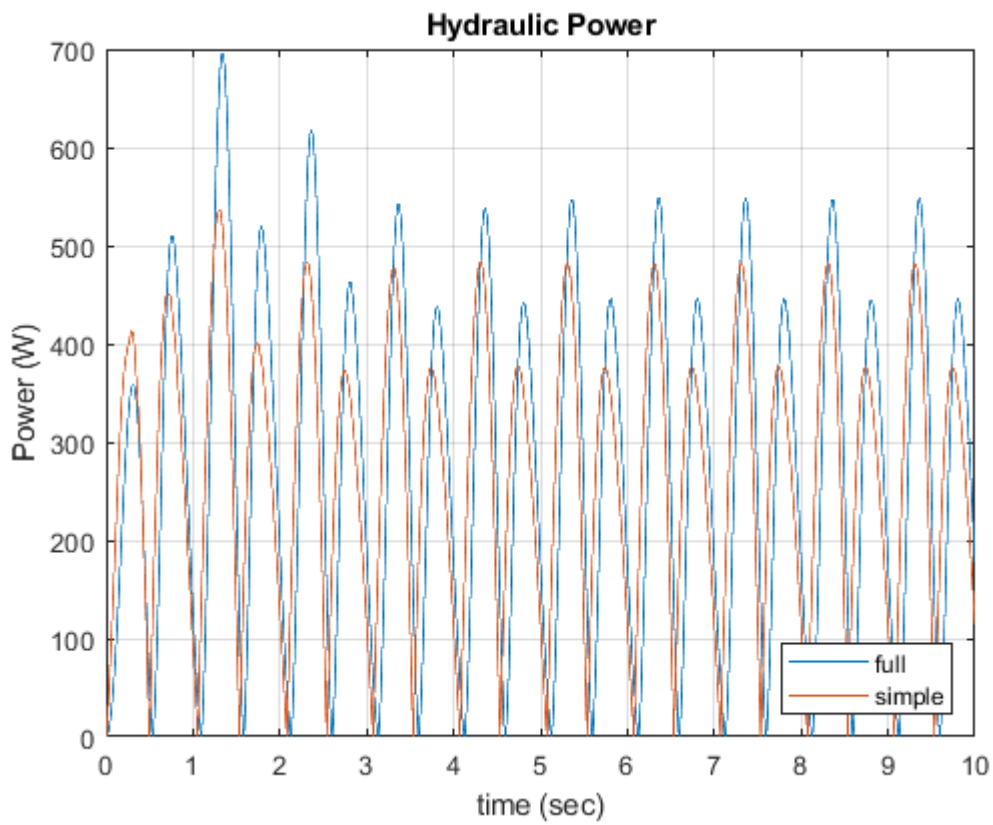


Figure 4-15: Time –Hydraulic power diagram

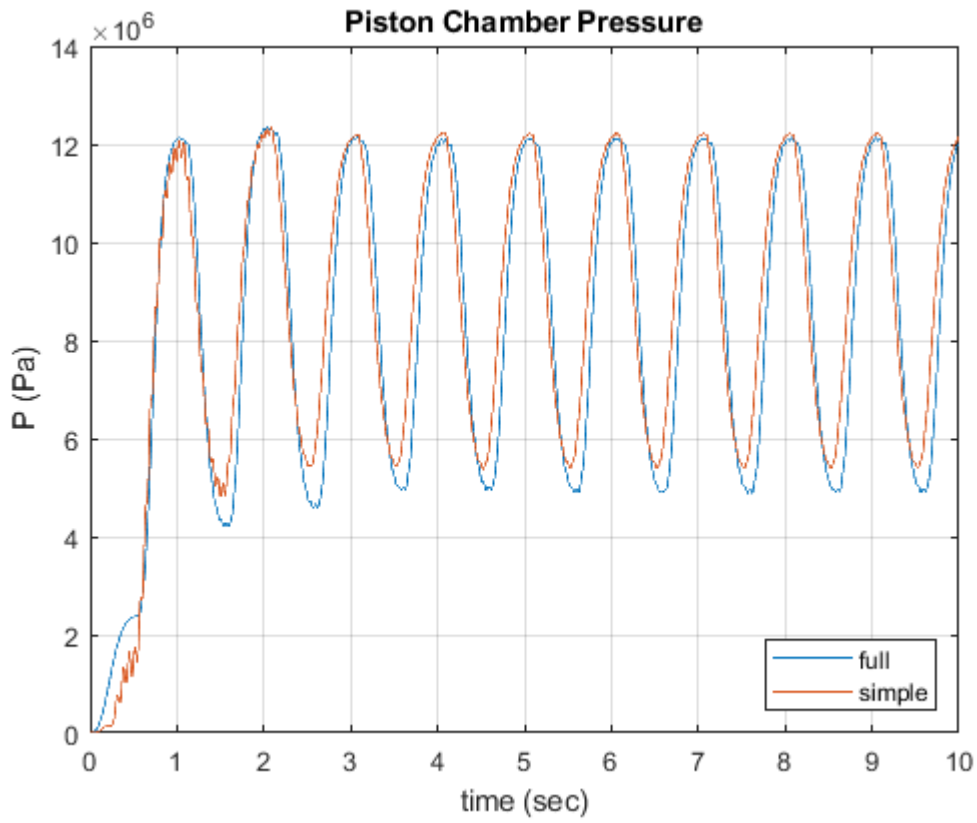


Figure 4-16: Time – Piston chamber pressure diagram

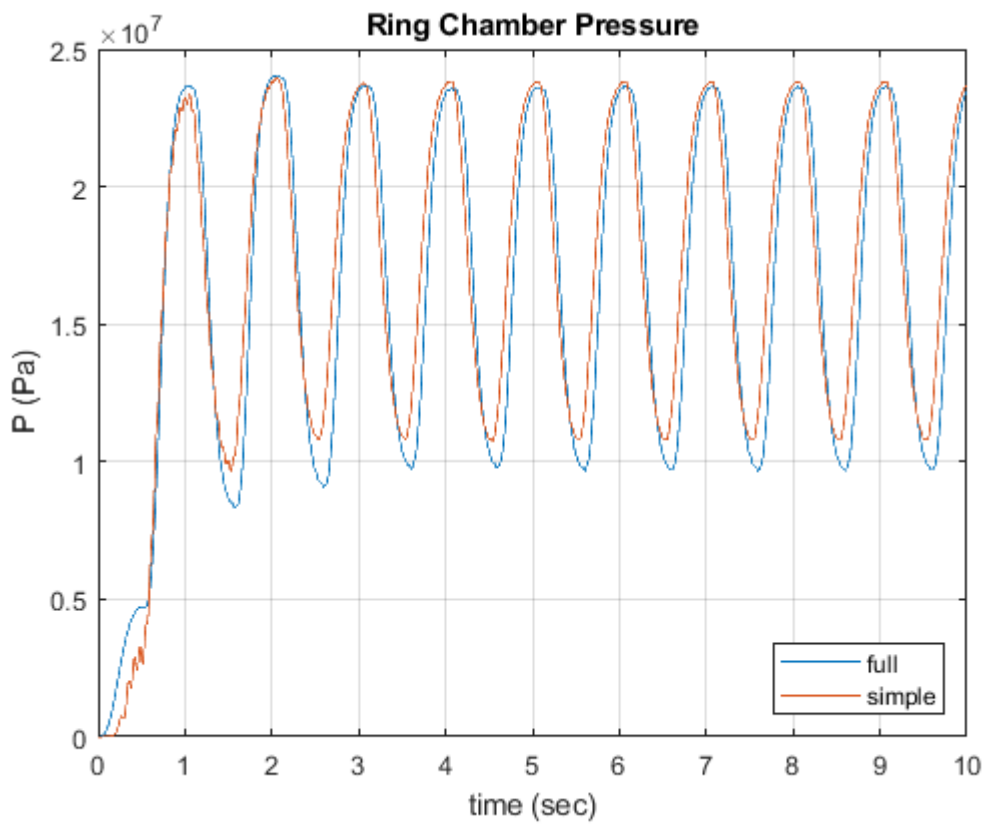


Figure 4-17: Time – Ring chamber pressure diagram

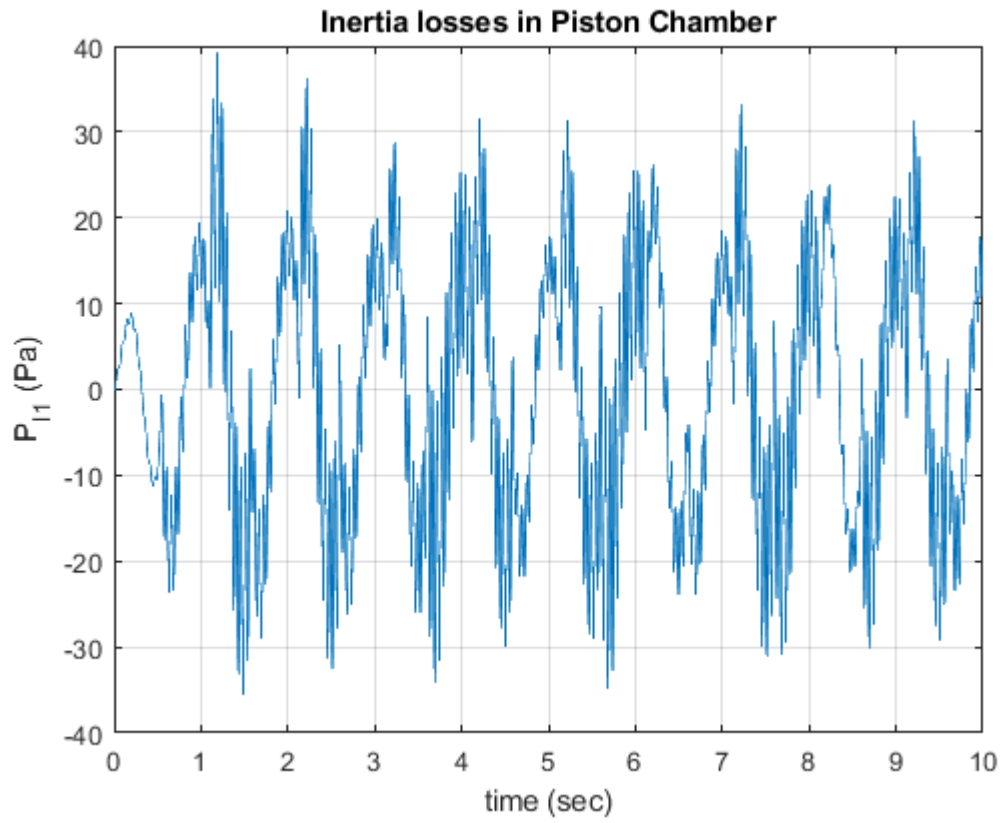


Figure 4-18: Time – Inertia losses in piston chamber diagram

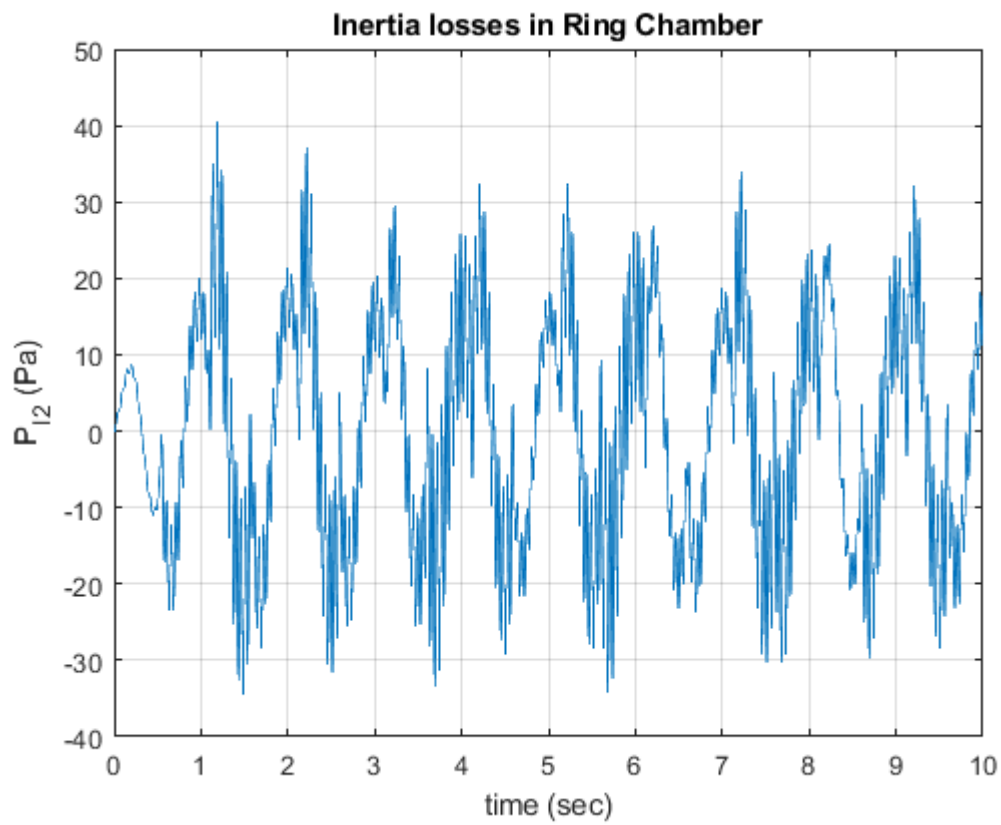


Figure 4-19: Time – Inertia losses in ring chamber diagram

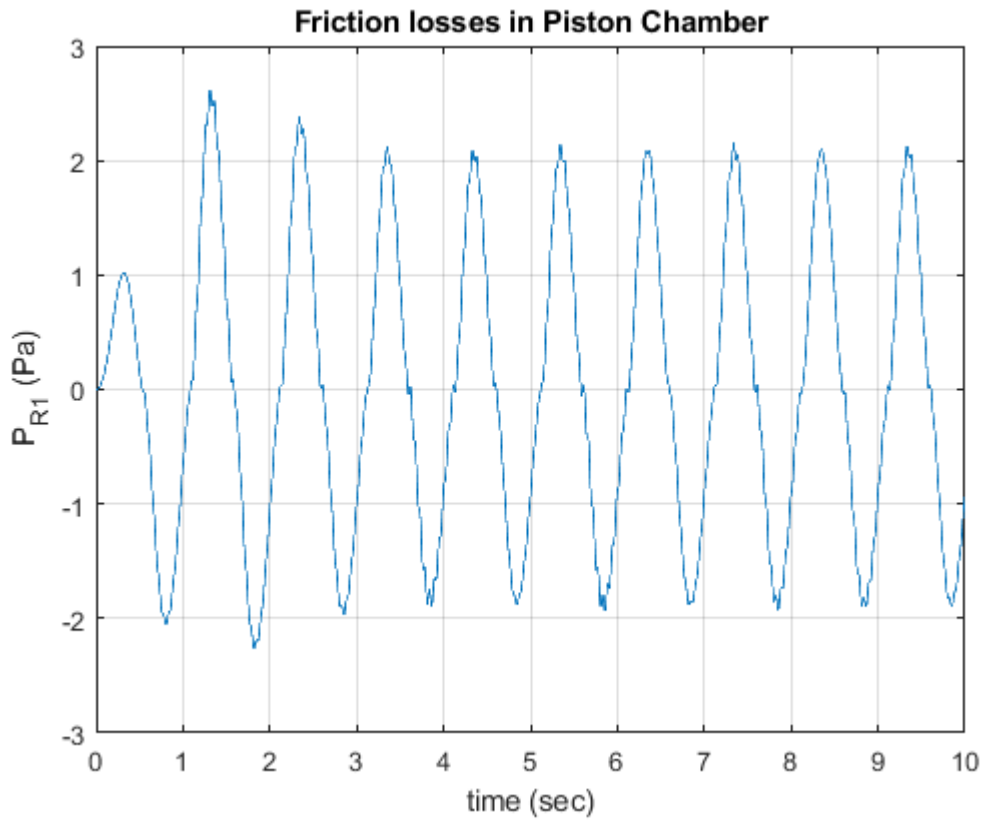


Figure 4-20: Time – Friction losses in piston chamber diagram

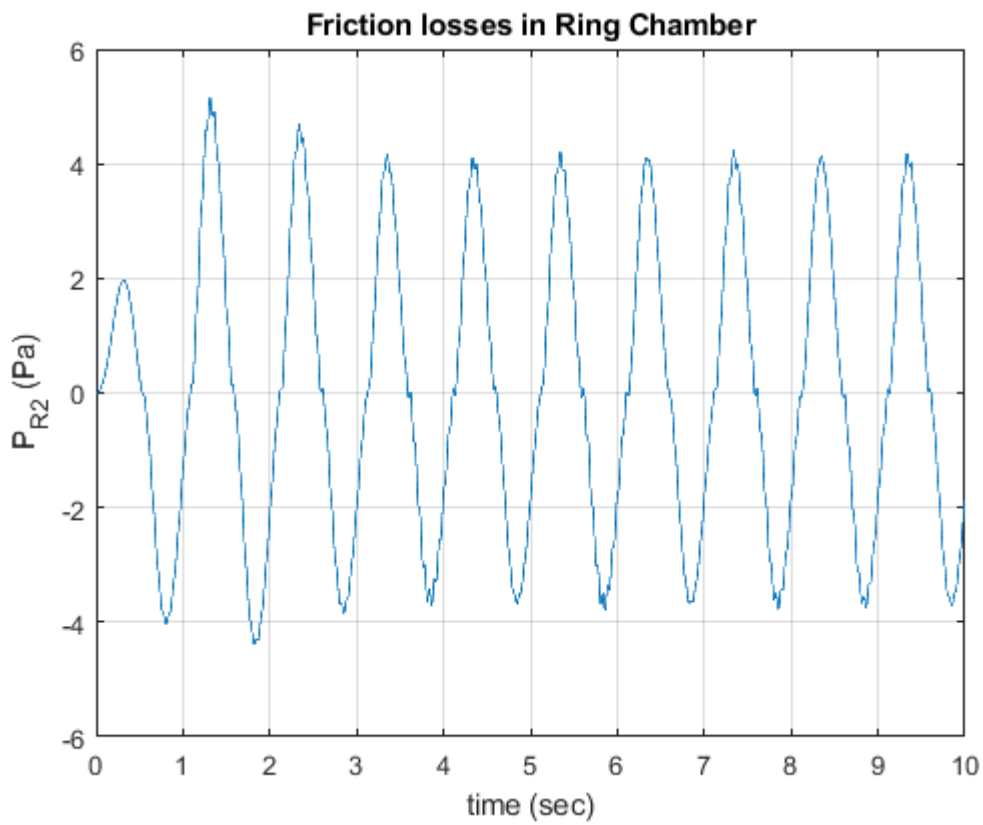


Figure 4-21: Time – Friction losses in ring chamber diagram

In addition to the above, another simulation of the full model was run at the same amplitude as the second simulation, but at a frequency of 10Hz. This was done to investigate the effect of frequency on hydraulic losses. It can be seen, in the figures below, that although the amplitude is the same, both inertia and friction losses have increased. Specifically, increasing the frequency of the system by ten times, increased the friction losses by almost the same amount. On the other hand, the inertia losses have increased by almost eighty times. This indicates that the inertia of the hydraulic fluid is affected intensively by the system frequency, as expected. Also, it is worth mentioning that the inertia losses of the final simulation are higher than those of the first, of amplitude 0.05m and frequency 1Hz. This means that although the amplitude decreased by twenty times, a ten times increase in frequency produces more inertia losses.

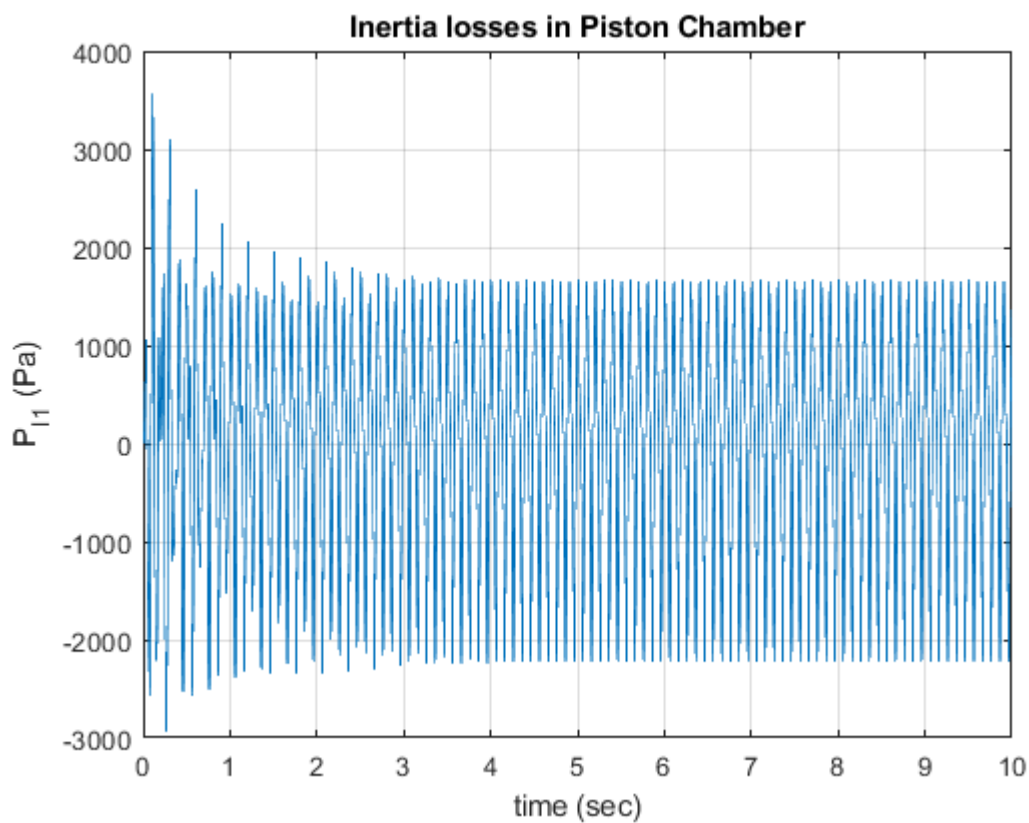


Figure 4-22: Time – Inertia losses in piston chamber diagram

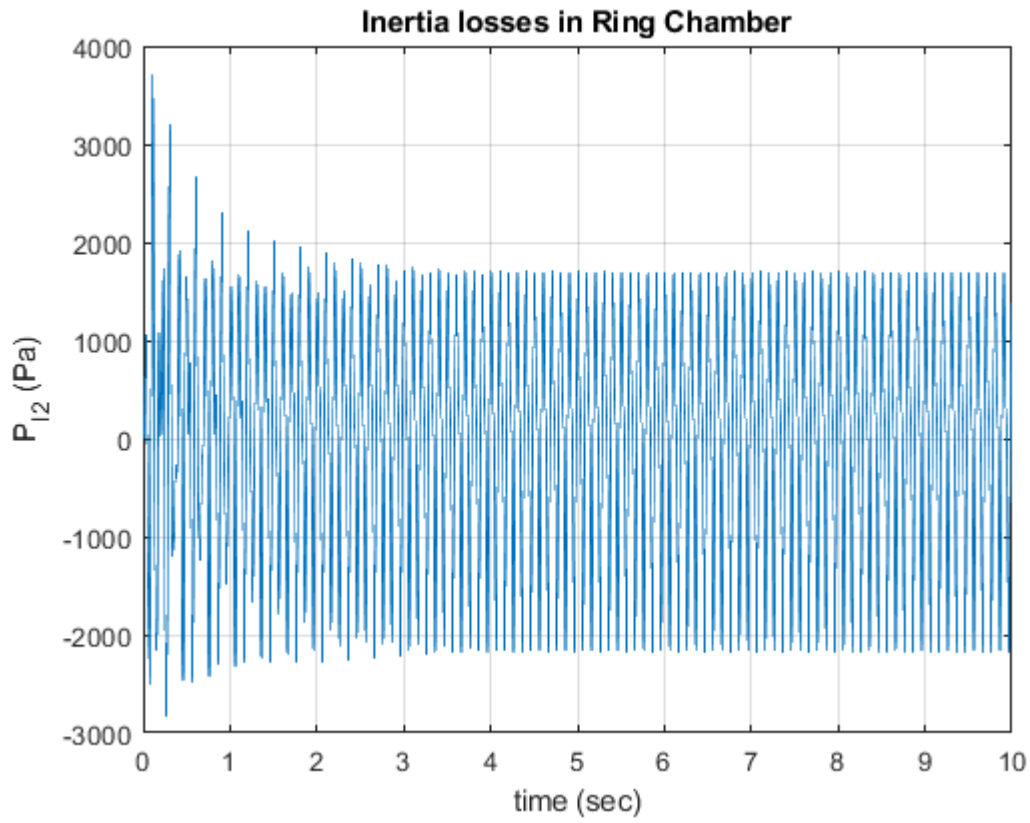


Figure 4-23: Time – Inertia losses in ring chamber diagram

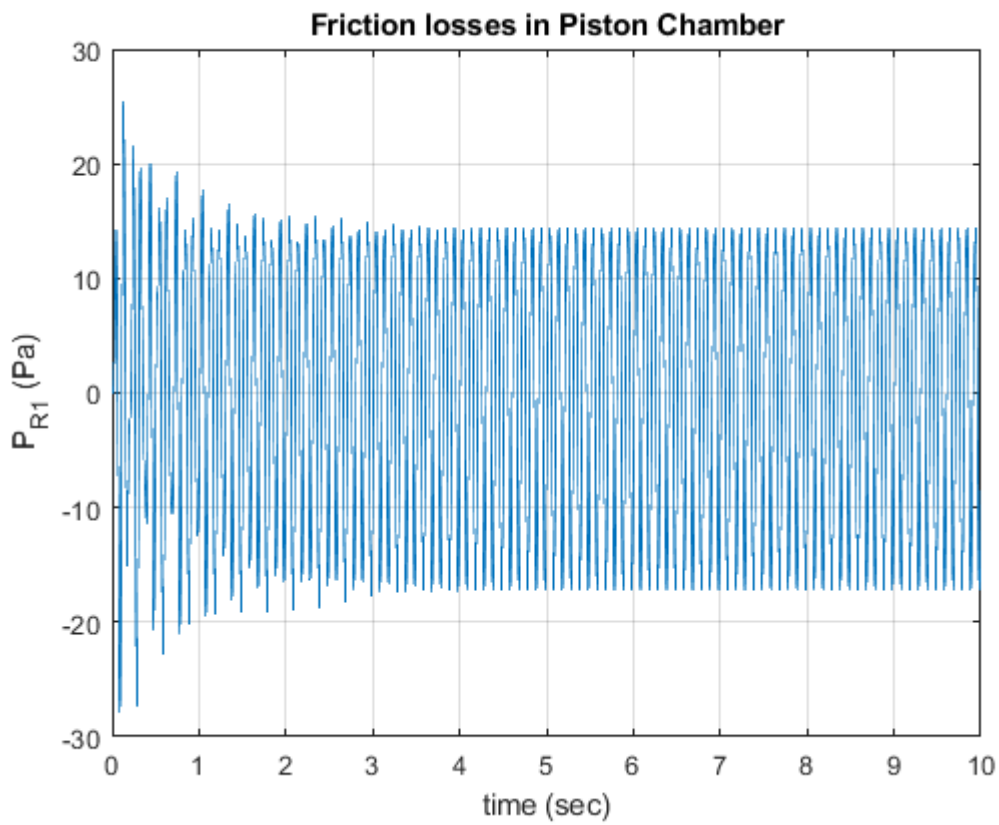


Figure 4-24: Time – Friction losses in piston chamber diagram

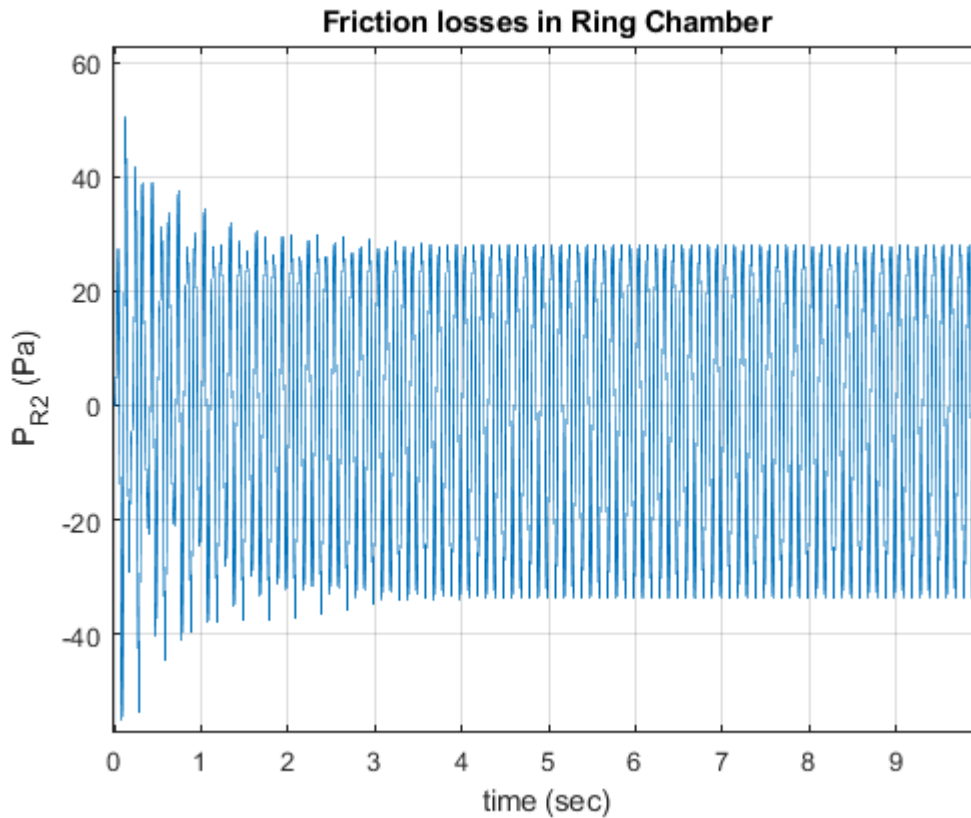


Figure 4-25: Time – Friction losses in ring chamber diagram

To conclude, both amplitude and frequency affect the hydraulic losses of the system, although the frequency of the system has a bigger impact at inertia losses. Also, the friction seems to have the least impact on the total pressure losses of the system. Even so, the maximum value of inertia losses is still very small compared to the pressure developed inside the cylinder chambers and so, both friction and inertia losses can be neglected without having much error in the results.

In the table below, the mean absolute value of the inertia and friction pressure losses are presented for each simulation.

Hydraulic Pressure Losses (Pa)				
Simulation	R1	R2	I1	I2
A = 0.05m / f = 1Hz	20.71	40.42	238.92	235.62
A = 0.0025m / f = 1Hz	1.1	2.15	12.93	12.95
A = 0.0025m / f = 10Hz	10.64	20.84	1010.43	1009.07

Table 4-1: Mean absolute values of the Pressure Losses

4.3. Hydraulic – Active system comparison

4.3.1. Main results

The comparison of the two systems was made by simulating them for various values of stroke frequency with constant amplitude. The frequencies that were used in the simulations range from 0.1 to 10Hz. The comparison variables that were selected are the power needed for each system, the mean pressure developed in each chamber of the hydraulic cylinder, the absolute position error and the percent position error. Also, a PID controller was used for the proper control of the two systems.

The main goal of this analysis is to examine whether there is a significant difference in power consumption between the two systems. For this reason, the two models must follow the same trajectories, otherwise the results would not be valid. For example, if the stroke for the active system with the control volume had a greater amplitude than the servo valve system, then a comparison between those two systems would be wrong. Based on the above, the PID controllers for both systems were tuned so that they are as fast as possible but without them being unstable and so that the amplitude of the piston stroke doesn't exceed the desired amplitude.

The figures below present the mean power needed for the electric motor for the active system, the mean mechanical power needed for the pump for the servo valve system and, as well as, the mean hydraulic power of the hydraulic oil. First of all, it can be seen that, for low frequencies, the active system has an almost constant minimum value for the power consumption. This is logical since the oil inside the cylinder chambers is pre-charged and so, a minimum power is needed in order for the electric motor to overcome this pressure.

By comparing the power consumption of the electric motor with the mechanical power for the two different size pumps, it can be deduced that the power consumption of the active system is greater for frequencies below 0.8Hz as shown clearly in figure (4-27). On the contrary, for frequencies above those values, the power consumption of the servo valve systems is increased drastically, while the smaller pump system has greater power consumption than the bigger pump system (figure 4-26). Additionally, it can be seen that the hydraulic power of the oil for both pump systems is almost the same.

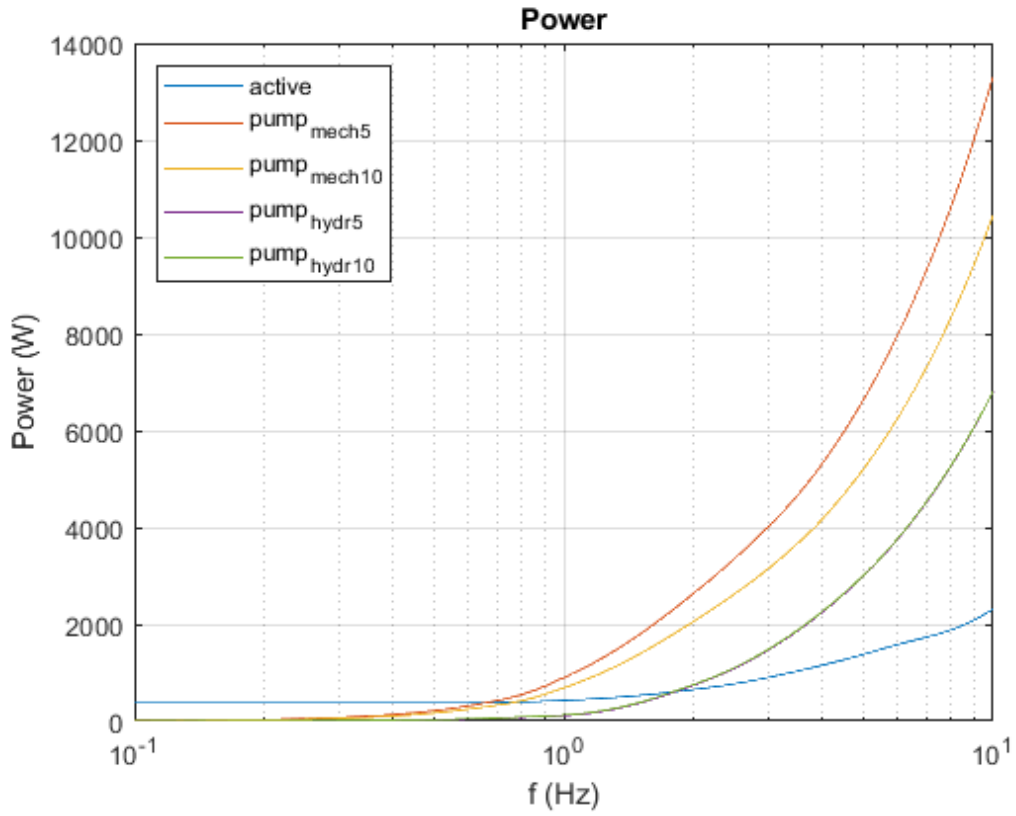


Figure 4-26: Frequency – Power diagram

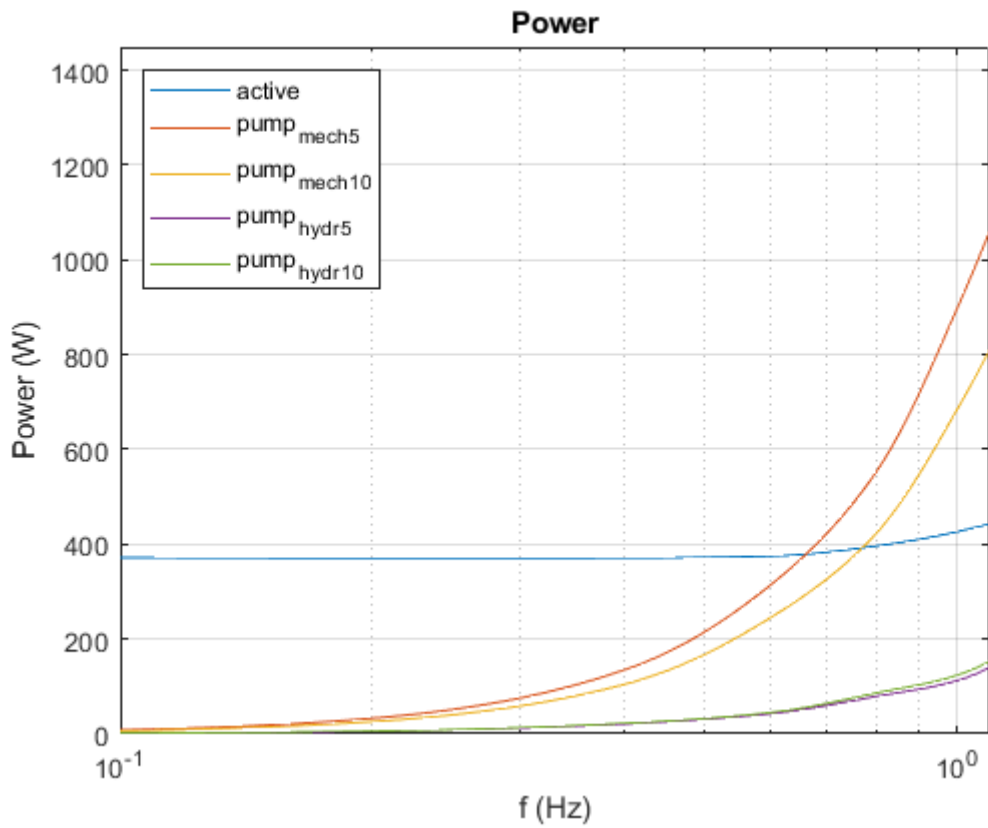


Figure 4-27: Frequency – Power diagram (detail)

In addition to the above, the percent power loss for the servo systems was calculated, using the mechanical and hydraulic power for each system, as shown in the figure below. It can be seen that, that the power loss curve for both systems is similar and that the small pump system has more power losses than the big pump system. Also, for both systems, the power loss increases slightly as the frequency increases up to 1Hz and for frequency above 1Hz, the power loss decreases drastically.

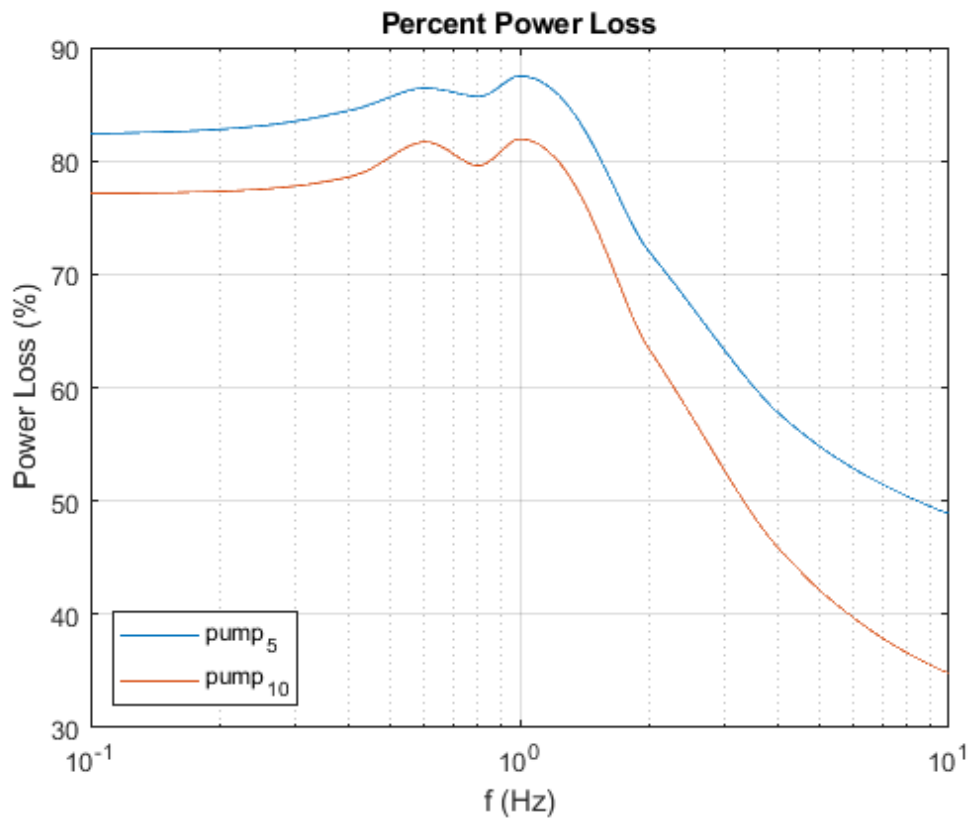


Figure 4-28: Frequency – Percent Power Loss diagram

The mean pressure of both hydraulic cylinder chambers for each system are shown in the diagrams below. The pressure for the active system is almost constant regardless of the frequency and greater than that of the two servo valve systems. On the contrary, the pressure for the servo valve systems is increased as the frequency increases, while having almost the same value except at frequencies ranging from 2 to 8Hz where the bigger pump system has greater mean pressure.

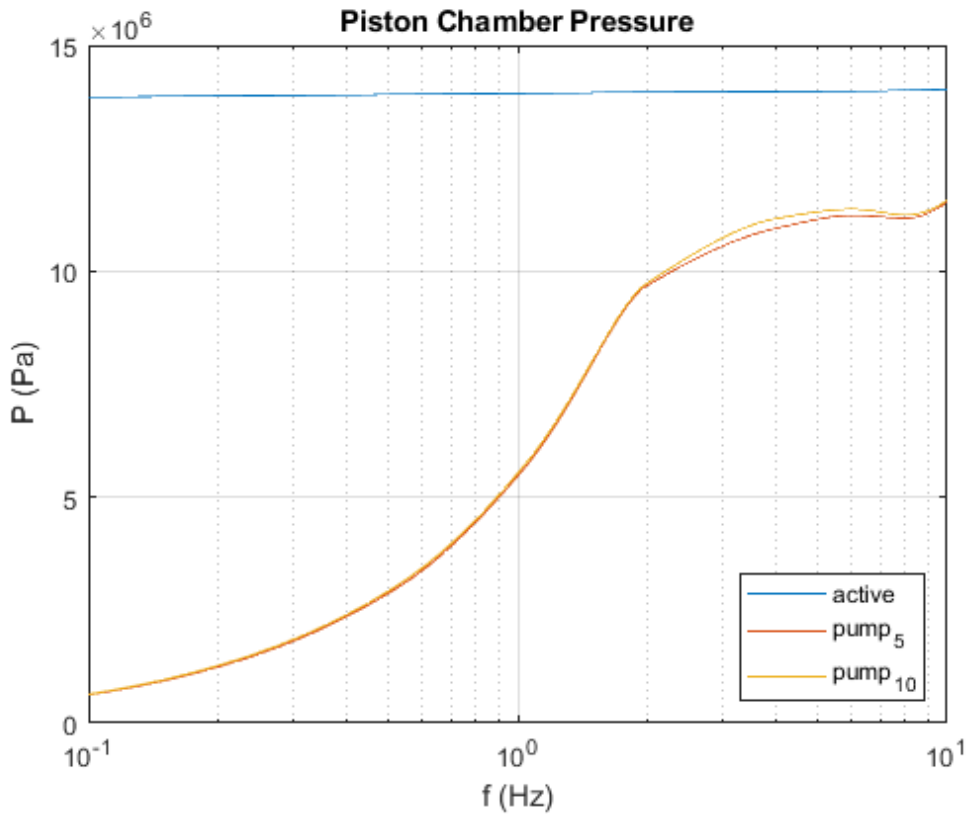


Figure 4-29: Frequency – Piston Chamber Pressure diagram

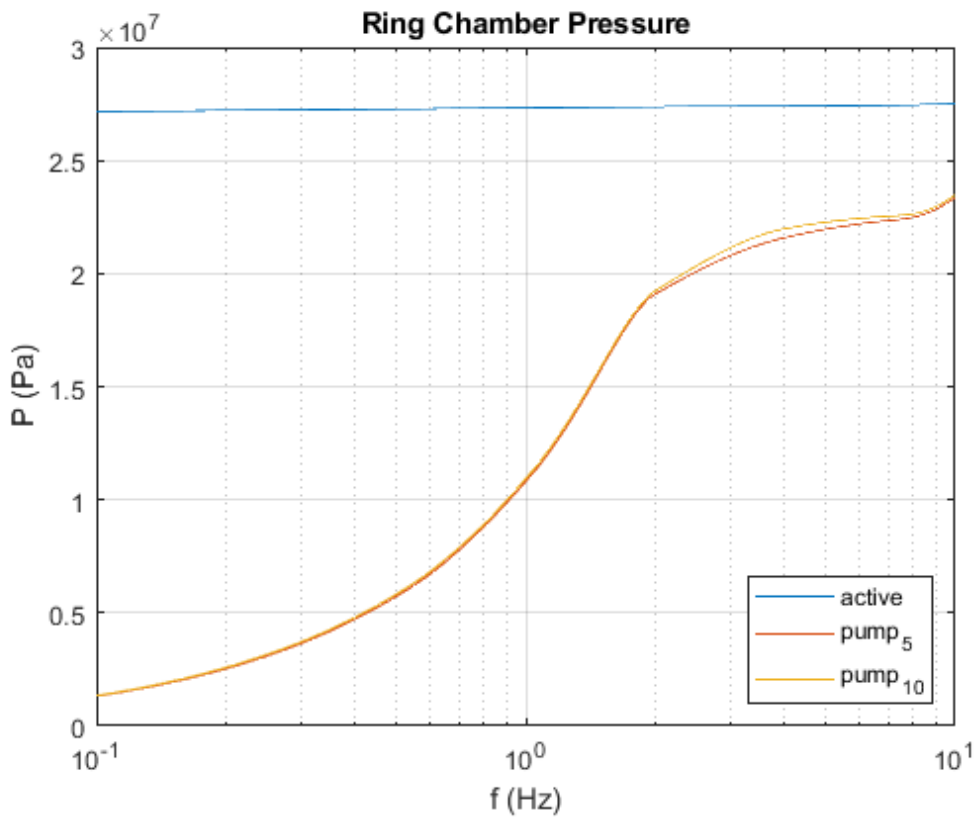


Figure 4-30: Frequency – Ring Chamber Pressure diagram

The mean absolute and percent position error are shown in the figures below. First of all, it can be easily concluded that the position of the active system is smaller than both the servo valve systems. Also, it can be seen that at frequencies above 1Hz the mean position error of the bigger pump system is greater than that of the smaller pump system, while both pump systems have the same mean error for frequencies below 1Hz.

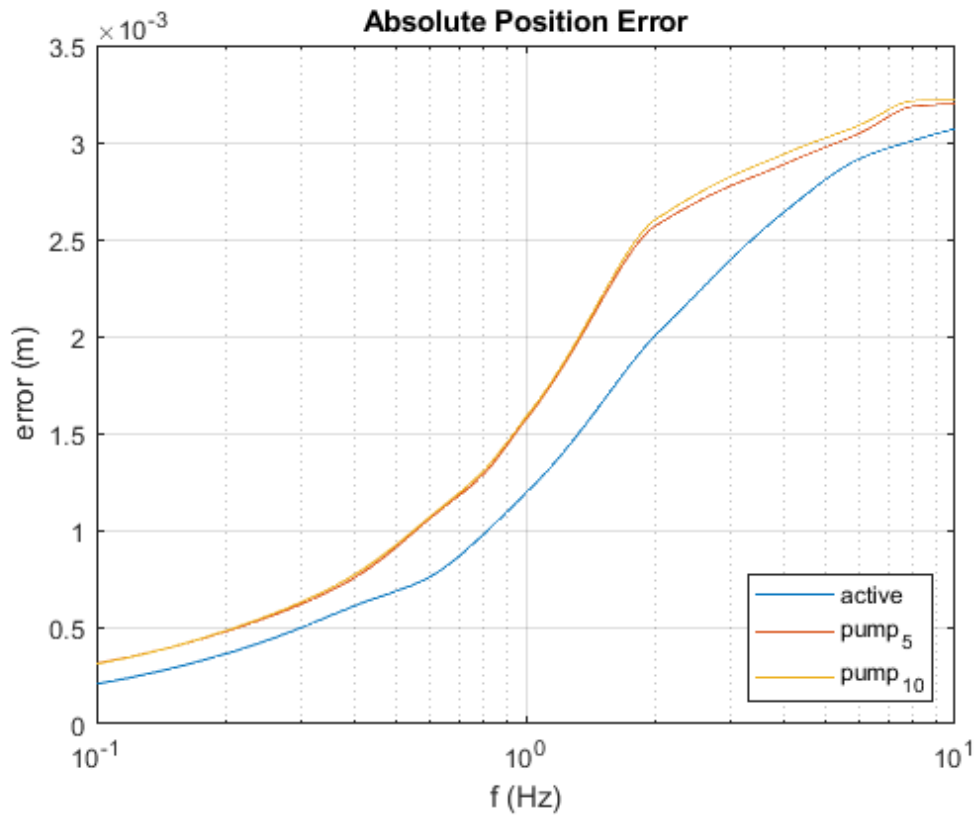


Figure 4-31: Frequency – Piston Absolute Position Error diagram

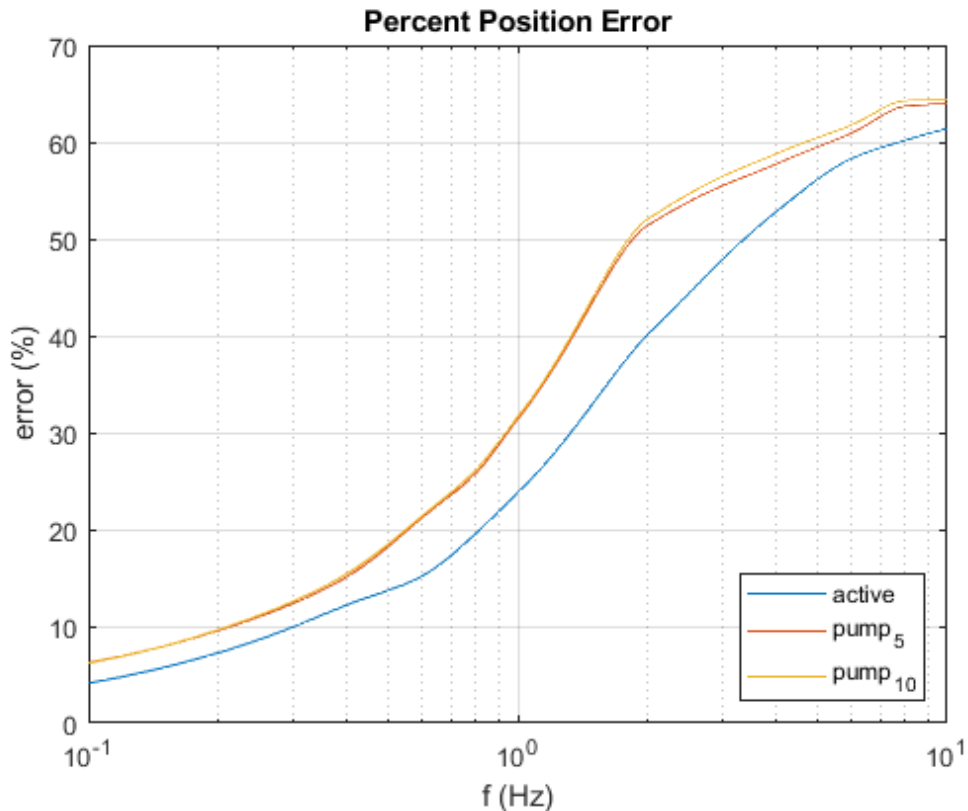


Figure 4-32: Frequency – Piston Percent Position Error diagram

Finally, the piston position at 10Hz is being shown in the diagrams below for the bigger pump system. The selection of the pump size is random, since the behavior of both servo valve systems is identical at high frequencies. Generally, as the frequency of the system increases above 4Hz, the response of all systems has overshooting from the desired position at the beginning of the simulation. More specifically, the servo valve systems have larger overshooting than the active system, but have smaller settling time. Also, for the active system, the piston at the beginning moves at the opposite direction than the desired one. This happens due to the pressure of the piston chamber exerting a force on the control volume and moving it out of chamber before the electric motor controls it and moves it to the desired position.

It can also be seen in both figures (4-32) and (4-33) that, for the retraction, the piston doesn't reach the lower desired position at has an error of about 0.25mm while it reaches the desired higher position (extension). This can be caused by an error at the simulation or due to the fact that oils needs to enter the ring area of the piston which has greater pressure and thus it is more difficult for the pump to produce the necessary flow. Generally, the main conclusion is that, for high frequencies, the active system has better behavior regarding the piston position.

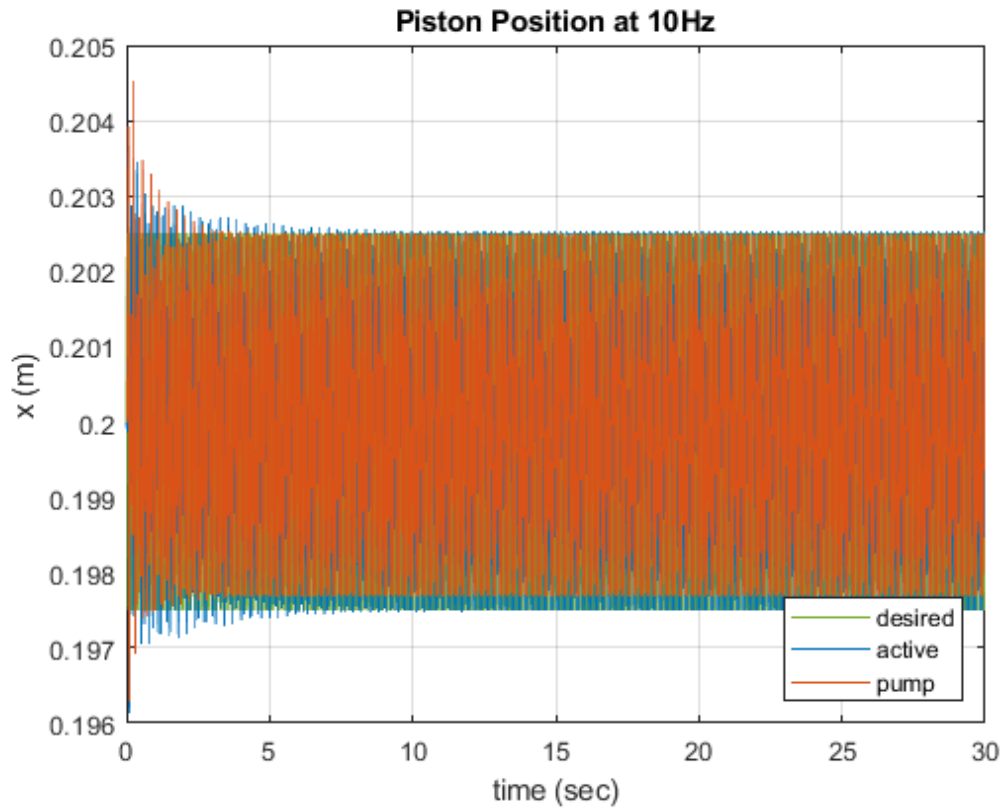


Figure 4-33: Frequency – Piston Position at 10Hz diagram

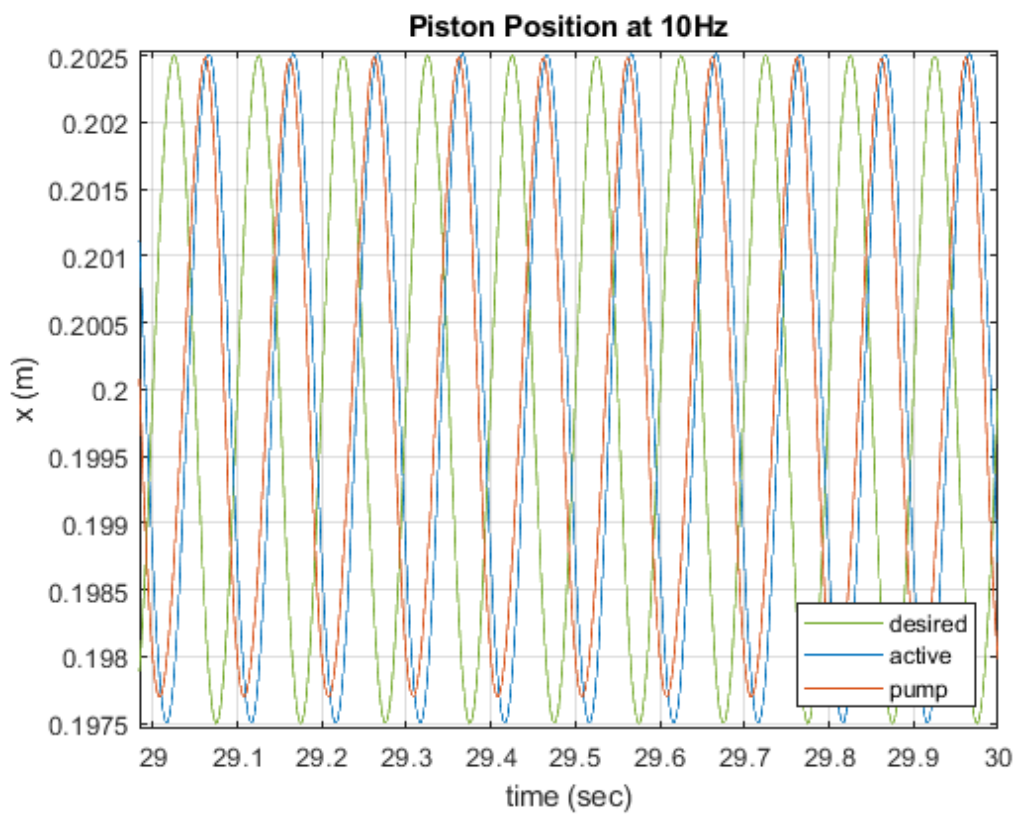


Figure 4-34: Frequency – Piston Position at 10Hz diagram (detail)

All simulation values are presented in Appendix A at the according tables.

4.3.2. Piston Position Results

The main conclusions, after all the simulations were finished, for the piston position are summarized below:

- Better response for the active system than the servo valve systems (more stable, equal retraction and extension range, no oscillations).
- For the servo valve systems, for frequencies of 8Hz and above the piston doesn't reach the lower desired position (retraction).
- For frequencies of 2Hz below the opposite happens, the piston seems to go easier further down to the lower position than to the higher position (extension).
- At 4Hz and 6Hz the response of the servo valve systems is more stable and the retraction and extension lengths are almost the same.
- At the transient state, the servo valve systems have greater overshooting than the active system. In contrast, the active system has greater settling time.
- At the start of the simulation, the piston at the active system moves at the opposite direction due to the pressurized oil inside the piston chamber.

The piston position diagrams for each frequency and pump size are presented in Appendix B. The codes used are presented in Appendix C.

4.4. Conclusion

Summing up this diploma thesis, some very interesting conclusions have surfaced. First of all, at low frequencies the power required for the active system is higher than the power required for both servo valve systems and seems to have a minimum value which is constant. This is due to the oil inside of the piston chambers being pre-pressurized and the value of the pre-charge pressure effects this minimum power value. The power required for the active system at 0.1Hz is 45.33 times greater than the power required for the small pump servo valve system and 57.5 times greater than the big servo valve system. On the other hand, the power required for the active system at 10Hz is 5.76 times smaller than the small pump servo valve system and 4.52 times smaller than the big servo valve system. So, it is easily deduced that the active system is more energy efficient at high frequencies than the servo valve systems.

Considering the system performance, the active system generally displays better response and smaller position error than the servo valve system, throughout all the range of frequencies. Specifically, the position error for the active system at 0.1Hz is 33.79% lower than the small pump servo system and 33.30% lower than the big pump servo system. At 10Hz, these values become 4.03% and 4.60% respectively.

The active system consists of the electrical subsystem, comprising of the electric motor, the hydraulic system, comprising of the hydraulic cylinder and the control volume, and the mechanical subsystem, comprising of the rack and pinion mechanism that converts the rotational to translational motion. The complexity of the active system is not considered superior than that of the servo valve system since servo valves are very intricate and costly mechanisms. Nevertheless, the manufacturing process to connect the control volume to the hydraulic cylinder must be of extremely high precision in order to prevent leakages, since the oil inside the cylinder chambers is at high pressure. It is also important to note that since the active system is a closed hydraulic system, it has no way to replace the oil lost due to leakages.

Additionally, the parameter values of the active system were selected for specific frequency and amplitude values. By adjusting the hydraulic cylinder and control volume size and, as well as, the pre-charge pressure of the oil, greater or smaller amplitudes and frequencies can be achieved. For example, lowering the value of the pre-charge pressure will lower the minimum required power for the active system, thus making it more energy efficient in low frequencies.

Some possible applications that could use the active hydraulic system are:

- the hydraulic KDamper, at controlling the meta-stable point at the initial position. “The KDamper is a novel passive vibration isolation and damping concept, based essentially on the optimal combination of appropriate stiffness elements, which include a negative stiffness element” [6]. The hydraulic KDamper aims to enhance the performance of the KDamper by replacing the negative stiffness spring configuration, used by the KDamper, with a hydraulic spring comprising of a bladder type accumulator connected with a hydraulic actuator which acts as a negative stiffness spring. More information on KDamper are presented in Appendix D.
- fatigue test machines that use dynamic load to determine the sturdiness of components and products.

Bibliography

- [1] M. Jelali and A. Kroll, *Hydraulic Servo-systems: Modeling, Identification and Control*, London: Springer-Verlag London Limited, 2004.
- [2] K.-E. Rydberg, *Hydraulic Servo Systems, Dynamic Properties and Control*, Linköping: Department of Management and Engineering, Linköping University, 2014.
- [3] M. G. Rabie, *Fluid Power Engineering*, Cairo: McGraw-Hill, 2009.
- [4] A. Milovanovic, M. Bjekić and S. Antic, "Permanent Magnet DC Motor Friction Measurement and Analysis of Friction's Impact," *International Review of Electrical Engineering (IREE)*, 2011.
- [5] R. N. K. Loh, W. Thanom, J. S. Pyko and A. Lee, "Electronic Throttle Control System: Modeling, Identification and Model-Based Control Designs," *SCIRP*, 2013.
- [6] A. I. Antoniadis, S. Kanarachos, I. Sapountzakis and K. Gryllias, "KDamping: A stiffness based vibration absorption concept," *Journal of Vibration and Control*, 2018.
- [7] F. J. Niemas Jr., *Selection Considerations for a Servovalve*, Orlando, Florida: University of Central Florida, 1977.
- [8] Z. Wu, Y. Xiang, M. Li, M. Y. Iqbal and G. Xu, "Investigation of Accumulator Main Parameters of Hydraulic Excitation System," *Journal of Coastal Research*, 2019.
- [9] D. C. Clark, "Selection and Performance Criteria for Electrohydraulic Servodrives," in *National Conference on Fluid Power*, 1969.
- [10] L. Pace, M. Ferro, F. Fraternali, M. D. Vedova, C. Antonio and P. Maggiore, "Comparative Analysis of a Hydraulic Servo-Valve," *International Journal of Fluid Power*, 2014.
- [11] P. Wolm, X. Q. Chen, J. G. Chase, W. Pettigrew and C. E. Hann, "Analysis of a PM DC Motor Model for Application in Feedback Design for Electric Powered Mobility Vehicles," *International Journal of Computer Applications in Technology*, 2010.
- [12] R. A. H. AL-Baldawi, Y. A. Faraj and R. E. J. Talabani, "A Study on the Effects of Servovalve Lap on the Performance of a Closed - Loop Electrohydraulic Position Control System," *AL-Rafidain Engineer Journal*, 2009.
- [13] N. N. Nise, *Control Systems Engineering*, John Wiley & Sons, 2014.

Appendix

A. Mean simulation values

Mean System Power [Watt]					
frequency [Hz]	Electric Motor	Mechanical Power Pump ($5 \text{ cm}^3/\text{rev}$)	Mechanical Power Pump ($10 \text{ cm}^3/\text{rev}$)	Hydraulic Power Pump ($5 \text{ cm}^3/\text{rev}$)	Hydraulic Power Pump ($10 \text{ cm}^3/\text{rev}$)
0.1	371.78	8.20	6.47	1.44	1.48
0.2	370.56	32.80	25.79	5.65	5.86
0.4	371.08	134.58	104.18	20.93	22.33
0.6	375.00	315.52	246.28	42.88	45.18
0.8	396.25	551.64	422.29	78.95	86.13
1.0	426.43	896.90	683.88	112.13	123.54
2.0	649.22	2623.89	2049.11	735.13	749.92
4.0	1139.82	5319.70	4174.35	2245.24	2260.80
6.0	1581.69	7985.51	6266.74	3764.08	3779.65
8.0	1885.62	10651.89	8357.53	5281.87	5298.97
10.0	2312.07	13315.91	10454.45	6805.21	6815.58

Table A-1: Mean System Power

Mean Piston Chamber Pressure [MPa]			
frequency [Hz]	Active	Pump ($5 \text{ cm}^3/\text{rev}$)	Pump ($10 \text{ cm}^3/\text{rev}$)
0.1	13.86	0.63	0.64
0.2	13.89	1.24	1.27
0.4	13.90	2.36	2.41
0.6	13.92	3.38	3.44
0.8	13.93	4.46	4.51
1.0	13.94	5.47	5.53
2.0	13.96	9.67	9.74
4.0	13.97	10.97	11.14
6.0	13.99	11.23	11.37
8.0	14.00	11.18	11.28
10.0	14.02	11.52	11.58

Table A-2: Mean Piston Chamber Pressure

Mean Ring Chamber Pressure [MPa]			
frequency [Hz]	Active	Pump ($5 \text{ cm}^3/\text{rev}$)	Pump ($10 \text{ cm}^3/\text{rev}$)
0.1	27.17	1.32	1.34
0.2	27.21	2.53	2.58
0.4	27.27	4.72	4.81
0.6	27.29	6.73	6.85
0.8	27.31	8.84	8.93
1.0	27.32	10.81	10.94
2.0	27.37	19.07	19.22
4.0	27.40	21.61	21.95
6.0	27.43	22.20	22.43

8.0	27.46	22.50	22.65
10.0	27.50	23.36	23.47

Table A-3: Mean Ring Chamber Pressure

Mean Absolute Error [mm]			
frequency [Hz]	Active	Pump (5 cm³/rev)	Pump (10 cm³/rev)
0.1	0.21	0.31	0.31
0.2	0.36	0.48	0.48
0.4	0.61	0.76	0.77
0.6	0.76	1.06	1.07
0.8	0.98	1.29	1.31
1.0	1.20	1.57	1.58
2.0	2.00	2.57	2.60
4.0	2.62	2.89	2.94
6.0	2.91	3.05	3.09
8.0	3.01	3.19	3.21
10.0	3.07	3.20	3.22

Table-A-4: Mean Absolute Error

Mean Percent Error [%]			
frequency [Hz]	Active	Pump (5 cm³/rev)	Pump (10 cm³/rev)
0.1	4.13	6.24	6.19
0.2	7.23	9.54	9.61
0.4	12.2	15.11	15.43
0.6	15.2	21.25	21.41
0.8	19.6	25.83	26.18
1.0	23.8	31.41	31.63
2.0	40.05	51.34	51.98
4.0	52.48	57.73	58.79
6.0	58.3	60.94	61.79
8.0	60.19	63.70	64.28
10.0	61.38	63.96	63.34

Table A-5: Mean Percent Error

B. Position plots

- $V_g = 5 \frac{\text{cm}^3}{\text{rev}}$

➤ $f = 0.1\text{Hz}$

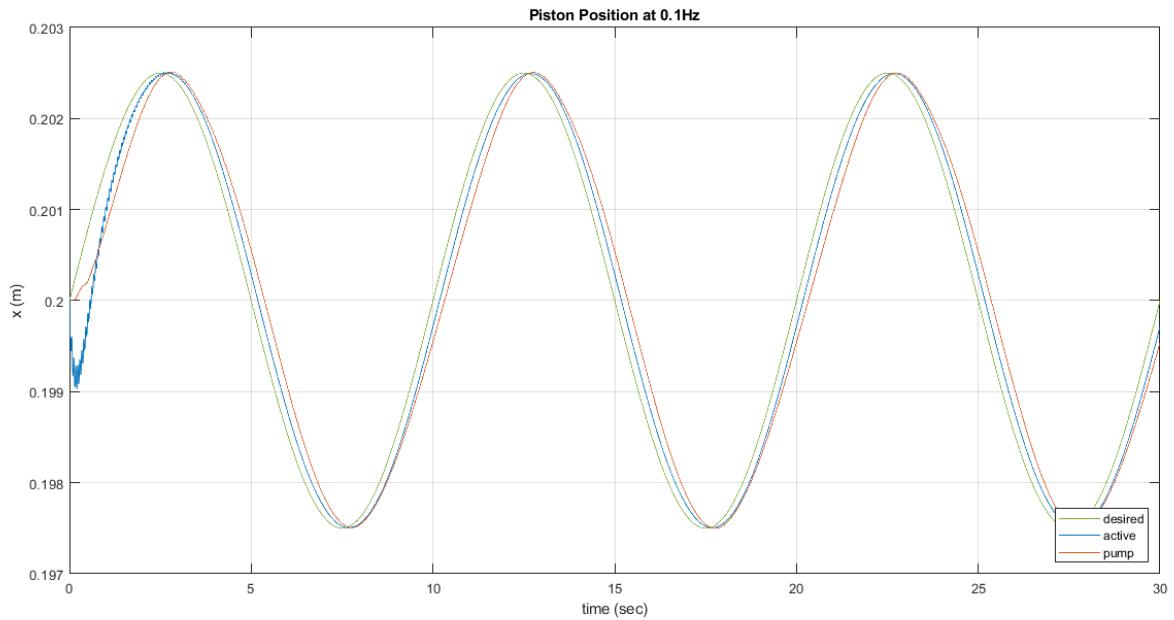


Figure B-1: Frequency – Piston Position at 0.1Hz diagram ($V_g = 5\text{cm}^3/\text{rev}$)

➤ $f = 0.2\text{Hz}$

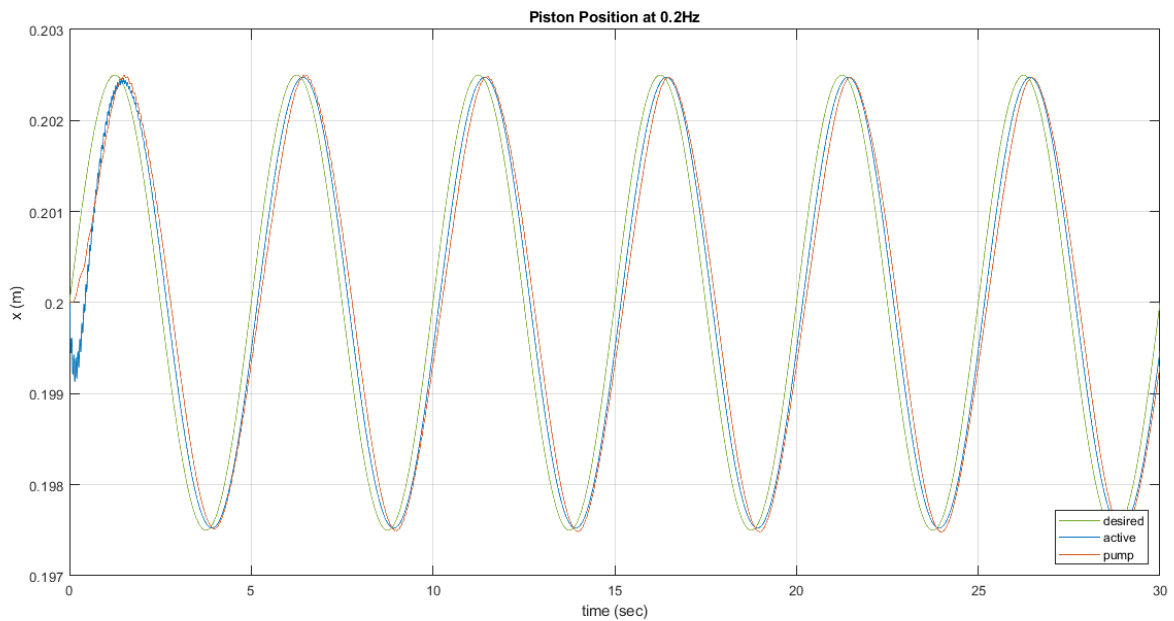


Figure-B-2: Frequency – Piston Position at 0.2Hz diagram ($V_g = 5\text{cm}^3/\text{rev}$)

➤ f = 0.4Hz

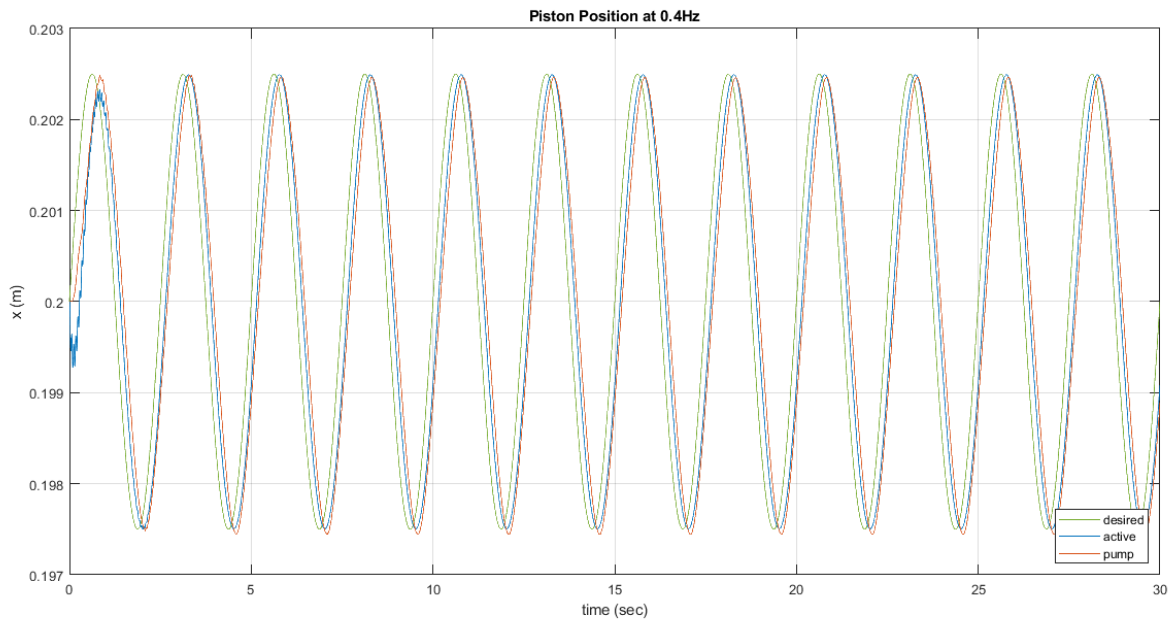


Figure B-3: Frequency – Piston Position at 0.4Hz diagram ($V_g = 5\text{cm}^3/\text{rev}$)

➤ f = 0.6Hz

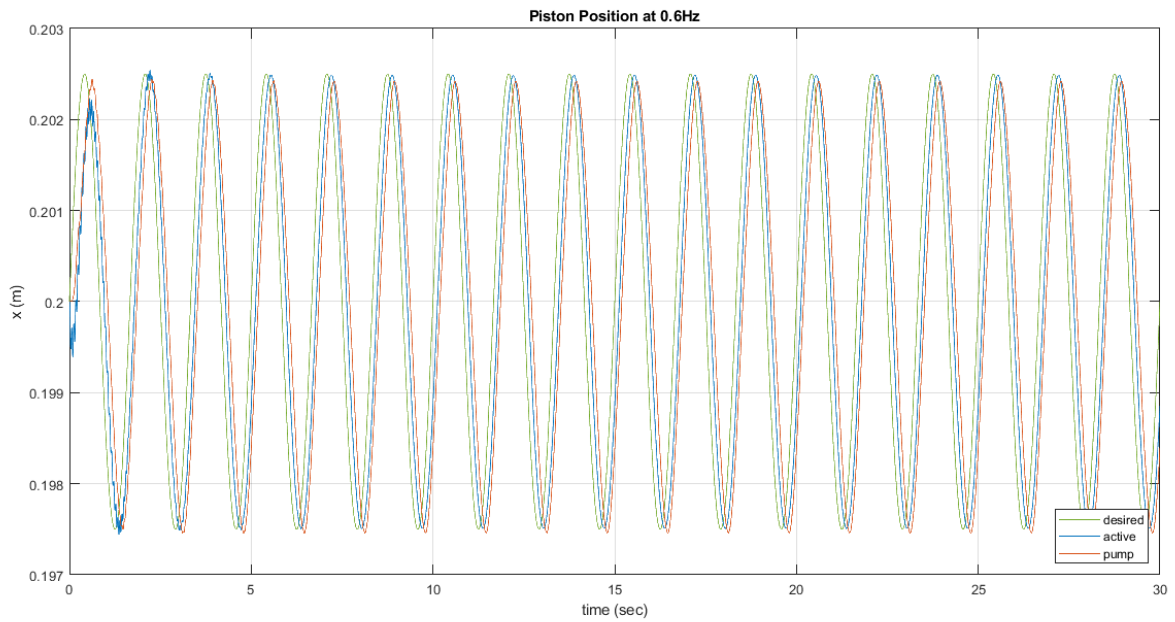


Figure B-4: Frequency – Piston Position at 0.6Hz diagram ($V_g = 5\text{cm}^3/\text{rev}$)

➤ $f = 0.8\text{Hz}$

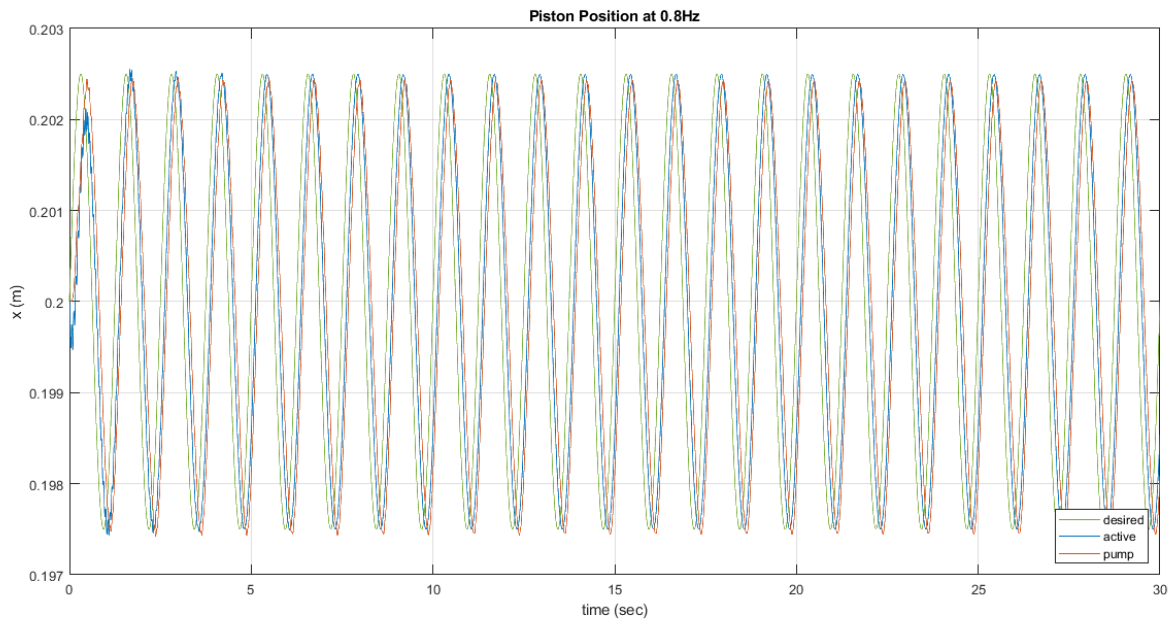


Figure B-5: Frequency – Piston Position at 0.8Hz diagram ($V_g = 5\text{cm}^3/\text{rev}$)

➤ $f = 1\text{Hz}$

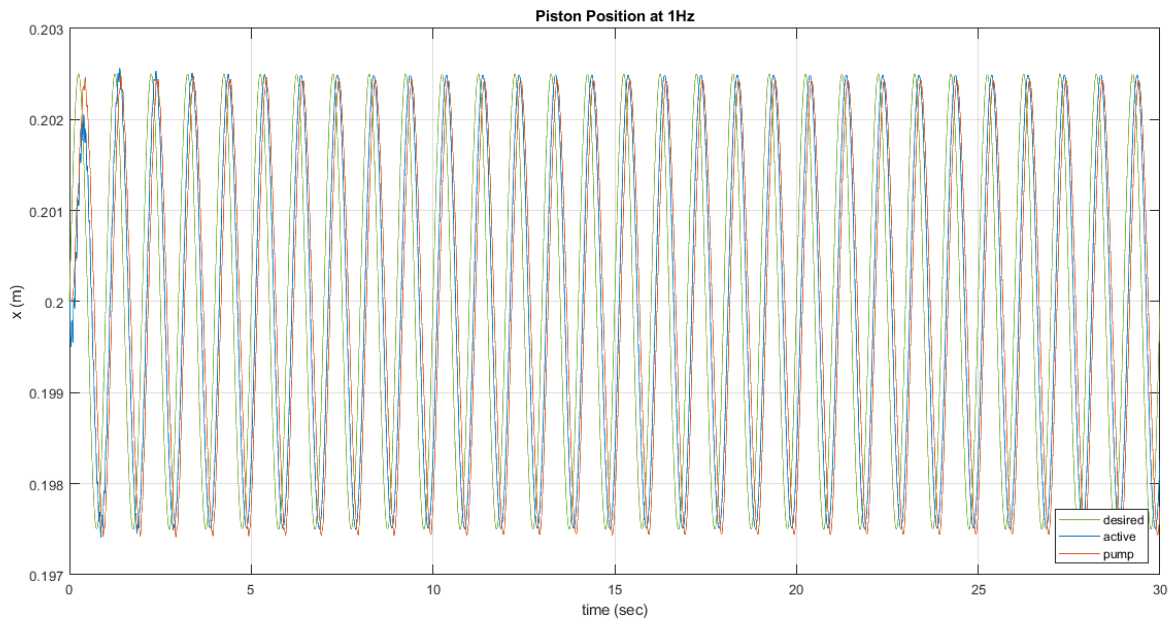


Figure B-6: Frequency – Piston Position at 1Hz diagram ($V_g = 5\text{cm}^3/\text{rev}$)

➤ f = 2Hz

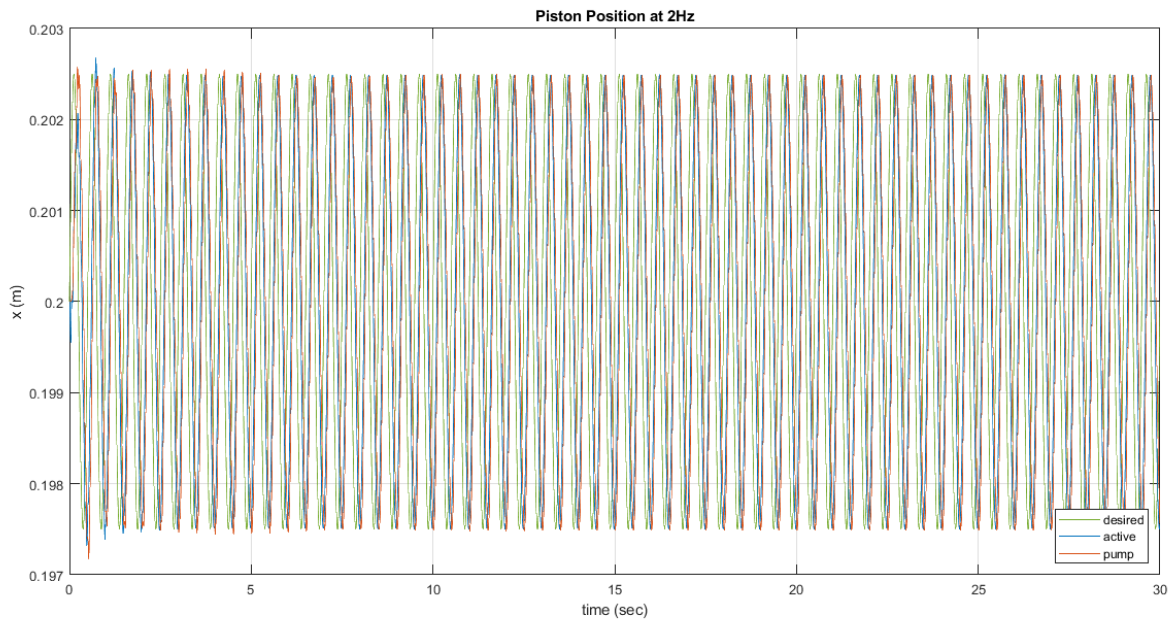


Figure B-7: Frequency – Piston Position at 2Hz diagram ($V_g = 5\text{cm}^3/\text{rev}$)

➤ f = 4Hz

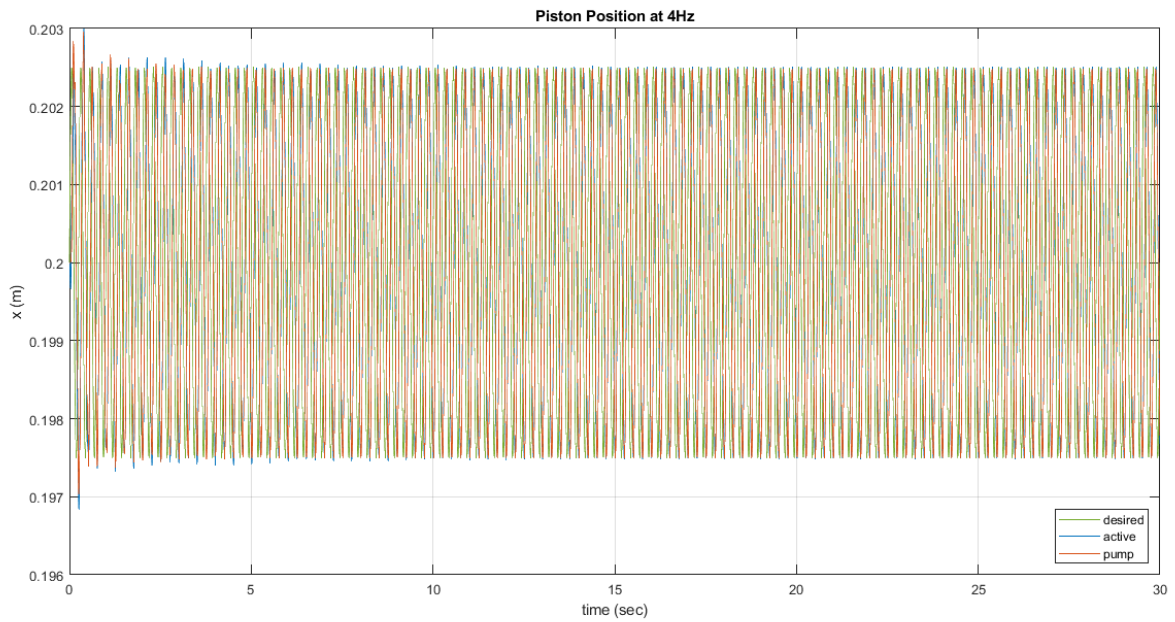


Figure B-8: Frequency – Piston Position at 4Hz diagram ($V_g = 5\text{cm}^3/\text{rev}$)

➤ f = 6Hz

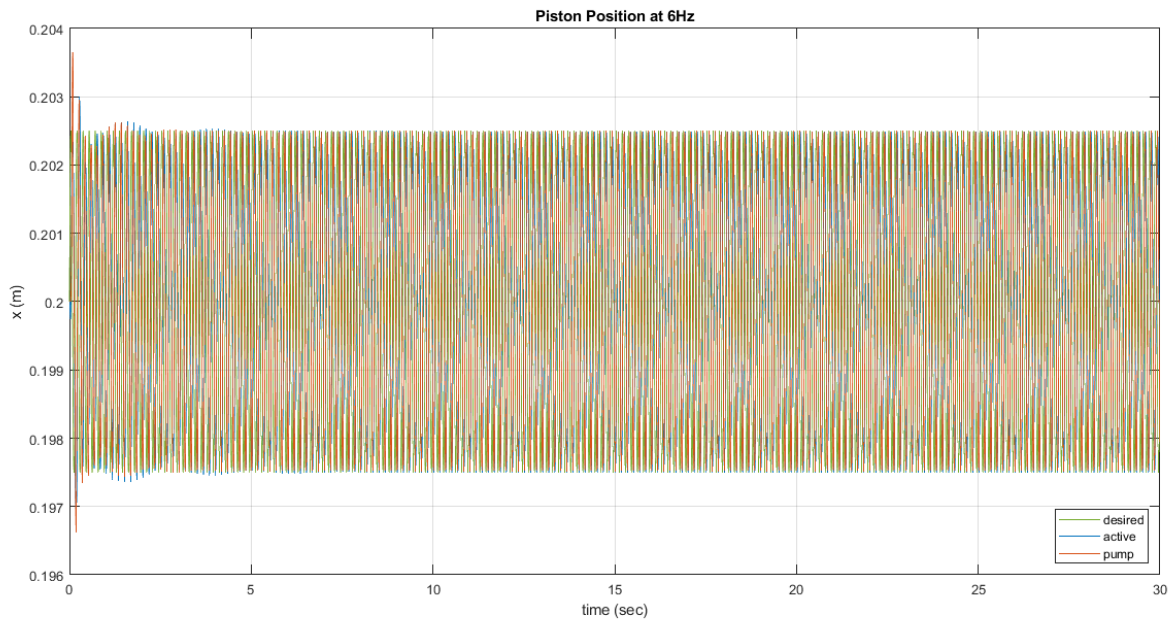


Figure B-9: Frequency – Piston Position at 6Hz diagram ($V_g = 5\text{cm}^3/\text{rev}$)

➤ f = 8Hz

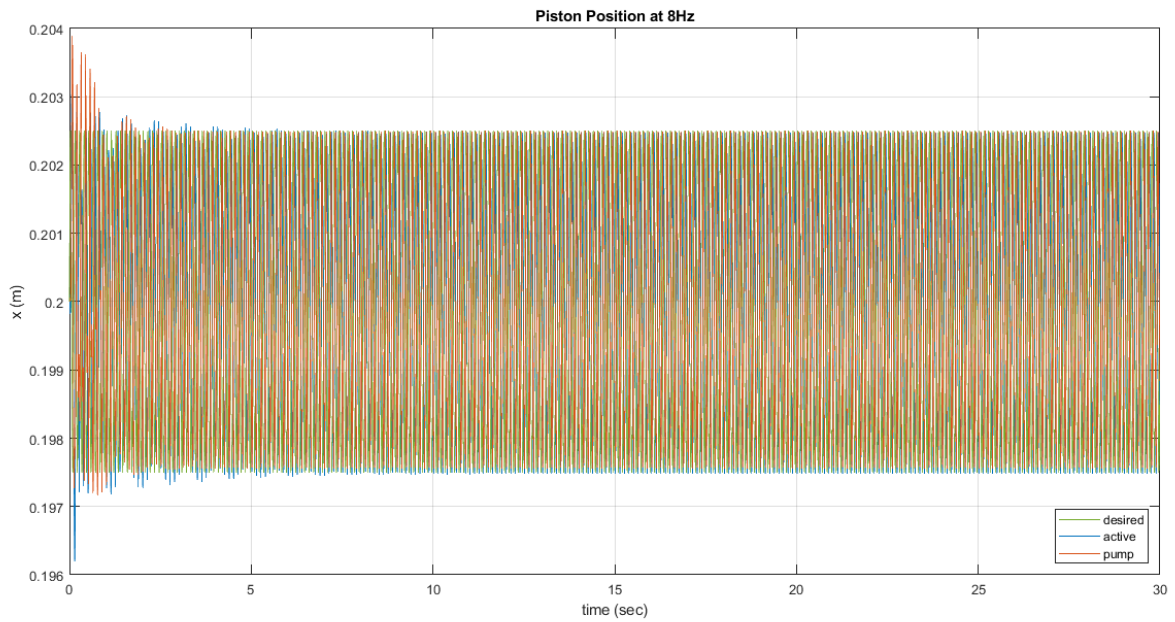


Figure B-10: Frequency – Piston Position at 8Hz diagram ($V_g = 5\text{cm}^3/\text{rev}$)

➤ $f = 10\text{Hz}$

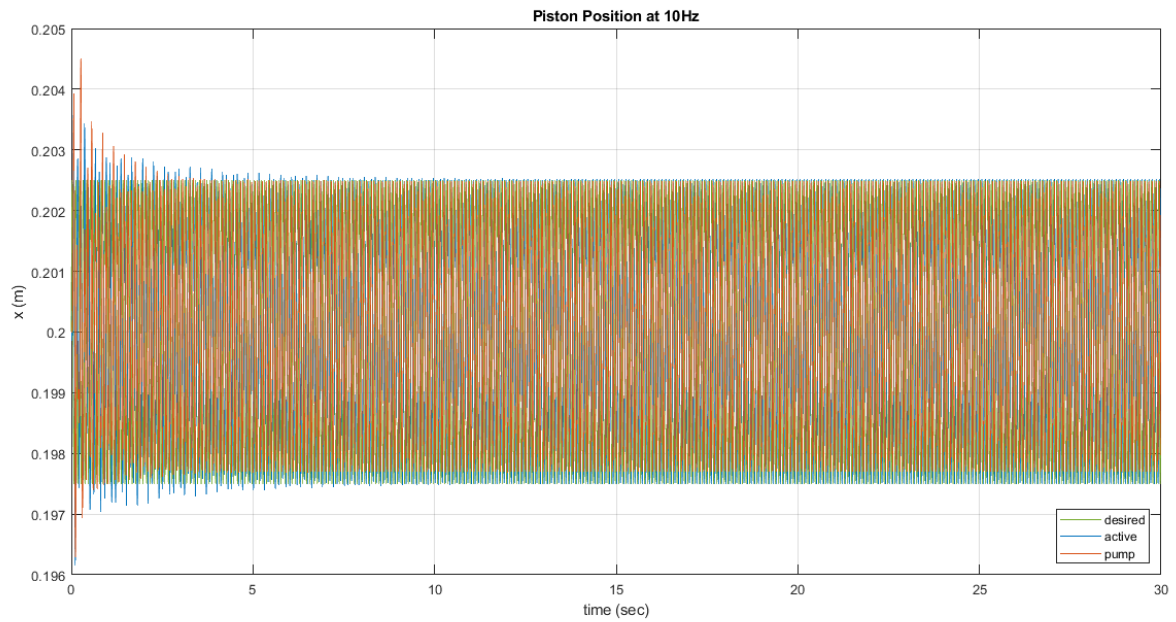


Figure B-11: Frequency – Piston Position at 10Hz diagram ($V_g = 5\text{cm}^3/\text{rev}$)

• $V_g = 10 \frac{\text{cm}^3}{\text{rev}}$

➤ $f = 0.1\text{Hz}$

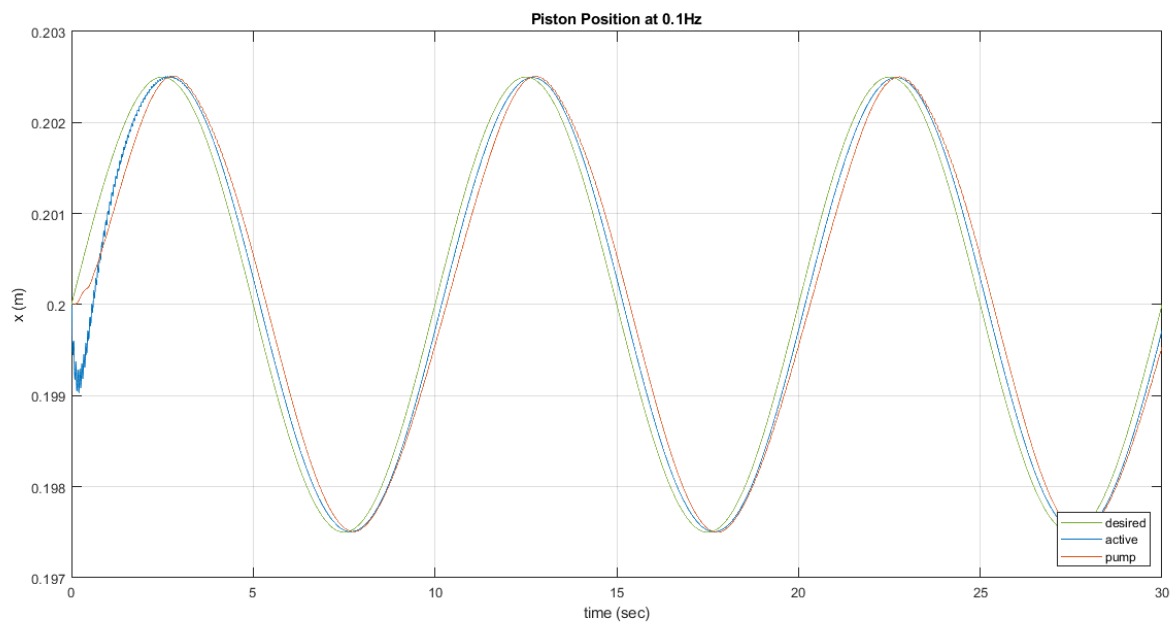


Figure B-12: Frequency – Piston Position at 0.1Hz diagram ($V_g = 10\text{cm}^3/\text{rev}$)

➤ f = 0.2Hz

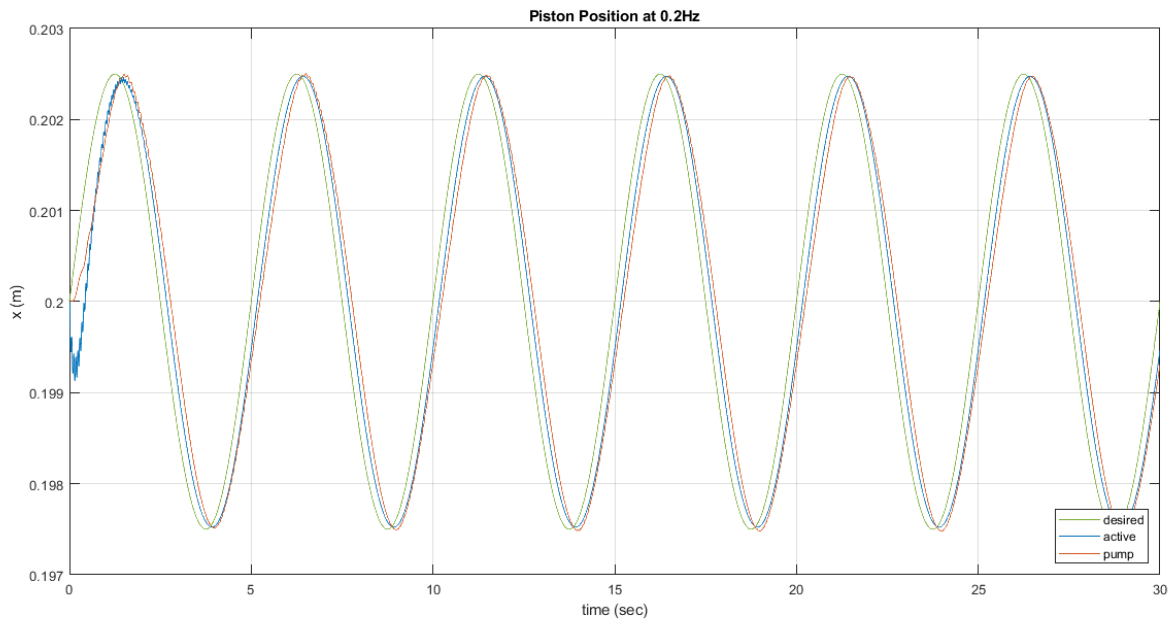


Figure B-13: Frequency – Piston Position at 0.2Hz diagram ($V_g = 10\text{cm}^3/\text{rev}$)

➤ f = 0.4Hz

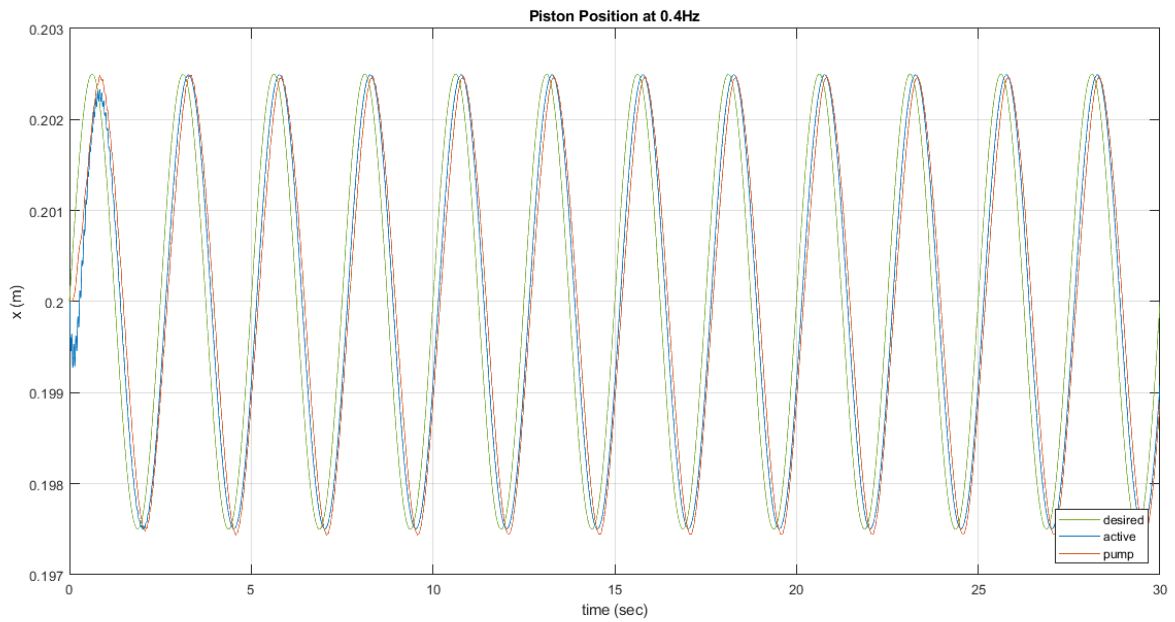


Figure B-14: Frequency – Piston Position at 0.4Hz diagram ($V_g = 10\text{cm}^3/\text{rev}$)

➤ f = 0.6Hz

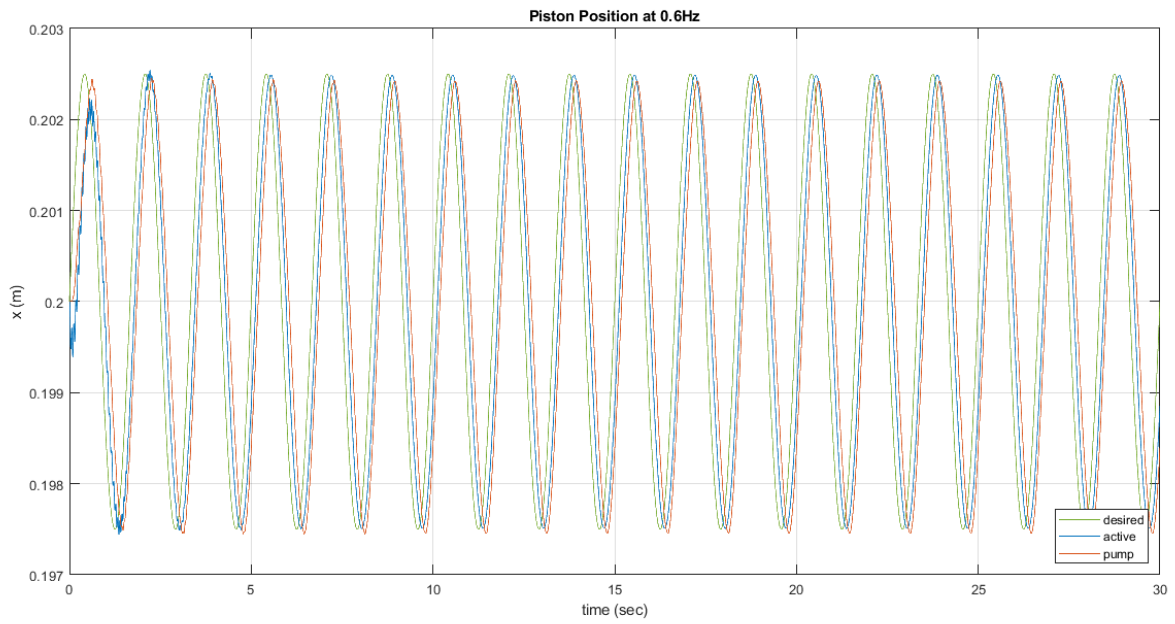


Figure B-15: Frequency – Piston Position at 0.6Hz diagram ($V_g = 10\text{cm}^3/\text{rev}$)

➤ f = 0.8Hz

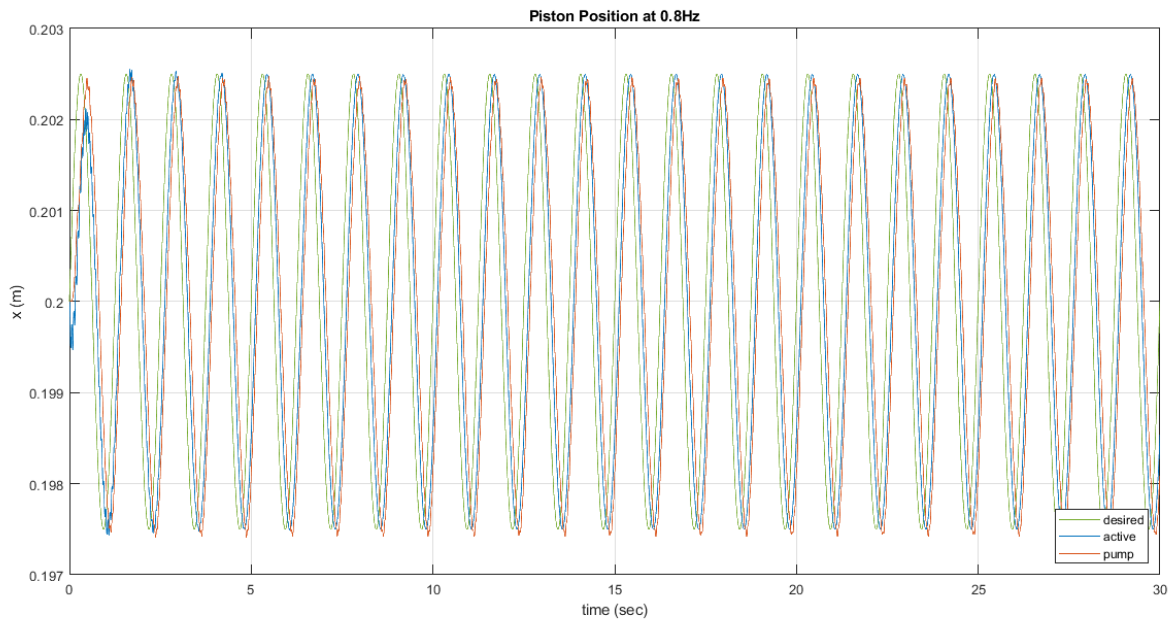


Figure B-16: Frequency – Piston Position at 0.8Hz diagram ($V_g = 10\text{cm}^3/\text{rev}$)

➤ f = 1Hz

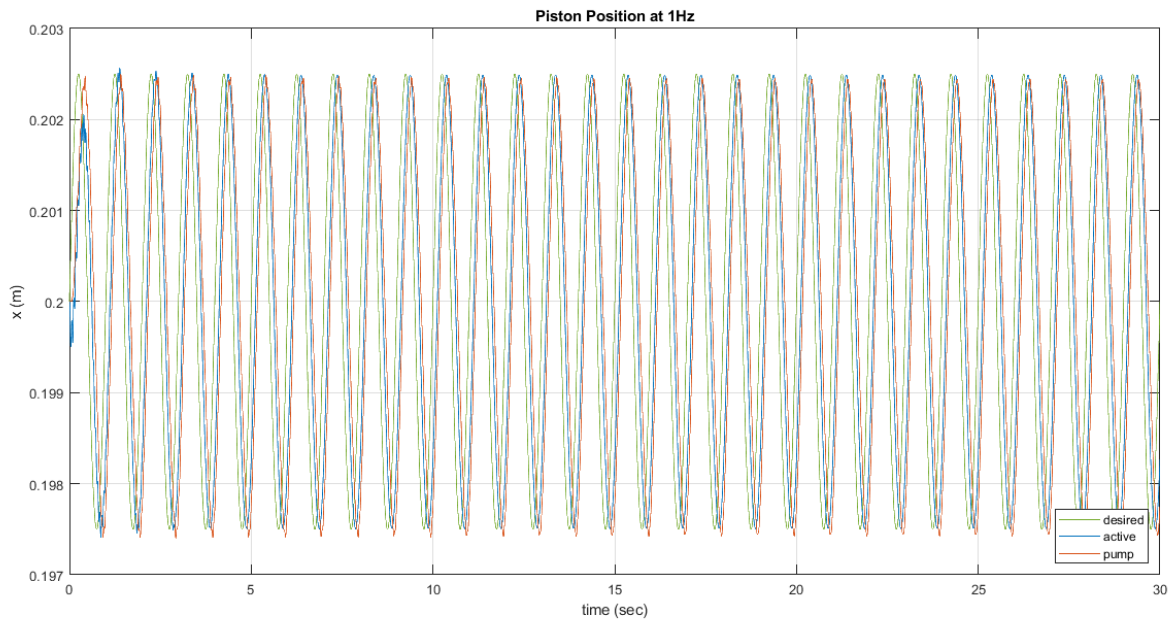


Figure B-17: Frequency – Piston Position at 1Hz diagram ($V_g = 10\text{cm}^3/\text{rev}$)

➤ f = 2Hz

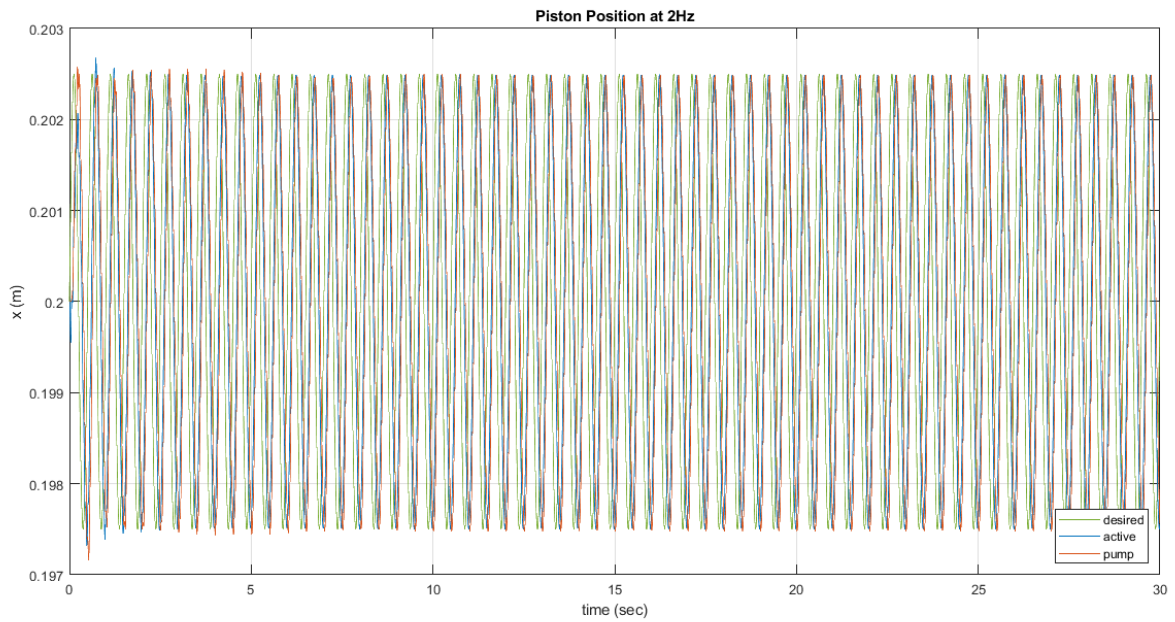


Figure B-18: Frequency – Piston Position at 2Hz diagram ($V_g = 10\text{cm}^3/\text{rev}$)

➤ f = 4Hz

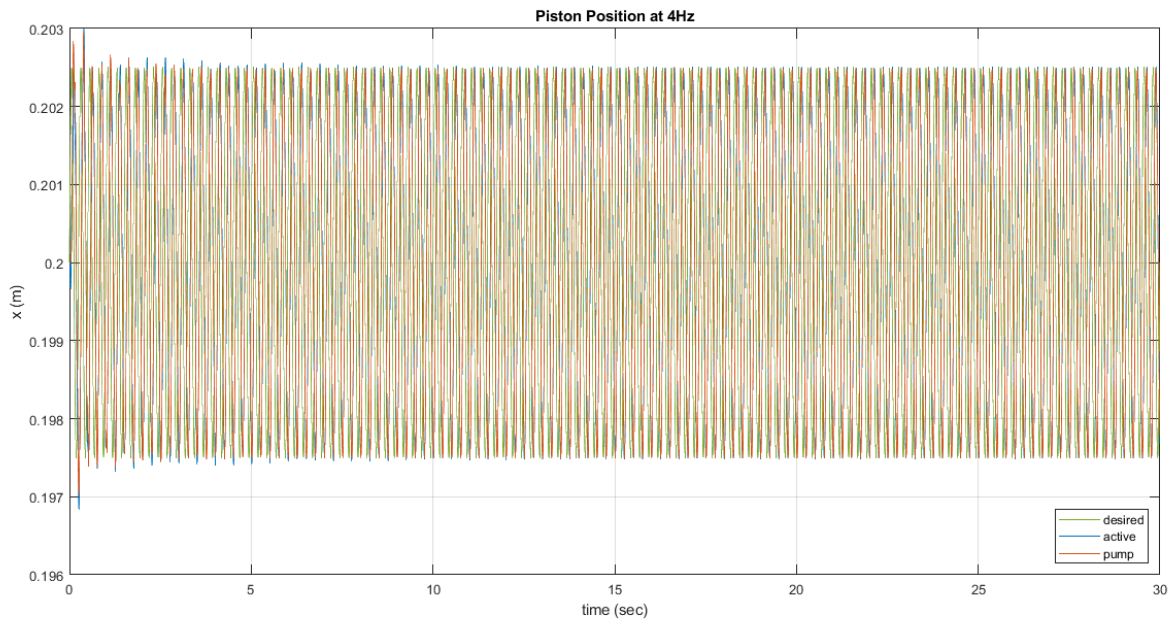


Figure B-19: Frequency – Piston Position at 4Hz diagram ($V_g = 10\text{cm}^3/\text{rev}$)

➤ f = 6Hz

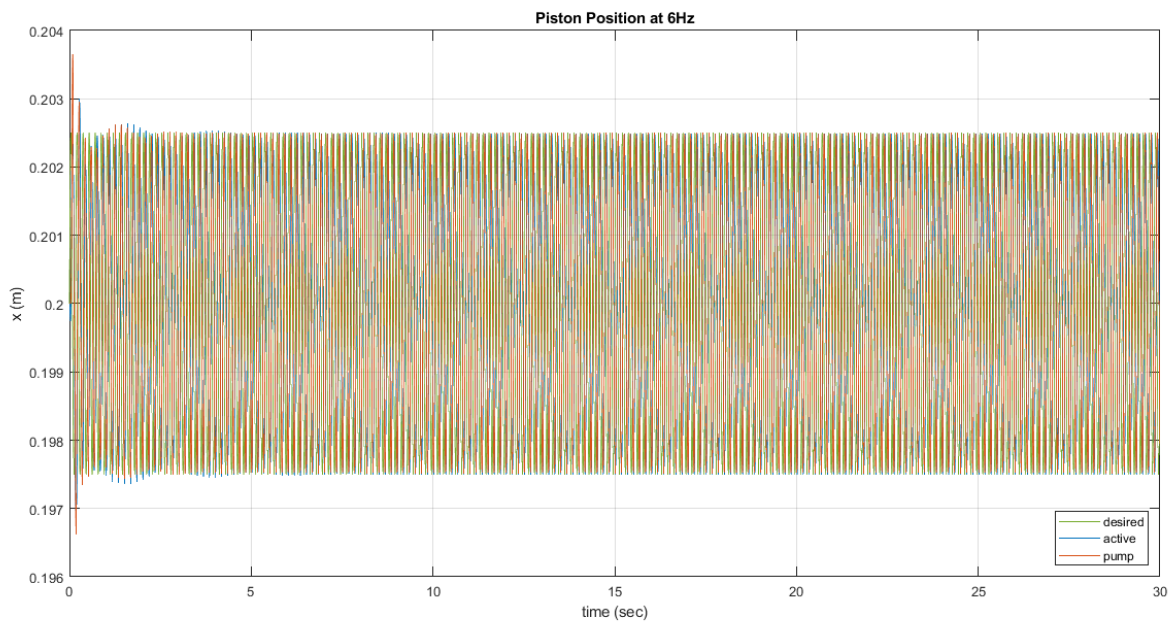


Figure B-20: Frequency – Piston Position at 6Hz diagram ($V_g = 10\text{cm}^3/\text{rev}$)

➤ f = 8Hz

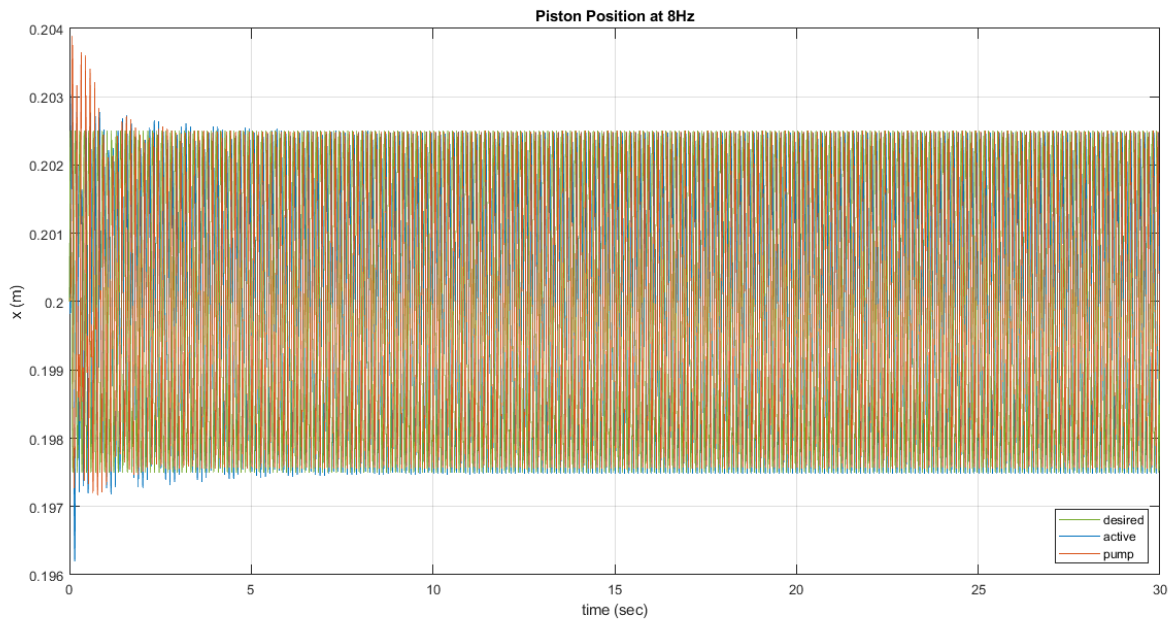


Figure B-21: Frequency – Piston Position at 8Hz diagram ($V_g = 10\text{cm}^3/\text{rev}$)

➤ f = 10Hz

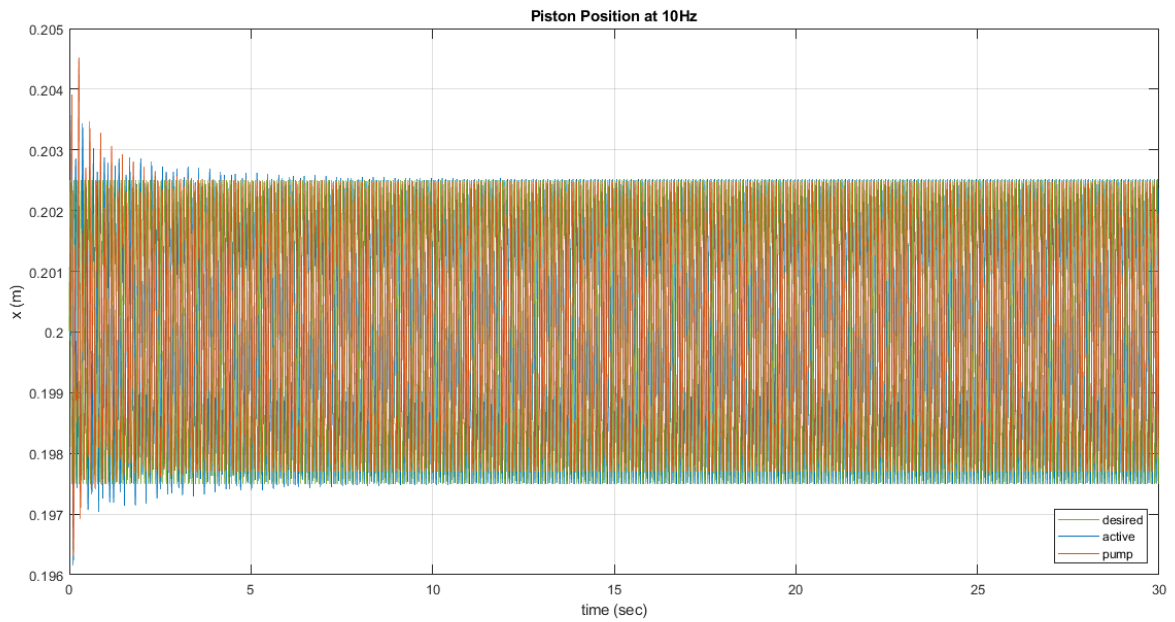


Figure B-22: Frequency – Piston Position at 10Hz diagram ($V_g = 10\text{cm}^3/\text{rev}$)

C. Matlab codes

a) Main code

```
close all
clear
clc
%% Manual test
% f = 10;
% w = 2*pi*f;
% Vg = 5;
%
% if Vg == 10
%     RPM = 130*f;
%     RPM_nom = 3150;
%     Ks_pump = 0.92e3;
%     J_pump = 0.0004;
%     P_nom = 400;
% elseif Vg == 23
%     RPM = 560;
%     RPM_nom = 2500;
%     Ks_pump = 2.56e3;
%     J_pump = 0.0012;
%     P_nom = 400;
% elseif Vg == 5
%     RPM = 260*f;
%     RPM_nom = 5600;
%     Ks_pump = 0.63e3;
%     J_pump = 0.00006;
%     P_nom = 350;
% end
% [k_act,ki_act,kd_act,k_pump,ki_pump,kd_pump] = PID_gains_new(f);
%% Simulation
simulation = 1;
%0 = no / 1 = yes
validation = 0;
%0 = no / 1 = yes
freq = [0.1,0.2,0.4,0.6,0.8,1,2,4,6,8,10];
%system frequency [Hz]
A = 0.0025;
%amplitude [m] (must be A < Xp_init)
Xp_max = 0.4;
%max piston stroke [m]
Xp_init = Xp_max/2;
%initial piston position [m]
Vg_pump = [10,5];
%pump displacement
%% servo valve
% Hydraulic system
D_piston = 0.04;
%piston no-rod side diameter [m]
D_rod = 0.028;
%piston rod side diameter [m]
Ps = 28e6;
%supply pressure [Pa]
Pt = 0;
%tank pressure [Pa]
Cd = 0.611;
%discharge coef
A1 = pi*D_piston^2/4;
%piston area chamber 1 [m^2]
```



```

A2 = pi*D_piston^2/4 - pi*D_rod^2/4;
%piston area chamber 2 [m^2]
D_servo = 0.0075*sqrt(20/40);
%servo valve port diameter [m]
A_servo = pi*D_servo^2/4;
%servo valve port area [m^2]
K_leak = 1e-14;
%internal leakage coef [Pasec/m^3]
Ki_leak = 1e-14;
%external leakage coef [Pasec/m^3]
%% active
P2_init = Ps;
%initial pressure in chamber 2 [Pa]
P1_init = P2_init*A2/A1;
%initial pressure in chamber 1 [Pa]

% ME1302 electric motor
Ja = 45e-4;
%motor inertia [kgm^2]
Ra = 0.013;
%armature resistance [Ohm]
La = 0.1e-3;
%armature inductance [H]
kt = 0.15;
%torque constant [Nm/A]
kb = kt;
%back-emf constant [Vsec/rad]
B = 0.001;
%motor viscous friction [Nmsec/rad]

% Control volume
Am = A1/5;
%Control volume area
Dm = sqrt(4*Am/pi);
%Control volume diameter [m]
Lm = D_piston;
%Control volume length [m]
dm = 7500;
%Control volume density [kg/m^3]
Mm = Am*Lm*dm;
%Control volume mass [kg]
R = 0.00625;
%pinion pitch radius [m]
Jm = Mm*R^2;
%Control volume moment of inertia [kgm^2]
Jtot = Ja + Jm;
%total moment of inertia [kgm^2]

% transfer function
a3 = Jtot*La;
a2 = Jtot*Ra + B*La;
a1 = B*Ra + kb*kt;
a0 = 0;
b0 = kt;
b11 = La;
b01 = Ra;
%% accumulator
Vo = 5e-3;
%acc total volume
P1 = 400;
%gas pressure at initial position

```

```

P2 = 600;
%max system pressure
Po = 0.9*P1;
%gas precharge pressure
V1 = Vo*(Po/P1)^(1/1.4);
%gas volume at initial position
V2 = Vo*(Po/P2)^(1/1.4);
%gas minimum volume
V_oil = Vo - V1;
%oil volume in acc at initial position
%% Load
Mt = 1000;
%mass [kg]
Bp = 1000;
%friction [Nsec/m]
Kp = 0;
%stiffness [N/m]
%% Oil - ISO VG 32
d = 857.2;
%oil density [kg/m^3]
nu = 31.8106e-6;
%kinematic viscosity [m^2/sec]
mu = nu*d;
%dynamic viscosity [Pasec]
be = 1.44756e9;
%bulk modulus [Pa]
%% Simulation
if (simulation == 1)
    for k = 1:length(Vg_pump)
        Vg = Vg_pump(k);
        if Vg == 10
            RPM_nom = 3150;
            Ks_pump = 0.92e3;
            J_pump = 0.0004;
            P_nom = 400;
        elseif Vg == 5
            RPM_nom = 5600;
            Ks_pump = 0.63e3;
            J_pump = 0.00006;
            P_nom = 350;
        elseif Vg == 23
            RPM_nom = 2500;
            Ks_pump = 2.56e3;
            J_pump = 0.0012;
            P_nom = 400;
        end
        for j = 1:length(freq)
            f = freq(j);
            [k_act,ki_act,kd_act,k_pump,ki_pump,kd_pump] =
PID_gains_new(f);
            w = 2*pi*f;
%angular frequency [rad/sec]
            T = 1/f;
%period [sec]
            if Vg == 10
                RPM = 130*f;
            elseif Vg == 23
                RPM = 56*f;
            elseif Vg == 5
                RPM = 260*f;
            end
        end
    end
end

```

```

%% simscape pump
out_pump = sim('servovalve_transfer_function_pump',30);
time_pump = out_pump.tout;
Xp_d_pump = out_pump.Xp_d_sim;
P1_pump = out_pump.P1_sim;
P2_pump = out_pump.P2_sim;
Xp_pump = out_pump.Xp_sim;
P_pump = out_pump.P_pump;
Q_pump = out_pump.Q_pump;
T_pump = out_pump.Torque_pump;
error_pump = out_pump.error_pump;
%% active
out_act = sim('active_sim_full_voltage',30);
time_act = out_act.tout;
P1_act = out_act.P1_act;
P2_act = out_act.P2_act;
Xp_act = out_act.Xp_act;
Va_act = out_act.Va_act;
Ia_act = out_act.Ia_act;
error_act = out_act.error_act;
%% Plots
figure (1)
plot(time_pump,Xp_d_pump,'Color',[0.4660, 0.6740,
0.1880])
title(['Piston Position at ' num2str(f) 'Hz'])
xlabel('time (sec)')
ylabel('x (m)')
hold on
grid on
plot(time_act,Xp_act,'Color',[0, 0.4470, 0.7410])
hold on
plot(time_pump,Xp_pump,'Color',[0.8500, 0.3250, 0.0980])
hold off

legend({'desired','active','pump'},'location','southeast')

pos_act{j} = Xp_act;
time_active{j} = time_act;
%% Power calculation
Power_motor{j} = (Va_act.*Ia_act)/0.9;
Power_motor_mean(j) = mean(abs(Power_motor{j}));
P1_act_mean(j) = mean(P1_act);
P2_act_mean(j) = mean(P2_act);
error_act_mean(j) = mean(abs(error_act));
error_act_mean_perc(j) = mean(100*abs(error_act/A/2));

Power_pump{k,j} = T_pump*RPM*pi/30;
Power_pump_hydro{k,j} = P_pump.*Q_pump;
if k == 1
    pos_pump_10{j} = Xp_pump;
    pos_des_10{j} = Xp_d_pump;
    time_pump_10{j} = time_pump;
    Power_pump_mean_10(j) = mean(abs(Power_pump{k,j}));
    Power_pump_hydro_mean_10(j) =
mean(abs(Power_pump_hydro{k,j}));
    P1_pump_mean_10(j) = mean(abs(P1_pump));
    P2_pump_mean_10(j) = mean(abs(P2_pump));
    error_pump_mean_10(j) = mean(abs(error_pump));
    error_pump_mean_perc_10(j) =
mean(100*abs(error_pump/A/2));

```

```

        power_loss_10(j) = (Power_pump_mean_10(j) -
Power_pump_hydro_mean_10(j))./Power_pump_mean_10(j);
        elseif k == 2
            pos_pump_5{j} = Xp_pump;
            pos_des_5{j} = Xp_d_pump;
            time_pump_5{j} = time_pump;
            Power_pump_mean_5(j) = mean(abs(Power_pump{k,j}));
            Power_pump_hydro_mean_5(j) =
mean(abs(Power_pump_hydro{k,j}));
            P1_pump_mean_5(j) = mean(abs(P1_pump));
            P2_pump_mean_5(j) = mean(abs(P2_pump));
            error_pump_mean_5(j) = mean(abs(error_pump));
            error_pump_mean_perc_5(j) =
mean(100*abs(error_pump/A/2));
            power_loss_5(j) = (Power_pump_mean_5(j) -
Power_pump_hydro_mean_5(j))./Power_pump_mean_5(j);
        end
    end
end
%% Plots
xq1 = 0.1:0.01:10;
figure (2)
Power_motor_meani = pchip(freq,Power_motor_mean,xq1);
semilogx(xq1,Power_motor_meani)
title('Power')
xlabel('f (Hz)')
ylabel('Power (W)')
grid on
hold on
Power_pump_mean_5i = pchip(freq,Power_pump_mean_5,xq1);
semilogx(xq1,Power_pump_mean_5i)
hold on
Power_pump_mean_10i = pchip(freq,Power_pump_mean_10,xq1);
semilogx(xq1,Power_pump_mean_10i)
hold on
Power_pump_hydro_mean_5i =
pchip(freq,Power_pump_hydro_mean_5,xq1);
semilogx(xq1,Power_pump_hydro_mean_5i)
hold on
Power_pump_hydro_mean_10i =
pchip(freq,Power_pump_hydro_mean_10,xq1);
semilogx(xq1,Power_pump_hydro_mean_10i)
hold off

legend({'active','pump_m_e_c_h_5','pump_m_e_c_h_1_0','pump_h_y_d_r_5'
,'pump_h_y_d_r_1_0'},'location','northwest')

figure (3)
P1_act_meani = pchip(freq,P1_act_mean,xq1);
semilogx(xq1,P1_act_meani)
title('Piston Chamber Pressure')
xlabel('f (Hz)')
ylabel('P (Pa)')
grid on
hold on
P1_pump_mean_5i = pchip(freq,P1_pump_mean_5,xq1);
semilogx(xq1,P1_pump_mean_5i)
hold on
P1_pump_mean_10i = pchip(freq,P1_pump_mean_10,xq1);
semilogx(xq1,P1_pump_mean_10i)
hold off

```

```

legend({'active', 'pump_5', 'pump_1_0'}, 'location', 'southeast')

figure (4)
P2_act_meani = pchip(freq, P2_act_mean, xq1);
semilogx(xq1, P2_act_meani)
title('Ring Chamber Pressure')
xlabel('f (Hz)')
ylabel('P (Pa)')
hold on
P2_pump_mean_5i = pchip(freq, P2_pump_mean_5, xq1);
semilogx(xq1, P2_pump_mean_5i)
hold on
grid on
P2_pump_mean_10i = pchip(freq, P2_pump_mean_10, xq1);
semilogx(xq1, P2_pump_mean_10i)
hold off
legend({'active', 'pump_5', 'pump_1_0'}, 'location', 'southeast')

figure (5)
error_act_meani = pchip(freq, error_act_mean, xq1);
semilogx(xq1, error_act_meani)
title('Absolute Position Error')
xlabel('f (Hz)')
ylabel('error (m)')
hold on
error_pump_mean_5i = pchip(freq, error_pump_mean_5, xq1);
semilogx(xq1, error_pump_mean_5i)
hold on
grid on
error_pump_mean_10i = pchip(freq, error_pump_mean_10, xq1);
semilogx(xq1, error_pump_mean_10i)
hold off
legend({'active', 'pump_5', 'pump_1_0'}, 'location', 'southeast')

figure (6)
error_act_mean_perci = pchip(freq, error_act_mean_perc, xq1);
semilogx(xq1, error_act_mean_perci)
title('Percent Position Error')
xlabel('f (Hz)')
ylabel('error (%)')
hold on
error_pump_mean_perc_5i = pchip(freq, error_pump_mean_perc_5, xq1);
semilogx(xq1, error_pump_mean_perc_5i)
hold on
grid on
error_pump_mean_perc_10i =
pchip(freq, error_pump_mean_perc_10, xq1);
semilogx(xq1, error_pump_mean_perc_10i)
hold off
legend({'active', 'pump_5', 'pump_1_0'}, 'location', 'southeast')

figure (7)
power_loss_5i = pchip(freq, power_loss_5, xq1);
power_loss_10i = pchip(freq, power_loss_10, xq1);
semilogx(xq1, 100*power_loss_5i)
title('Percent Power Loss')
xlabel('f (Hz)')
ylabel('error (%)')
grid on
hold on

```

```

        semilogx(xq1,100*power_loss_10i)
        hold off
        legend({'pump_5','pump_1_0'},'location','southwest')
end
%% Piston position plots
% i = 11;
% f = freq(i);
% figure (1)
% plot(time_pump_5{i},pos_des_5{i},'Color',[0.4660, 0.6740, 0.1880])
% title(['Piston Position at ' num2str(f) 'Hz'])
% xlabel('time (sec)')
% ylabel('x (m)')
% hold on
% grid on
% plot(time_active{i},pos_act{i},'Color',[0, 0.4470, 0.7410])
% hold on
% plot(time_pump_5{i},pos_pump_5{i},'Color',[0.8500, 0.3250, 0.0980])
% hold off
% legend({'desired','active','pump'},'location','southeast')
%% Validation simulation
if validation == 1
    A = 0.05;
    f = 1;
    K = 0.05;
    K_full = 0.09;
    ki = 0.375;
    w = 2*pi*f;
%angular frequency [rad/sec]
    T = 1/f;
%period [sec]
    if A == 0.05
        K = 0.05;
        Ki = 0;
        K_full = 0.09;
        Ki_full = 0;
    elseif A == 0.0025
        if f == 1
            K = 0.005;
            Ki = 0.0439;
            K_full = 0.013;
            Ki_full = 0.1775;
        elseif f == 10
            K = 0.038;
            Ki = 0.96;
            K_full = 0.08;
            Ki_full = 5.45;
        end
    end
end
%% full model
out_full = sim('FINAL_BD_asymmetric_full',10);
time = out_full.tout;
Xp = out_full.Xp;
Xp_d = out_full.Xp_d;
Xp_dot = out_full.Xp_dot;
Q1 = out_full.Q1;
Q2 = out_full.Q2;
Q_leak = out_full.Q_leak;
P1 = out_full.P1;
P2 = out_full.P2;
Xv = out_full.Xv;
R1 = out_full.R1_loss;

```

```

R2 = out_full.R2_loss;
I1 = out_full.I1_loss;
I2 = out_full.I2_loss;
%% simscape simple model
if f ~= 10
    out_simple = sim('servovalve_transfer_function',10);
    time_simple = out_simple.tout;
    Q1_simple = out_simple.Q1_sim;
    Q2_simple = out_simple.Q2_sim;
    Xp_simple = out_simple.Xp_sim;
    Xv_simple = out_simple.Xv_sim;
    P1_simple = out_simple.P1_sim;
    P2_simple = out_simple.P2_sim;
%% Full-simple models comparisson
for i = 1:length(Xv)
    if Xv(i) > 0
        P_eff(i,1) = P1(i);
        Q_eff(i,1) = Q1(i);
    elseif Xv(i) < 0
        P_eff(i,1) = P2(i);
        Q_eff(i,1) = Q2(i);
    else
        P_eff(i,1) = 0;
        Q_eff(i,1) = 0;
    end
end

for i = 1:length(time_simple)
    if Xv_simple(i) > 0
        Q_eff_simple(i,1) = Q1_simple(i);
    elseif Xv_simple(i) < 0
        Q_eff_simple(i,1) = Q2_simple(i);
    else
        Q_eff_simple(i,1) = 0;
    end
end

Power_full = Ps*Q_eff;
Power_simple = Ps*Q_eff_simple;
Power_full_mean = mean(Power_full)
Power_simple_mean = mean(Power_simple)

figure (8)
plot(time,Xp_d,'Color',[0.4660, 0.6740, 0.1880])
title('Piston Position')
xlabel('time (sec)')
ylabel('x (m)')
hold on
grid on
plot(time,Xp,'Color',[0, 0.4470, 0.7410])
hold on
plot(time_simple,Xp_simple,'Color',[0.8500, 0.3250, 0.0980] )
hold off
legend({'desired','full','simple'},'location','southeast')

figure (9)
plot(time,Power_full)
title('Hydraulic Power')
xlabel('time (sec)')
ylabel('Power (W)')

```

```

hold on
grid on
plot(time_simple,Power_simple)
hold off
legend({'full','simple'},'location','southeast')

% Pressure 1
figure (10)
plot(time,P1)
title('Piston Chamber Pressure')
xlabel('time (sec)')
ylabel('P (Pa)')
hold on
grid on
plot(time_simple,P1_simple)
hold off
legend({'full','simple'},'location','southeast')

% Pressure 2
figure (11)
plot(time,P2)
title('Ring Chamber Pressure')
xlabel('time (sec)')
ylabel('P (Pa)')
hold on
grid on
plot(time_simple,P2_simple)
hold off
legend({'full','simple'},'location','southeast')

% flow rate 1
figure (12)
plot(time,Q1)
title('Piston Chamber 1 Flow Rate')
xlabel('time (sec)')
ylabel('Q (m^3/sec)')
hold on
grid on
plot(time_simple,Q1_simple)
hold off
legend({'full','simple'},'location','southeast')

% flow rate 2
figure (13)
plot(time,Q2)
title('Piston Chamber 2 Flow Rate')
xlabel('time (sec)')
ylabel('Q (m^3/sec)')
hold on
grid on
plot(time_simple,Q2_simple)
hold off
legend({'full','simple'},'location','southeast')
%%
% effective flow rate
figure (14)
plot(time,Q_eff)
title('Effective Flow Rate')
xlabel('time (sec)')
ylabel('Q (m^3/sec)')

```



```

        grid on
        hold on
        plot(time_simple,Q_eff_simple)
        hold off
    end
    %% Losses
    figure (15)
    plot(time,I1)
    title('Inertia losses in Piston Chamber')
    xlabel('time (sec)')
    ylabel('P_I_1 (Pa)')
    grid on

    figure (16)
    plot(time,I2)
    title('Inertia losses in Ring Chamber')
    xlabel('time (sec)')
    ylabel('P_I_2 (Pa)')
    grid on

    figure (17)
    plot(time,R1)
    title('Friction losses in Piston Chamber')
    xlabel('time (sec)')
    ylabel('P_R_1 (Pa)')
    grid on

    figure (18)
    plot(time,R2)
    title('Friction losses in Ring Chamber')
    xlabel('time (sec)')
    ylabel('P_R_2 (Pa)')
    grid on

    I1_mean = mean(abs(I1))
    I2_mean = mean(abs(I2))
    R1_mean = mean(abs(R1))
    R2_mean = mean(abs(R2))
end

```

b) PID Gains

```

function [k_act,ki_act,kd_act,k_pump,ki_pump,kd_pump] =
PID_gains_new(f)

if f == 10
    k_act = 1500;
    ki_act = 225000;
    kd_act = 200;

    k_pump = 0.032;
    ki_pump = 2.2;
    kd_pump = 0.001;

elseif f == 8
    k_act = 1400;
    ki_act = 173000;
    kd_act = 200;

    k_pump = 0.025;

```

```

ki_pump = 1.655;
kd_pump = 0.001;

elseif f == 6
k_act = 1250;
ki_act = 112000;
kd_act = 200;

k_pump = 0.023;
ki_pump = 1.12;
kd_pump = 0.001;

elseif f == 4
k_act = 1200;
ki_act = 56500;
kd_act = 200;

k_pump = 0.0175;
ki_pump = 0.56;
kd_pump = 0.001;

elseif f == 2
k_act = 1000;
ki_act = 17700;
kd_act = 200;

k_pump = 0.0115;
ki_pump = 0.16;
kd_pump = 0;

elseif f == 1
k_act = 1000;
ki_act = 7500;
kd_act = 200;

k_pump = 0.015;
ki_pump = 0.056;
kd_pump = 0;

elseif f == 0.8
k_act = 1000;
ki_act = 6300;
kd_act = 200;

k_pump = 0.017;
ki_pump = 0.04;
kd_pump = 0;

elseif f == 0.6
k_act = 1000;
ki_act = 5250;
kd_act = 200;

k_pump = 0.018;
ki_pump = 0.026;
kd_pump = 0;

elseif f == 0.4
k_act = 800;

```

```

    ki_act = 4000;
    kd_act = 200;

    k_pump = 0.0225;
    ki_pump = 0.015;
    kd_pump = 0;

elseif f == 0.2
    k_act = 800;
    ki_act = 3100;
    kd_act = 200;

    k_pump = 0.027;
    ki_pump = 0.0045;
    kd_pump = 0;

elseif f == 0.1
    k_act = 800;
    ki_act = 2800;
    kd_act = 200;

    k_pump = 0.031;
    ki_pump = 0.0015;
    kd_pump = 0;

end

```

c) Sizing

```

close all
clear
clc
%%
m = 1000;
%mass
B = 1000;
%friction
f = 10;
%frequency
A = 0.0025;
%amplitude
Ps = 35e6;
%supply pressure
%%
w = 2*pi*f;
%angular frequency
t = atan(-m*w/B)/w + 1/f;
%time when dF/dt = 0
F_max_th = -m*A*w^2*sin(w*t) + B*A*w*cos(w*t)
%theoretical max value
%%
L = 10000;
time = linspace(0,1/f,L);
a = -A*w^2*sin(w*time);
u = A*w*cos(w*time);
F_a = m*a;
F_u = B*u;
F_tot = F_a + F_u;
F_max = max(F_tot)
Power = F_tot.*u;

```

```

figure(1)
plot(time,F_a)
xlabel('time (sec)')
% yyaxis left
ylabel('Force (N)')
grid on
hold on
plot(time,F_u)
hold on
plot(time,F_tot)
% yyaxis right
% plot(time,Power)
% ylabel('Power (W)')
legend({'F_a','F_u','F_t_o_t'},'location','southeast')
hold off
%% Diameter
A2 = F_max_th/Ps
A1 = A2*2
D_piston = sqrt(4*A1/pi)
%% pump
Q_max = (max(u)*pi*0.04^2/4)*60000
Vg = 5;
n = Q_max*1000/Vg/0.92
%% Power
figure (2)
plot(time,Power)
xlabel('time (sec)')
ylabel('Power (W)')
grid on
Power_max = max(abs(Power))
Power_mean = mean(abs(Power))
%% FFT
Fs = L;
% Sampling frequency
T_fft = 1/Fs;
% Sampling period
t_fft = (0:L-1)*T_fft;
% Time vector
Fa = (-A*m*w^2*sin(w*t_fft));
Fu = B*A*w*cos(w*t_fft);
v = A*w*cos(w*t_fft);
P = (Fa + Fu).*v;
Y = fft(P);
P2 = abs(Y/L);
P1 = P2(1:L/(L/f/10)+1);
P1(2:end-1) = 2*P1(2:end-1);
freq = Fs*(0:(L/(L/f/10)))/L;
xq1 = 0:0.01:max(freq);
P1(1) = 0;
P1_chip = pchip(freq,P1,xq1);
figure (3)
plot(xq1,P1_chip)
title('Single-Sided Amplitude Spectrum of Power(t)')
xlabel('f (Hz)')
ylabel('|P1(f)|')
grid on

```

D. KDamper

The figure below presents the fundamental concept of the KDamper. It can be seen that it uses a negative stiffness element k_N in order to achieve better damping effect. The main requirement of the KDamper is that the overall static stiffness of the system is constant.

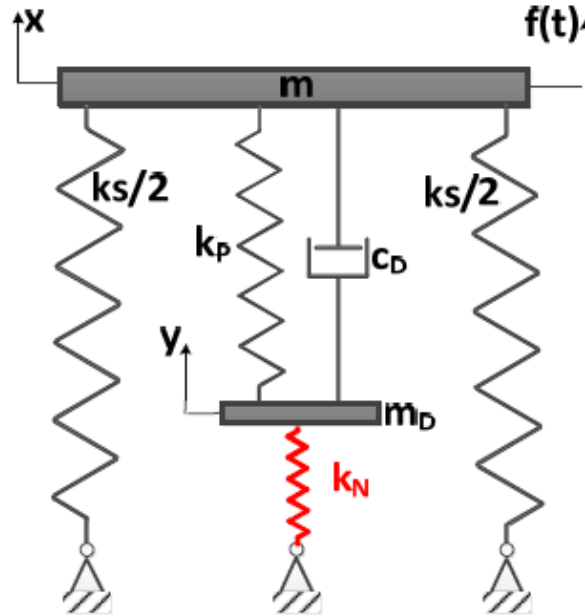


Figure D-1: Schematic presentation of KDamper

An example for an implementation of the KDamper is depicted in Figure D-2. It consists of a mass m which is connected with two parallel linear springs of stiffness k_s and k_p respectively and by a damper with constant damping coefficient c_D . The damper c_D and the spring k_p are in turn connected to a mass m_D . To implement the negative stiffness spring, a set of two symmetric linear horizontal springs are used with constants k_H , which support the mass m_D by an articulated mechanism. The static equilibrium position of the system is depicted in Fig D-2(a), under the action of the gravity force. The perturbed position after an external dynamic excitation $f(t)$ can be seen in Fig D-2(b).

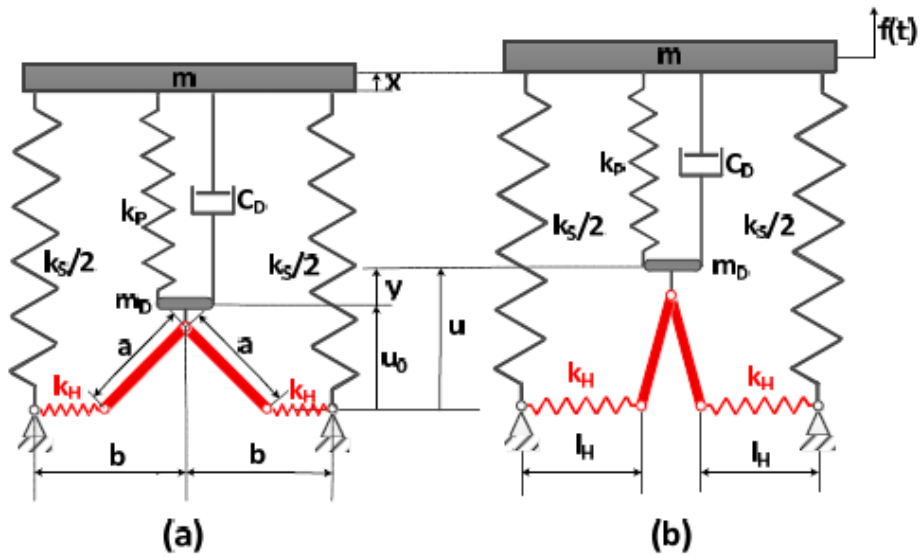


Figure D-2: K-Damper: (a) Static equilibrium under gravity force, (b) perturbed position after dynamic excitation

For the enhancement of K-Damper's performance, the use of hydraulic springs is being investigated. The hydraulic spring comprises of a bladder type accumulator connected with a hydraulic actuator which acts as a negative stiffness spring replacing the horizontal spring k_H .

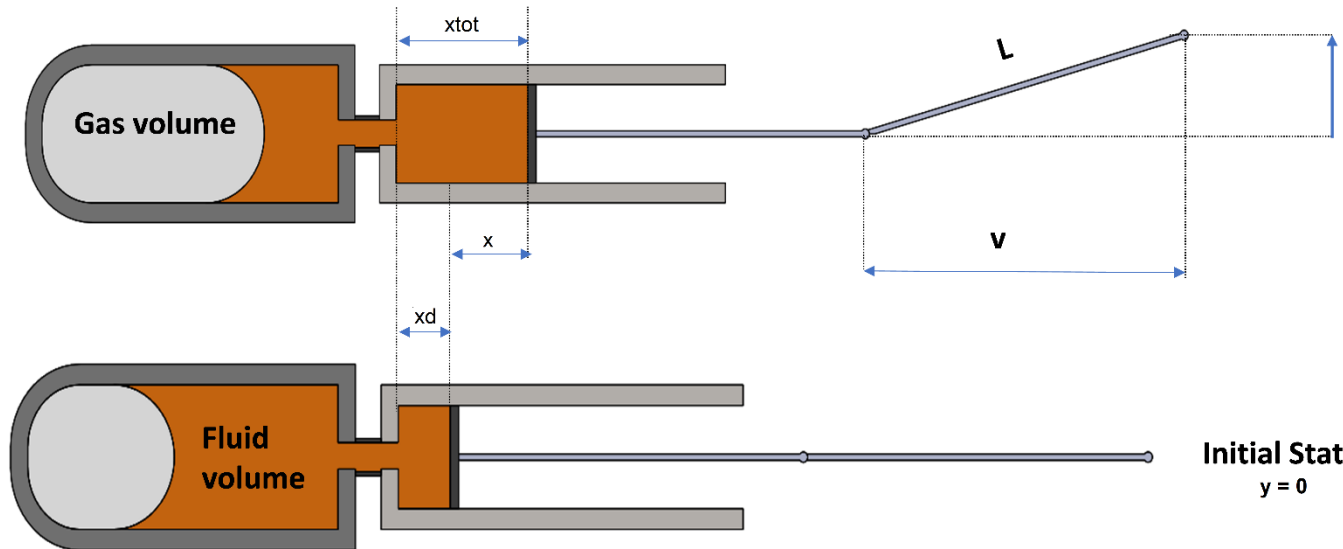


Figure D-3: Conceptual configuration of the negative stiffness spring in K-Damper

From the above configuration it can be deduced that:

$$v = \sqrt{L^2 - y^2} \quad (D-1)$$

Assuming that the length x is zero when the configuration is horizontal ($y = 0$), the value of x is calculated as follows:

$$x = L - \sqrt{L^2 - y^2} \quad (D-2)$$

Deriving the above equation (D-2), the velocity and acceleration of the actuator piston are calculated:

$$\dot{x} = \frac{y\dot{y}}{\sqrt{L^2 - y^2}} \quad (D-3)$$

$$\ddot{x} = \frac{y(L^2 - y^2)\ddot{y} + L^2\dot{y}^2}{(L^2 - y^2)^{\frac{3}{2}}} \quad (D-4)$$

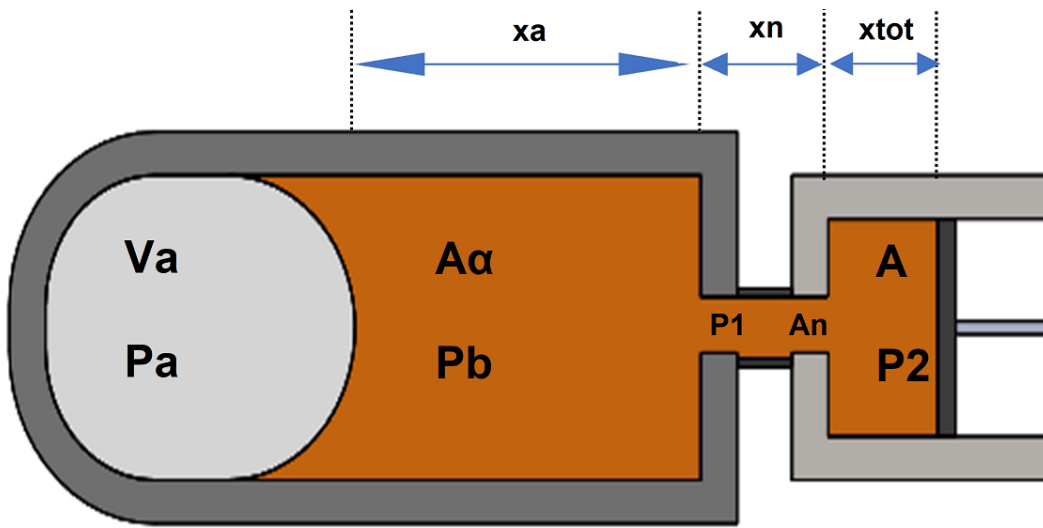


Figure D-4: Simplified model of the hydraulic actuator

Assuming that the gas inside the gas chamber is ideal, the following equation is being satisfied between two states of the accumulator:

$$P_a V_a^n = P_{a0} V_{a0}^n = C \quad (D-5)$$

where index 0 is used to denote the initial conditions of the accumulator and n is the gas constant.

Deriving the above equation (D-5) results in:

$$\begin{aligned} \frac{dP_a}{dt} V_a^n + P_a n V_a^{n-1} \frac{dV_a}{dt} &= 0 \Rightarrow \frac{dV_a}{dt} = -\frac{V_a}{n P_a} \frac{dP_a}{dt} \\ &= -\frac{V_{a0}}{n P_{a0}} \frac{dP_a}{dt} \xrightarrow{\text{laplace}} \end{aligned}$$

$$\begin{aligned}
sV_{a(s)} - V_{a0} &= -\frac{V_{a0}}{nP_{a0}}(sP_{a(s)} - P_{a0}) \Rightarrow P_{a(s)} \\
&= -\frac{nP_{a0}}{V_{a0}}V_{a(s)} + \frac{(n+1)}{s}P_{a0}
\end{aligned} \tag{D-6}$$

The force of the gas inside the gas chamber is given by the equation:

$$\begin{aligned}
(P_b - P_a)A_a &= k_g \frac{V_a}{A_a} + B_g \frac{1}{A_a} \frac{dV_a}{dt} \Rightarrow P_b - P_a \\
&= k_g \frac{V_a}{A_a^2} + B_g \frac{1}{A_a^2} \frac{dV_a}{dt}
\end{aligned} \tag{D-7}$$

where:

- P_b : oil pressure inside the accumulator
- P_a : gas pressure in the gas chamber
- A_a : cross-sectional area of the accumulator
- V_a : gas volume in the gas chamber
- k_g : gas stiffness coefficient
- B_g : gas damping coefficient.

The gas damping coefficient is calculated by the following equation:

$$B_g = 8\pi\mu_g \frac{V_a}{A_a} \tag{D-8}$$

where μ_g is the viscosity coefficient of the gas.

The gas stiffness coefficient is a variable that describes the change in gas volume as pressure changes and is calculated as:

$$k_g = \frac{\Delta F}{\Delta X} = \frac{\Delta P A_a}{\Delta V / A_a} = A_a^2 \frac{dP}{dV} = -A_a^2 \frac{nP_{a0} V_{a0}^n}{V_a^{n+1}} \tag{D-9}$$

The hydraulic oil inside the liquid chamber is very difficult to compress because of its high rigidity and thus it can be assumed that the hydraulic oil is practically incompressible. Therefore, the change of gas volume in the gas chamber is equal to the flow rate of the oil entering or exiting the accumulator.

$$Q = \frac{dV_a}{dt} \tag{D-10}$$

The force of the hydraulic oil inside the accumulator is calculated as:

$$P_1 A_n - P_b A_a = m_{ac} \frac{1}{A_a} \frac{d^2 V_a}{dt^2} + B_e \frac{1}{A_a} \frac{dV_a}{dt} \quad (D-11)$$

where:

- P_1 : pressure of the oil in the inlet of the accumulator
- A_n : cross-sectional area of the inlet of the accumulator
- m_{ac} : mass of the oil inside the accumulator
- B_e : viscous damping coefficient of the hydraulic oil

The viscous damping coefficient of the hydraulic fluid is given by the following equation:

$$B_e = 8\pi\mu_o x_a \quad (D-12)$$

where:

- μ_o : dynamic viscosity of the hydraulic oil
- x_a : length of the oil in the accumulator.

Assuming that:

$$A_n = k A_a \quad (D-13)$$

and combining equations (D-11) and (D-13), the general equation that describes the accumulator is:

$$k P_1 - P_a = \frac{1}{A_a^2} \left(m_{ac} \frac{d^2 V_a}{dt^2} + B_e \frac{dV_a}{dt} + B_g \frac{dV_a}{dt} + k_g V_a \right) \quad (D-14)$$

The pressure for the connection line between the accumulator and the hydraulic actuator is given by the equation:

$$P_2 - P_1 = \frac{8\pi\mu_d x_n}{A_n^2} Q + \frac{\rho x_n}{A_n} \dot{Q} \quad (D-15)$$

where:

- P_2 : oil pressure inside the hydraulic actuator
- x_n : length of the pipeline
- μ_d : dynamic viscosity of the oil inside the pipeline
- ρ : oil density

The force applied by the hydraulic actuator, neglecting the friction losses, is given by the following equation:

$$F = P_2 A_p + m' \ddot{x} \quad (D-16)$$

where:

- A_p : piston area
- m' : mass of the hydraulic oil inside the hydraulic cylinder plus the mass of the piston
- \ddot{x} : piston acceleration

Since the hydraulic oil is considered to be incompressible, the velocity of the piston can be expressed as:

$$\dot{x} = \frac{Q}{A_p} = \frac{1}{A_p} \frac{dV_a}{dt} \quad (D-17)$$

Combining equations (D-16) and (D-17) results in:

$$\begin{aligned} F &= \left(P_1 + \frac{8\pi\mu_d l_n}{A_n^2} Q + \frac{\rho l_n}{A_n} \dot{Q} \right) A_p + m' \frac{1}{A_p} \dot{Q} = \\ &= \left(P_1 + \frac{8\pi\mu_d l_n}{A_n^2} \frac{dV_a}{dt} + \frac{\rho l_n}{A_n} \frac{d^2 V_a}{dt^2} \right) A_p + m' \frac{1}{A_p} \frac{d^2 V_a}{dt^2} \end{aligned} \quad (D-18)$$

Using equations (D-14) and (D-18), the following equation for the force applied by the hydraulic actuator is obtained:

$$\begin{aligned} F &= \left[\frac{1}{k A_a^2} \left(m_{ac} \frac{d^2 V_a}{dt^2} + B_e \frac{dV_a}{dt} + B_g \frac{dV_a}{dt} + k_g V_a \right) + \frac{P_a}{k} \right. \\ &\quad \left. + \frac{8\pi\mu_d x_n}{A_n^2} \frac{dV_a}{dt} + \frac{\rho x_n}{A_n} \frac{d^2 V_a}{dt^2} \right] A_p + m' \frac{1}{A_p} \frac{d^2 V_a}{dt^2} \Rightarrow \\ \Rightarrow F &= \left(\frac{m_{ac} A_p}{k A_a^2} + \frac{\rho x_n A_p}{A_n} + \frac{m'}{A_p} \right) \frac{d^2 V_a}{dt^2} \\ &\quad + \left(\frac{(B_e + B_g) A_p}{k A_a^2} + \frac{8\pi\mu_d x_n A_p}{A_n^2} \right) \frac{dV_a}{dt} + \frac{k_g A_p}{k A_a^2} V_a \\ &\quad + \frac{A_p}{k} P_a = m_{eq} \frac{d^2 V_a}{dt^2} + B_{eq} \frac{dV_a}{dt} + \frac{k_g A_p}{k A_a^2} V_a + \frac{A_p}{k} P_a \end{aligned} \quad (D-19)$$

Applying the Laplace transformation on equation (D-19) results in:

$$F_{(s)} = m_{eq}(V_{a(s)}s^2 - V_{a0}s - \dot{V}_{a0}) + B_{eq}(V_{a(s)}s - V_{a0}) + \frac{k_g A_p}{k A_a^2} V_{a(s)} + \frac{A_p}{k} P_{a(s)} \quad (D-20)$$

Combining equations (D-6) and (D-20):

$$\begin{aligned} F_{(s)} &= m_{eq}(V_{a(s)}s^2 - V_{a0}s - \dot{V}_{a0}) + B_{eq}(V_{a(s)}s - V_{a0}) \\ &\quad + \frac{k_g A_p}{k A_a^2} V_{a(s)} + \\ &\quad + \frac{A_p}{k} \left(-\frac{n P_{a0}}{V_{a0}} V_{a(s)} + \frac{(n+1)}{s} P_{a0} \right) = \\ &= m_{eq}(V_{a(s)}s^2 - V_{a0}s - \dot{V}_{a0}) + B_{eq}(V_{a(s)}s - V_{a0}) \\ &\quad + \left(\frac{k_g A_p}{k A_a^2} - \frac{n P_{a0} A_p}{V_{a0} k} \right) V_{a(s)} + \frac{(n+1) A_p}{k s} P_{a0} \Rightarrow \end{aligned}$$

$$\begin{aligned} F_{(s)} &= m_{eq}(V_{a(s)}s^2 - V_{a0}s - \dot{V}_{a0}) + B_{eq}(V_{a(s)}s - V_{a0}) \\ &\quad + K_{eq} V_{a(s)} + \\ &\quad \frac{(n+1) A_p}{k s} P_{a0} \Rightarrow \end{aligned}$$

$$\begin{aligned} F_{(s)} &= m_{eq} V_{a(s)} s^2 + B_{eq} V_{a(s)} s + K_{eq} V_{a(s)} - m_{eq} V_{a0} s - m_{eq} \dot{V}_{a0} \\ &\quad - B_{eq} V_{a0} + \frac{(n+1) A_p}{k s} P_{a0} \end{aligned} \quad (D-21)$$

Considering that the flow at the initial moment is zero, the final equation that describes the force applied by the hydraulic actuator is:

$$\begin{aligned} F_{(s)} &= m_{eq} V_{a(s)} s^2 + B_{eq} V_{a(s)} s + K_{eq} V_{a(s)} - m_{eq} V_{a0} s - B_{eq} V_{a0} \\ &\quad + \\ &\quad \frac{(n+1) A_p}{k s} P_{a0} \Rightarrow \\ F_{(s)} &= (m_{eq} s^2 + B_{eq} s + K_{eq}) V_{a(s)} - (m_{eq} s + B_{eq}) V_{a0} \\ &\quad + \frac{(n+1) A_p}{k s} P_{a0} \end{aligned} \quad (D-22)$$

where:

- $m_{eq} = \frac{m_{ac} A_p}{k A_a^2} + \frac{\rho x_n A_p}{A_n} + \frac{m'}{A_p}$
- $B_{eq} = \frac{(B_e + B_g) A_p}{k A_a^2} + \frac{8 \pi \mu_d x_n A_p}{A_n^2}$
- $K_{eq} = \frac{k_g A_p}{k A_a^2} - \frac{n P_{a0} A_p}{V_{a0} k}$

The proposed configuration is a closed hydraulic circuit and hence the total mass of the hydraulic oil remains practically the same. Nevertheless, the oil mass in each of

the individual components is variable. The oil mass inside the pipeline can be calculated as follows:

$$m_{ln} = \rho x_n A_n \quad (D-23)$$

Next, the oil mass in the hydraulic cylinder is calculated:

$$m_{cyl} = \rho x_{tot} A_p = \rho (x_d + x) A_p \quad (D-24)$$

where x_d is the dead length of the cylinder.

Finally, the oil mass in the accumulator is calculated:

$$m_{ac} = \rho x_a A_a \quad (D-25)$$

$$x_a = \frac{V_{tot} - V_a}{A_a} \quad (D-26)$$

$$V_a = x A_p + V_{a0} \quad (D-27)$$

Combing equations (D-25), (D-26) and (D-27) the oil mass inside the accumulator is:

$$m_{ac} = \rho (V_{tot} - x A_p - V_{a0}) \quad (D-28)$$